Sustainable Materials and Technologies 41 (2024) e01077

Contents lists available at ScienceDirect

Sustainable Materials and Technologies

journal homepage: www.elsevier.com/locate/susmat

Lignocellulosic bioplastics in sustainable packaging – Recent developments in materials design and processing: A comprehensive review

M.J. Ahmed[a,b,e], J. Ashfaq[b,c], Z. Sohail[b,d], I.A. Channa[b,c,*], A. Sánchez-Ferrer[e], S.N. Ali[a,b], A.D. Chandio[b,c]

[a] Department of Chemistry, NED University of Engineering and Technology, Main Campus, Karachi 75270, Sindh, Pakistan
[b] Thin-Film Lab, Advanced Materials and Sustainable Environment (AMSE) Group, NED University of Engineering and Technology, Main Campus, Karachi 75270, Sindh, Pakistan
[c] Department of Metallurgical Engineering (fmr. Materials and Metallurgical Engineering), NED University of Engineering and Technology, Main Campus, Karachi 75270, Sindh, Pakistan
[d] Department of Biomedical Engineering, NED University of Engineering and Technology, Main Campus, Karachi 75270, Sindh, Pakistan
[e] Wood Materials Science Group, Holzforschungs Munchen (HFM), Technical University of Munich (TUM), Winzererstrasse 45, DE-80797 Munich, Germany

ARTICLE INFO

Keywords:
Lignocellulosic waste
Valorisation
Packaging
Sustainability
Process structure-property relations
Cellulose bioplastics

ABSTRACT

Lignocellulosic materials, despite their abundance and attractiveness, have long been marred with challenges in optimising the cost-functionality-quality trade-off. This comprehensive authoritative review paper explores how various lignocellulosic feedstock have been utilised to prepare marketable and sustainable bioplastics, as potential substitutes to conventional petroleum-based packaging. Dependence on hydrocarbon-derived plastics is increasingly being supplanted by both consumer-driven and sustainability-oriented materials design. This comprehensive paper encompasses a broad review relating to recent research (2013–2023) on the innovations and heuristic approaches to modify lignocellulose for the production of packaging films. The review paper holds extensive focus across various lignocellulosic materials such as - but not limited to - cellulose nanomaterials, cellulose esters and grafted cellulose. Advances in processes reported to date such as mechanochemical, chemical, thermochemical, biochemical and other novel methods have been studied. The materials design and process implications in terms of its cost, energy input and sustainability in its true sense, for all known techniques have been extensively investigated in this review paper. The review paper has further provided an elaborate process-structure-property-performance framework that characterises how material properties could be fine-tuned *via* different process considerations. A techno-economic feasibility overview for said processes and materials' use is also described herein.

Abbreviations & Symbols

AX	Arabinoxylanase
CA	Cellulose Acetate
CAGR	Compound Annual Growth Rate
CE	Carbohydrate Esterase
ChCl/LA	Choline Chloride/Lactic Acid
CP	Cellophane
CSTR	Continuous Stirred Tank Reactor
DBNHAc	1,5-Diazabicyclo[4.3.0]non-5-enium Acetate
DES	Deep Eutectic Solvent
DS	Degree of Substitution
EMIMLac	1-Ethyl-3-methylimidazolium L-(+)-Lactate
FACE	Fatty Acid Cellulose Ester
FDCA	2,5-Furandicarboxylic Acid
GGM	Gluco-Galactomannanase
GH	Glycoside Hydrolase
GT	Glycosyltransferase
HDPE	High-Density Polyethylene
LCA	Life Cycle Assessment
LCNF	Lignocellulosic Nanofibres

(*continued on next page*)

---

* Corresponding author.
E-mail addresses: ahmed4000166@cloud.neduet.edu.pk, muz.hfm_jalil@tum.de (M.J. Ahmed), jaweriaashfaq72@gmail.com (J. Ashfaq), zarmeen.ssoomro@gmail.com (Z. Sohail), iftikharc@neduet.edu.pk (I.A. Channa), sanchez@hfm.tum.de (A. Sánchez-Ferrer), saeeda@neduet.edu.pk (S.N. Ali), alidad@neduet.edu.pk (A.D. Chandio).

https://doi.org/10.1016/j.susmat.2024.e01077
Received 16 April 2024; Received in revised form 12 July 2024; Accepted 6 August 2024

(*continued*)

LDPE	Low-Density Polyethylene
LFR	Liquid Foam Reactor
LPMO	Lytic Polysaccharide Monooxygenase
LB	Lignocellulosic Biomass
LW	Lignocellulosic Waste
MCC	Microcrystalline Cellulose
NC	Nanocellulose
NCC	Nanocrystalline Cellulose
NFC	Nanofibrilliated Cellulose
MMT	Montmorillonite
NIPAM	*N*-Isopropylacrylamide
NMMO	*N*-Methylmorpholine *N*-Oxide
OP	Oxygen Permeability
OTR	Oxygen Transmission Rate
PAA	Poly(Acrylamide-*co*-Acrylic Acid)
PBAT	Poly(Butylene Adipate-*co*-Terephthalate)
PBS	Poly(Butylene Succinate)
PCL	Polycaprolactone
PE	Polyethylene
PEAA	Poly(Ethylene-*co*-Acrylic Acid)
PET	Poly(Ethylene Terephthalate)
PGA	Poly(Glycolic Acid)
PHA	Polyhydroxyalkanoate
PHB	Poly(3-Hydroxybutyrate)
PHBV	Poly(3-Hydroxybutyrate-*co*-3-hydroxyvalerate)
PLA	Poly(Lactic Acid)
PMMA	Poly(Methyl Methacrylate)
PP	Polypropylene
PS	Polystyrene
PTFE	Polytetrafluoroethylene
PVA	Poly(Vinyl Alcohol)
PVDC	Poly(Vinyl Dichloride)
rPET	Recycled Poly(Ethylene Terephthalate)
sIPN	Semi-Interpenetrating Network
$Sn(Oct)_2$	Tin (II) Octanoate
TFA/TFAA	Trifluoroacetic Acid/Trifluoracetic Anhydride system
V/U	Valorisation and Utilisation Approach
WVP	Water Vapour Permeability
WVTR	Water Vapour Transmission Rate
XyG	Xyloglucanase
εCL	ε-Caprolactone

1. Introduction

Lignocellulosic waste (LW) has long been a common, renewable resource for cellulose, with an abundance in an estimated lignocellulosic biomass/waste production between 10 and 100 billion metric tonnes [1]. This versatile substance has various applications, ranging from building materials to natural fabrics for clothing, bioethanol, solvents (such as Cyrene), as well as paper or cardboard products [2,3,4]. One of the drawbacks of cellulose as a potential substitute for conventional plastics is its high affinity and absorption for water due to the presence of hydroxyl groups (OH) that interact with water by hydrogen bonding making such a polymer hydrophilic [5]. Nevertheless, cellulose has a relatively high degree of crystallinity that, *a priori*, should work as a gas barrier, but the presence of amorphous domains together with its hydrophilic character negatively affects this barrier's properties against water. Moreover, the huge amounts of intra- and intermolecular hydrogen bonds in the crystalline domains difficult the processability of this biopolymer. As a result, cellulose can neither be melt-processed nor solubilised in most solvents [6]. The use of a circular strategy to upcycle the so-called 'forever' plastic wastes, *e.g.*, polyethene (PE), polystyrene (PS), and polyethylene terephthalate (PET), offers high-functionality of the recyclate, higher availability, and attractive cost margins. However, their use has both medium- and long-term environmental and health risks, as evidenced by the problem of microplastics and poor techno-economical sustainability [7].

The European Union's Waste Framework Directive (WFD) and the Circular Economy Action Plan (CEAP) are cornerstones in the transformation of make-use-dispose (linear) to make-use-upcycle/recycle (circular) economic processes. This action plan provides extensive regulations regarding the gradual phasing-off of non-renewable sources of energy and materials in consumer products by *ca.* 65% in 2035 [8,9,10]. The shift to renewable resources and precursors for biodegradable polymer using LW has been an extensive area of research, whereby alternative fuels [2], greener textiles [11], valued-added chemicals and biopolymers [12] have piqued considerable interest from the biorefinery concept. Research on value-added chemicals and biopolymers from LW, specifically for packaging, has undergone a significant increase since the 2010s (Fig. 1) as the World attempts to shift to greener packaging alternatives. (See Table 1.)

Recent innovations in both materials design and processes for the development of these green packaging alternatives need to be reviewed extensively in a manner that focuses on inventive and state-of-the-art research. The following work, thus, pertains to a comprehensive material- and process-design-focused review in the topic area. The authors of the present work have found literature on LW valorisation for packaging to be uncommon and relatively scarce, wherein review literature to date presents a generalised view of the topic. The review, prior most, establishes the state-of-the-art of LW.

valorisation and the corresponding reported use in packaging. The later sections encompass a comprehensive critical assessment of the recent advances in materials and process designs as well as the challenges that have been overcome or still exist. The authors further provide perspectives regarding the techno-economic feasibility of these innovations and their implications for commercialisation and scalability. Establishing a state-of-the-art LW valorisation for packaging can prove vital in driving critical innovations in packaging materials and processes.

This comprehensive review has considered research of significance from the last 10 years, especially, in terms of the development of lignocellulosic materials, including (but not limited to): (nano)cellulose, cellulose esters and grafted cellulose, but not non-cellulosic materials. The selection criteria for the materials considered and the processes used therewith, *i.e.,* mechanochemical, chemical, thermochemical, biochemical and other novel methods among others are of particular interest. Contemporary reviews and studies tend to generalise the impact of material and process design on the final packaging film or thermoplastic. To the authors' knowledge, studies are uncommon that establish or investigate process-structure-property-performance (PSPP) correlation(s) between the methods and materials used. Further the technoeconomic aspects of such processes have also not been explored and investigated. The PSPP can help researchers engaged in material chemistry and engineering how material properties could be fine-tuned *via* different process considerations to attain what could be the right packaging candidates.

2. Lignocellulosic waste valorisation approaches and its implications for packaging

Valorisation has long been the workhorse of circular economy developments. More particularly the increasing preference to shift in advanced economies and the developing world towards sustainable materials has rendered wastes that were invaluable as key raw material commodities [3]. Eliminating/transforming waste is a key aspect of lean management in the industrial value chain, which has become imperative for chemical industries [10]. More specifically, LW and/or biomasses produced from textile, agrochemical, paper and pulping industries, are a ready-to-use source for these industries to meet their energy and certain material input requirements.

2.1. *Agro-industrial lignocellulosic biomass – Characteristics and compositions*

Agro-industrial lignocellulosic biomasses (LBs) have acquired considerable interest for their use in biorefineries to synthesise value-

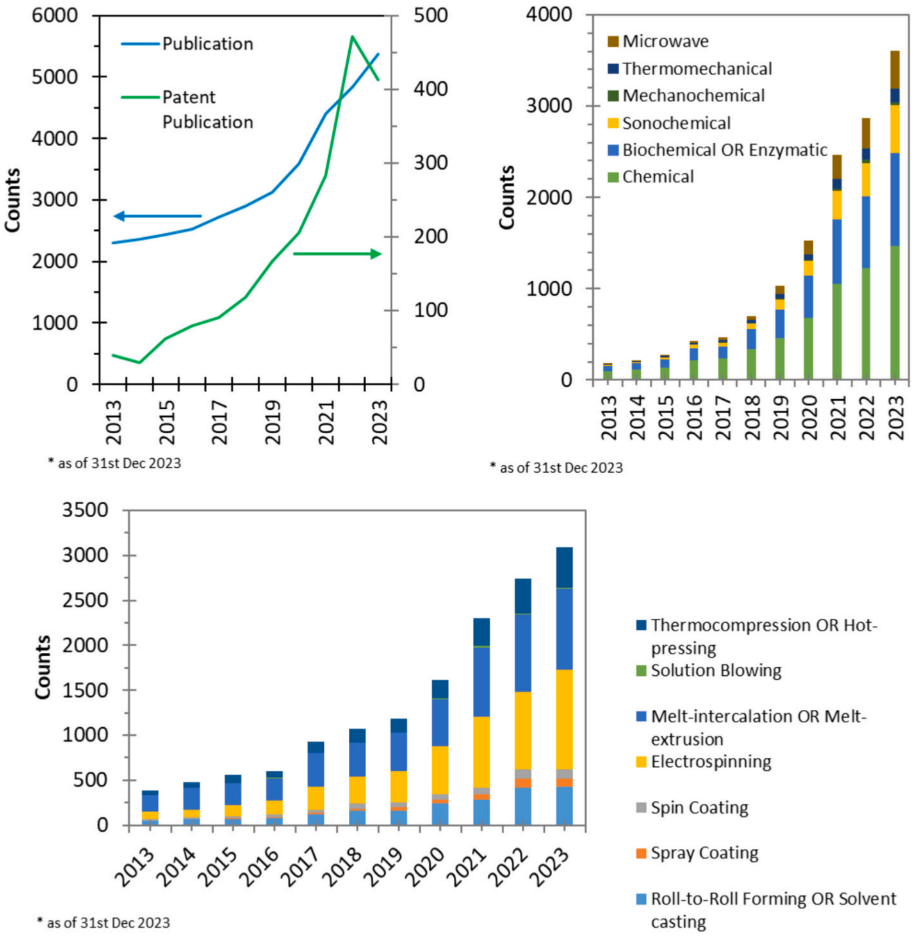

Fig. 1. Increase in number of publications and patents published from 2013 to 2023. Publications on the valorisation technique and by packaging film-forming technique used are also shown. Data relates to LW valorisation for Packaging applications — data from Google Scholar (2023) and Google Patents (2023).

added products. This demand for lignocellulosic materials has not been limited to biorefineries but rather has found use in multiple consumer goods research and innovation applications, such as bioplastics, wearable sensors, and ultrafiltration membranes to name a few [36,37,38]. The utilisation of agro-industrial LB in various applications is extensively dependent on the material structure and properties resulting from different chemical, mechanical, mechanochemical, and enzymatic methods [39,40,41,42]. Further, the composition of biomass components such as lignin, hemicelluloses and cellulose in the LB has a significant impact on the application. These impacts are particularly associated with the fibre-matrix strength, stability and the extent of degradation throughout the material's lifecycle [43].

The composition of LB typically comprises cellulose, lignin and hemicelluloses. The total polysaccharide fraction from wood, straw or bagasse-based LBs is the so-called holocellulose. The percentage composition of each of these components varies in different plant sources due to the nature and make of their cell walls (Fig. 2) (M. A. [13,1]). Cellulose is the fundamental component of the native plant fibres, comprising linear polymer chains of glucose units connected by β-(1–4) glycosidic bonds. Native cellulose can have four distinct crystalline polymorphs, of which Cellulose I and Cellulose II (Fig. 3) are of significance for film-forming and functional characteristics (K. [44]). The former is characterised by flat parallel chains that are H-bonded in a side-by-side fashion. In Cellulose II, the H-bonding occurs inter-planarly and in tandem across anti-parallel chains. Alkaline conditions bring about interconversion between these two polymorphs. Cellulose I and Cellulose II imbue distinct structural and morphological properties that render their suitability for certain applications. Cellulose I is generally more capable of film formation than its counterpart, which is instead a potential candidate for bioethanol feedstocks (M. M. [45]).

Hemicelluloses in contrast to cellulose, refer to complex, shorter, branched, and amorphous polyoses in plant cellular walls (*i.e.*, matrix polysaccharides). Hemicelluloses are typically composed of xylans, mannans or glucans or their copolymers with pentose sugars such as arabinoxylans, glucomannans and xyloglucans [46] and are responsible for dispersing and connecting cellulose into the amorphous lignin matrix. Lignins are complex, polyphenolic polymers partially crosslinked present in the plant's cell wall, which together with pectin are the major components in the middle lamellar in the plant's cellular structure. These heterogenic aromatic compounds are characterised by their mechanical strengths and hydrophobicity which impart anti-microbial resistance to the cellulosic fibres [47]. The presence of lignin can be a hindrance to packaging as it can reduce the transparency due to its high chromophoricity, and thermal stability of the final biopolymer film; though it can improve fibre strength by interfering with interfibrillar H-bonding (Y. [48]).

The ternary diagram in Fig. 4 illustrates the spread of various lignocellulosic sources, whereby, agricultural crops (herbaceous biomass) such as rice, corn, sugarcane, wheat, flax, cotton and others.

Biomass sources such as deciduous (hardwood – *e.g.*, beech, birch and oak) and coniferous (softwood – *e.g.*, fir, spruce and pine) trees have an apparent, higher lignin content which can limit their use for transparent packaging use. However, these agro-industrial LBs could still be used for kraft lignin and paper pulp packaging as they are used contemporarily [42]. The extremity of cotton in terms of cellulose content is evident, though its major application is for textiles and fabrics

Table 1
Lignocellulosic compositions in agro-industrial LBs from various plant sources.

Plant Source	Lignocellulosic Composition (%)				References
	Cellulose	*Hemi-celluloses*	*Holo-cellulose*	*Lignin*	
Sugarcane bagasse [a]	47	33	80	23	Mahmud and Anannya [13]
	46	29	75	24	
	41	30	71	21	
Jute [a]	61	14	75	12	
	72	20	92	13	
Cotton [a]	85	1	86	1	
	90	3	93	2	
Rice husk [a,b]	53	5	58	20	Khandanlou et al. [14]
Rice straw [a]	30	26	56	7	Johar et al. [15]
	36	17	53	23	
Corn husk [c]	50	39	89	8	Kambli et al. [16]
Wheat straw [c]	49	28	77	9	
Pineapple leaf [c]	36	23	59	28	
Pine bark (pinus *spp.*) [a]	25	15	40	45	[17]
Douglas Fir [a]	17	8	24	44	Pan et al. [18]
	23	14	37	44	
Spruce bark [d]	29	22	51	25	[19]
Bamboo[e]	33	27	60	30	Rusch et al. [20]
	47	23	70	20	
Birch bark [a,e]	40	36	76	20	Buzała et al. [21]; Kuznetsov et al. [22]
	47	30	77	23	
Poplar [a]	34	41	75	25	Boundzanga et al. [23]; Rego et al. [24]
	35	41	75	25	
	49	23	72	27	
Willow [e]	42	17	58	29	Díez et al. [25]
Peanut hulls [e]	45	6	50	36	Pączkowski et al. [26]
Coconut coir [e]	37	23	59	42	Felgueiras et al. [27]
Cotton stalks [e]	45	20	65	21	G. Li et al. [28]
Hemp [e,f]	57	9	66	5	Stevulova et al. [29]
	77	14	91	9	
Sisal [e]	64	20	84	10	Pirah et al. [30]
	65	27	92	13	
Flax[e]	65	13	78	5	Zommere et al. [31]
	75	26	102	7	

Characterisations based on:
[a] TAPPI T212 OS-74, TAPPI T222 OM-11, TAPPI T249 OM-09 ([32]; [33]).
[b] AOAC Standard, *Official Methods of Analysis*, 22e [34].
[c] Halliwell's Method (1997) [16].
[d] ASTM D1106–96 (2007).
[e] Other, modified chemical compositional analysis; methods based on those in note 1 (*vide supra*).
[f] NREL/TP-510-4262 (2008) [35].

production. Arguably, a higher cellulose or hemicellulose content is responsible for a higher fibrous characteristic of the agro-industrial LB, which could be useful for fibre-based packaging [49]. This yields another prospect opportunity for the use of cotton materials such as post-consumer textiles for packaging textiles.

2.2. Lignocellulosic wastes as candidate materials for sustainable packaging – Market viability and trends

Bio-based alternatives like cellulose acetate have a relatively lower impact depending on how it has been produced. Concurrent materials selection and design have been constantly looking for new routes of polymer preparation [50]. The use of abundant LW for sustainable packaging has grown much in prominence since the 2010s as consumers are growing increasingly aware of the implications and far-reaching consequences of common hydrocarbon-derived plastics. With many countries and regions such as the EU, the UK and the US banning the so-called single-use plastic, agro-industrial LBs have become ever more relevant and worthwhile candidates for packaging [51]. Often post-consumer plastic is downcycled for reuse, *i.e.*, reduced in value – or lost value - in terms of its original properties. This will lead to a significant reduction in carbon dioxide emissions (CO_2e) and greenhouse gas (GHG) emissions. The dependence on non-renewables such as petroleum can be minimised effectively.

The market valuation for agro-industrial LBs across its components, cellulose, hemicelluloses and lignin has been predominantly captured in the biorefinery (*i.e.*, bioethanol and low carbon fuel alternatives) and utilisation domains (*i.e.*, packaging and textiles). The estimated cost of agro-industrial LBs ranges from US $24.00 - US $121.00 per metric tonne; depending on the crop, its yield, the region where it was produced and the valuation assessment [52]. Annual production of agro-industrial LB is estimated to be around 181.5 bn metric tonnes [53]. Bioplastic production has been following a steadily increasing trend and is expected to reach 7.59 m metric tonnes by 2026; as shown in Fig. 5a and c (European [54,55]). Cellulose films and starch blends accounted for a total of 21.5% of the global bioplastic production in 2022; as shown in Fig. 5b [56].

Additionally, sustainable or biodegradable packaging was valued at US $99.33 bn in 2023 and is forecasted to reach a staggering US $132.74 bn in 2028 with a compound annual growth rate (CAGR) of 5.97% [57]. Sustainable packaging for this purpose, has largely pertained to identifying the right materials for ensuring a closed-loop circular production of consumer plastics. Agro-industrial LBs have offered an unprecedented advantage for green technology businesses and the plastics industry to combat waste disposal problems and bolster efforts towards responsible production and consumption of natural resources (wood or agro-industrial wastes and pulps).

3. Advances in lignocellulosic waste processing for packaging

3.1. Developments in chemical valorisation and utilisation approaches for packaging

LW utilisation has been much focused on developing sustainable reaction pathways for value-added chemicals, biopolymers and bio-composites for versatile usage across construction, and consumer products.

Lignocellulosic valorisation has featured multifaceted strategies to improve the yield, and scalability, and preserve the fibre characteristics of the cellulose nanofibrils in agro-industrial LB for use in such sustainable applications [51]. These fibre characteristics are among the sole features that define the versatility of cellulose nanofibrils for use across multiple applications. The quality of fibre characteristics preserved defines the mechanical, optoelectronic, thermal and functional properties, *i.e.*, characterise cellulose's multifunctionality [58]. These strategies have involved pioneering research involving mechanochemistry, pyrolysis, and chemical and biotechnology approaches. Each approach is uniquely tailored to achieve the desired properties in a cost-effective and energy-efficient manner. Various chemical valorisation approaches and their variations are also illustrated in Fig. 6.

3.1.1. Mechanochemical approach

The use of mechanochemistry has been much inspired by improving the atom economy, reactant dosage and energy efficiency of synthetic and valorisation procedures. Ball-milling has taken the centre-stage in agro-industrial LB valorisation and utilisation owing to its synergistic use of chemical reactions and mechanical forces to bring about simultaneous size reduction (nanocellulose preparation) and functionalisation of the cellulose microfibrils [66]. The mechanical forces are said to provide the necessary shearing forces that allow for a more profound hydrolysis and breaking of lignocellulose. The mechanochemical approach to valorising agro-industrial LB has been typically considered

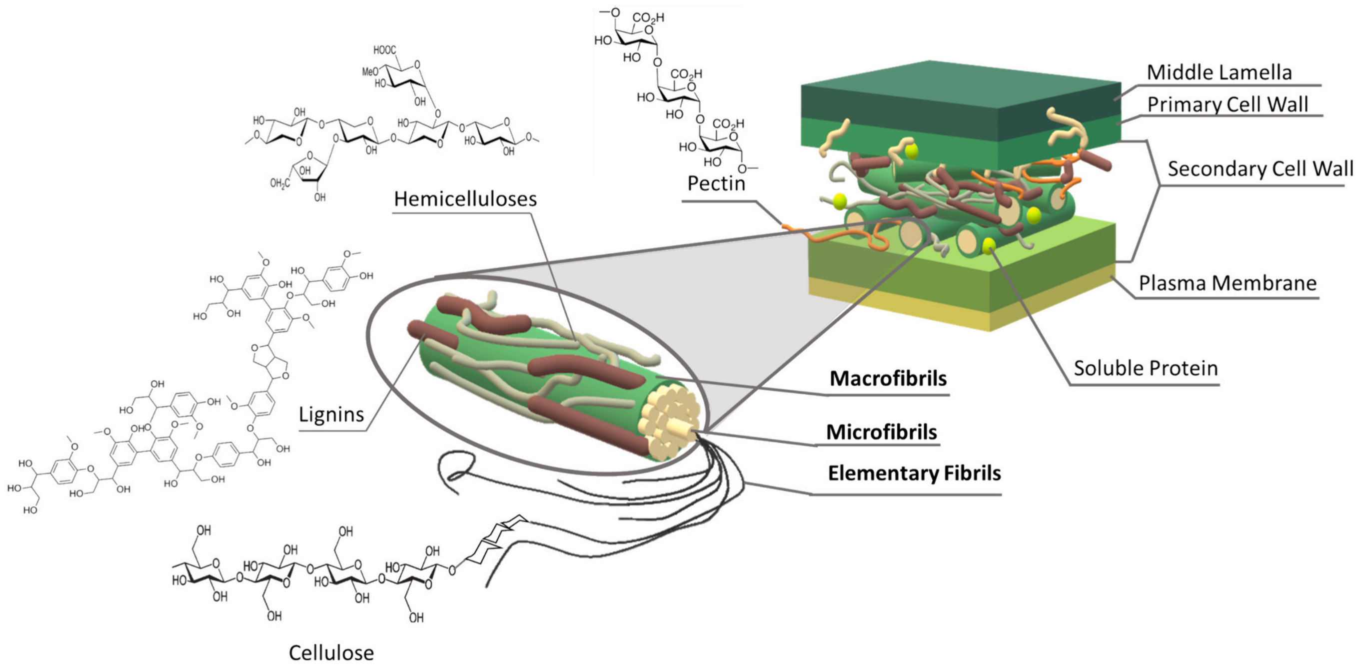

Fig. 2. Lignocellulosic arrangement and make-up of the plant cell walls and their components.

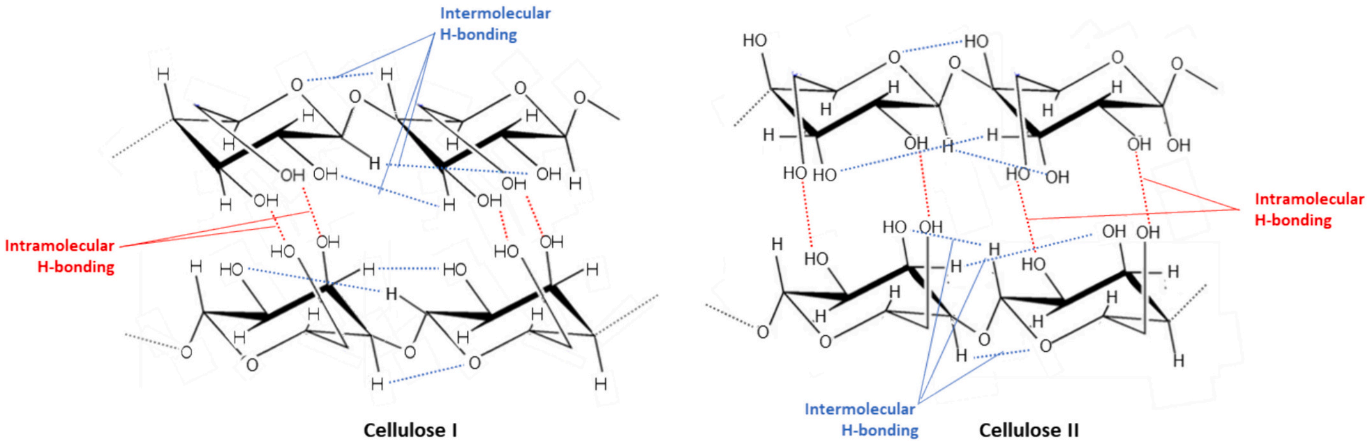

Fig. 3. Crystalline polymorphs of cellulose with the corresponding intermolecular (blue) and intramolecular (red) hydrogen bonding.

suitable for obtaining thermoplastic cellulose esters at a more improved efficiency [67]. Despite the known energy intensity of cellulose mechanical defibrillation, it is reportedly preferred owing to the capacity to handle the abundant lignocellulosic feedstock in a single run, *i.e.*, scalability. Abe [44] reported a mechanochemical method, *i.e.*, alkaline planetary ball-milling, of preparing regenerated nanocellulose with high crystallinity and high Young's modulus of 9.3 GPa. Ilyas et al. [68] mentioned a cellulose nanofibre preparation process using mechanical pre-treatment *via* ball-milling treatment, followed by a high-pressure mechanical homogenisation to defibrillate the cellulose fibres by shear and impact forces. The procedure yielded nanofilms of appreciable modulus from 59 to 121 MPa with a relatively higher degree of crystallinity of 81%.

The high degree of substitution (DS) - or rather the degree of esterification - with $C_{\geq 11}$ fatty acids yields thermoplastics with good film-forming characteristics and mechanical strengths that resemble commercial packaging films based on LDPE, HDPE and PS ([69]; Y. [70]). The chain length in this regard is pivotal in determining the FACE thermoplasticity. Hu et al. [71] mention a mechanochemical synthesis of cellulose esters of varying chain lengths in the presence of co-reactants like acetic anhydride. The later method refers to the acetic anhydride system used commonly as a green esterification reaction for preparing cellulose esters [72]. Hu and co-workers reported appreciable DS values for cellulose octanoate esters (2.04–2.41), cellulose laurate esters (1.80–2.07) and cellulose palmitate esters (2.07–2.27). The use of nanocelluloses derived from a mechanochemical reaction with organic acids such as oxalic acid yields thermoplastics with good crystallinity and thermoplastic characteristics, as Zhao et al. [73] described. Hou et al. [59] mentioned a solventless mechanochemical method for cellulose oleate thermoplastics using a ball-mill, with an appreciable degree of substitutions in the 1.29–2.55 range, with a high tensile strength value of 8.3 MPa for FACEs prepared at 400 rpm during 4 h, and a high glass transition temperature (T_g) ranging from 54 to 173 °C. By contrast, natural cellulose exhibits a T_g value of *ca.* 230 °C (amorphous regions) and melting temperature (T_m) at *ca.* 260 °C (crystalline regions). As substitution reactions (especially with hydrophobic components) imbue greater amorphousness to cellulose, it further lowers the T_g; making the cellulose derivative more thermally processable and thermoplastic. To this end, the DS is inversely related to the T_g of most cellulose derivatives [74]. Hu et al. [71] also mentioned the use of mechanochemical

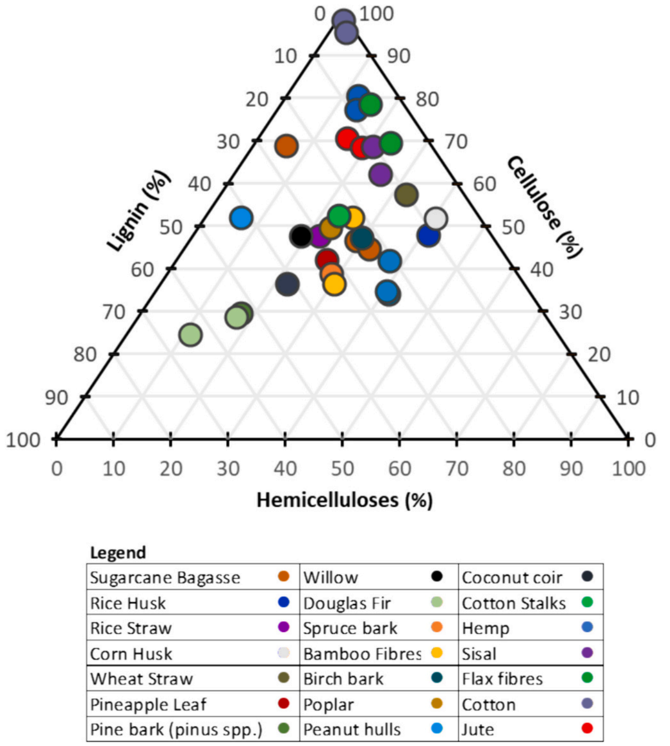

Fig. 4. Ternary diagram for cellulose, hemicelluloses and lignin distribution in various lignocellulosic feedstocks or raw materials. A dataset in per cent proportion of lignocellulosic content (extractive-free).

methods of esterifying nanocellulose, yielding high DS values in cellulose esters.

3.1.2. *Thermochemical and/or thermomechanical approaches*

Thermal approaches are key to deriving value-added sustainable materials form LW. Notably, the use of thermal approaches has been limited to the derivation of low-carbon solid and liquid fuels. However, pre-treatments of lignocellulosic materials have starred methods such as steam explosion, and fluidised fibre explosion techniques that aim to disrupt cell wall structure and enhance lignocellulose depolymerisation [75].

3.1.2.1. Steam explosion. Steam explosion utilises high temperatures ranging from 160 to 270 °C, and initial pressures of 20–50 atm [42] with a more rapid and severe breakdown of the glycosidic bonds achieved. The technique has been known to yield greater lignin-carbohydrate matrix fractionation, which can allow for more efficient packaging applications.

3.1.2.2. Fluidised fibre explosion. Alternatively, fluidised fibre explosion utilising liquid ammonia and supercritical-CO_2, have been utilised under high pressure (1.72–2.06 MPa) and temperature values (60–120 °C). The use of liquid ammonia promotes a more pronounced depolymerisation which can lead to a rapid lignocellulose biomass breakdown. Supercritical-CO_2 fluidised fibre explosion despite the relative similarity in terms of operability is greener [76]. It involves the dissolution of CO_2 under high pressure in water, leading to the formation of carbonic acid that can hydrolyse lignocellulose biomasses. The compressed supercritical-CO_2 is relatively less toxic, safer and non-flammable and easy to separate from the hydrolysate by depressurisation [42]. A major disadvantage associated with compressed supercritical-CO_2 is the cost of high-pressure equipment that could negatively impact cost-effectiveness and long-term operational sustainability.

The use of such explosion-based techniques has only proven practical for the derivation of nanocellulose from LBs. The resulting properties of the nanocellulose derived from the steam explosion are said to have a higher surface area [77,78]. This is a property that can allow for more efficient functionalisation and solvation for preparing packaging bioplastics such as FACEs or as self-supporting films by themselves. Anisotropic properties in the crystalline regions of the derived cellulosic material can lead to variations in crystallinity and polymerisation degrees that could, in turn, impact the filmogenic, mechanical and thermal properties of that material [79]. A higher aspect ratio and surface area of the nanocellulose are characterised by more elongated fibres [80]. These fibres can prove crucial to developing high-strength, ductile and flexible packaging films. The cellulose fibres obtained from thermal techniques such as those mentioned above are said to be more accessible for subsequent hydrolysis steps. Subsequently, the high-temperature treatment tends to transform lignin and facilitates the pyrolytic depolymerisation of LW [81]. The fluidised fibre explosion techniques are relatively milder, more merchantable, less energy- and cost-intensive than steam explosion.

3.1.3. *Chemical approach*

There exists a diverse range of chemical approaches to valorise LB, each with its unique capabilities to convert biomass into valuable bioplastics and biopolymers [42]. Chemical valorisation to date has featured acidic/alkaline hydrolysis methods, as well as peroxide-based hydrolysis methods, ionic liquids (ILs), and ozonolysis. There are also mechanochemical methods and thermochemical methods that have been discussed prior in Section 3.2.1 and 3.2.3. Oxidation-based methods are also popular in the chemical valorisation of LWs.

3.1.3.1. Acid hydrolysis. Hydrolytic methods are based on acid hydrolysis of lignocellulose wastes such as those based on the use of inorganic acids like 65%–86% H_2SO_4, 41% HCl, and 85% H_3PO_4. Acid hydrolysis methods have used dilute concentrations to allow for controlled hydrolysis of lignocellulose biomass into its components [82]. Acid hydrolysis has typically been conducted at temperatures around 60–70 °C, though procedures at elevated temperatures of *ca.* 130–200 °C have also been reported [42,83]. Further, the pressure has relatively been kept to atmospheric levels, although low-pressures have also been reported to significantly yield highly hydrolysed microcrystalline cellulose (MCC) and even nanocrystalline cellulose (NCC) - up to 100% hemicellulose hydrolysis [84]. While process cost-effectiveness could be improved by varying hydrolysis parameters, the use of strong inorganic acids has been known to incur low to medium yields, a greater likelihood of the over-hydrolysis of the lignocellulose into monomeric sugars and saccharides [84]. Quilez-Molina et al. [85] reported the use of mild acidic conditions using 1 M acetic acid for the hydrolysis of walnut shell lignocellulose at 30 °C for 24 h. Despite a high lignin content (60%), the thermoplastic films produced *via* blending yield materials with appreciable mechanical and optical properties. Walnut shell lignocellulose particle size was further reduced by *ca.* 25%; also leading to certain porogenic effects owing to hydrolysis of the holocellulose and slight delignification.

Acid hydrolysis however offers more rapid hydrolysis reactions with less residence time ($\leq$ 60–120 min), albeit at a greater risk of the loss of cellulose as monomeric sugars [86]. The use of inorganic acids has been historically popular owing to the availability of the chemicals, and their ability to cleave the cellulosic microfibrils and extract cellulose from the overall lignocellulosic biomass [87]. Liu et al. [88] reported the use of *p*-TsOH for acid hydrolysis of lignocelluloses, yielding microfibrils with low crystallinity values, but high lignin removal (>83.5–96.3%). Li et al. [89] mentioned the use of oxalic acid as a simultaneous hydrolysing and esterifying agent in a one-pot reaction. Oxalic acid provides for a mild green, solvent-free, biodegradable, highly recyclable and efficient hydrolysis (T. [90]), provided there exist apparent concerns regarding its toxicity and health hazards over long periods of exposure to its powder

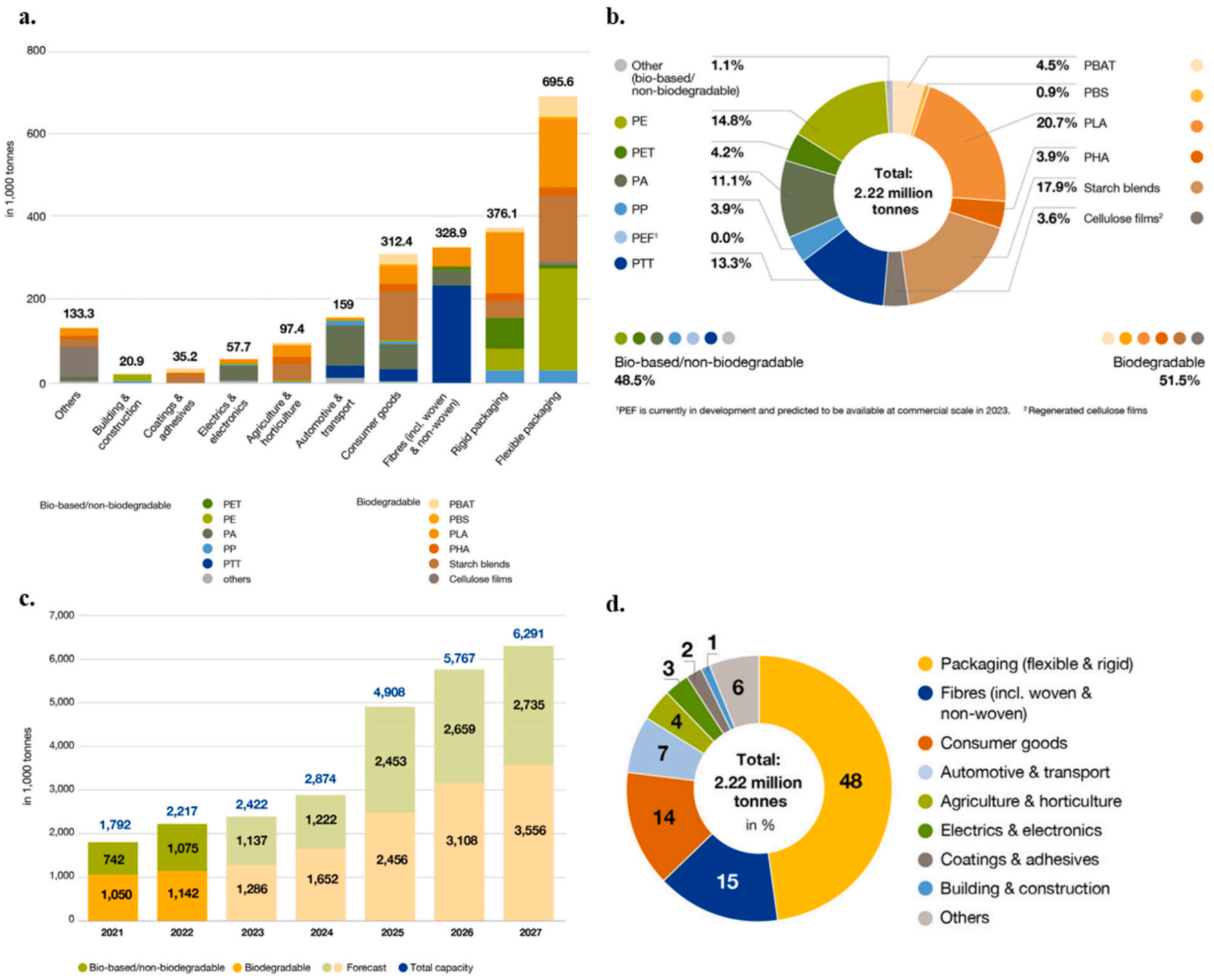

Fig. 5. Global production capacities of bioplastics by: a. Material types in market segments, b. Material type by share c. Material type by production, and d. Market segmentation. Adapted from a – b European Bioplastics [56] and c – d European Bioplastics [54].under Creative Commons Licence CC BY NY.

form. The reaction conditions involved a solvent-free system where the lignocellulose (softwood dissolving pulp) was mixed with molten oxalic acid dihydrate at 110 °C for 30–60 min at optimum. The cellulose oxalates formed were individual rods as compared to fibrils; having an aspect ratio of L/W of 9.35 to 11. Transparent films were prepared by solvent casting that indicated high polarizability, a 68% - 71% degree of crystallinity and better yields than other acid hydrolysis methods (81% *vs.* 30–50%) [5].

3.1.3.2. Alkaline hydrolysis and alkaline peroxide hydrolysis. Alkaline hydrolysis and alkaline peroxide hydrolysis, in comparison, have emerged as promising methods for lignocellulose valorisation, particularly for deriving cellulose-based materials suitable for sustainable packaging applications ([82,91,92]1 M NaOH or 1 M KOH at elevated temperatures facilitates the disruption of lignin-hemicelluloses bonds, resulting in the selective extraction of cellulose [93]. Alkaline hydrogen peroxide (AHP) hydrolysis, incorporating H_2O_2 as an oxidative agent, has garnered attention for its ability to enhance the delignification efficiency, thereby yielding cellulose with improved purity and crystallinity [94]. The use of NaOH/H_2O_2 leads to the swelling of the lignocellulosic fibres that improve the intercalation of the hydrolysing hydroxide ions (OH^-) and the hydroxyl radicals ($OH^\bullet$). These are optimally generated at pH 11.5. AHP hydrolysis at 5%–7% H_2O_2 concentration after conventional alkaline hydrolysis led to the production of cellulose with enhanced tensile strength and thermal stability [95,96]. This provides biopolymer material that is a viable candidate for sustainable packaging materials with superior mechanical properties. A transesterification approach for preparing FACEs has also been reported by Cao et al. [97], who utilised an aqueous DMSO/NaOH (20 g/L NaOH) and DMSO/KOH system to prepare cellulose acetate, propionate and butyrate with high DS (2.14–2.34) in 5 min at room temperature and, then, at 100 °C to initiate the transesterification process.

Temperature considerations for AHP hydrolysis are similar to acid hydrolysis (*i.e.*, 60–70 °C) and elevated temperatures are rarely attempted as such parameters could lead to over-hydrolysis and loss of valuable cellulose [98]. Residence times are also between 60 and 120 min with yields as high as 73.7% [99,96]. Song and Othman [100] reported the use of AcOH-H_2O_2 aqueous system (1:2) in the AHP bleaching process instead of the conventional H_2SO_4-H_2O_2 aqueous system for crude (microcrystalline) cellulose preparation from oil palm long dried fibres, where the use of AcOH allows for a greener, industrially viable and safe bleaching/delignification process. The use of chemical hydrolysis for lignocellulose biomasses has significant impacts on the microstructure of the cellulose fibres that would be extracted using the method, leading to lower fibre aspect ratios (<15), high cellulosic degree of crystallinity of 81–90% with a high T_g value of 198 °C considering low amorphousness. Often strengths and barrier performances are observed for the hydrolysed cellulosic materials which, if used in sustainable packaging, may lead to unviable applications [101,102].

These approaches are relatively greener and softer than acid hydrolysis methods and do not incur significant saccharification/glycolysis of the cellulose extracted. Further, the yield and purity of cellulose

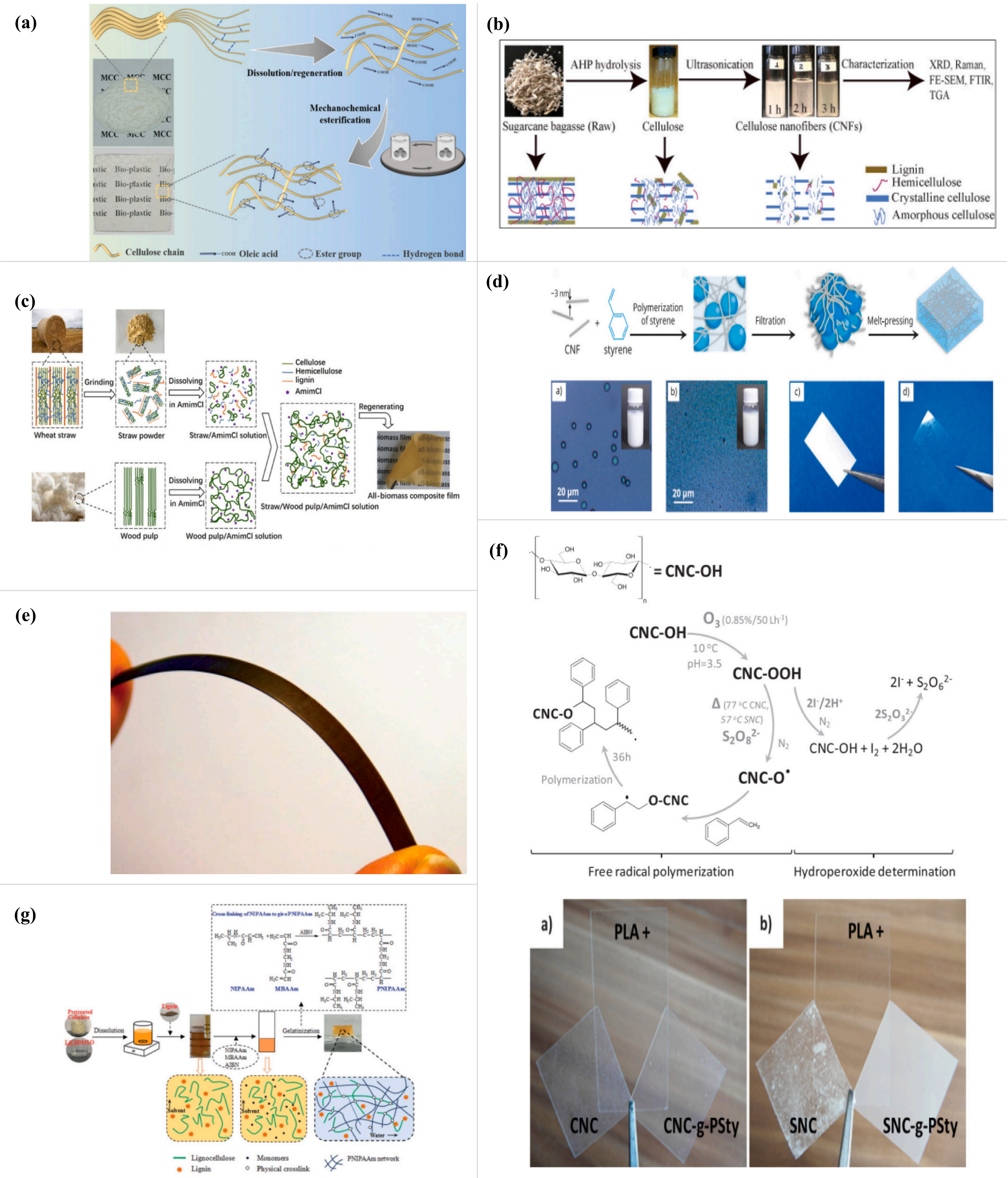

Fig. 6. Overview of various LB valorisation approaches for potential or intended packaging applications. (a) Mechanochemical V/U approach, (b) AHP-derived lignocellulosic material for potential packaging use, (c) Straw-based biomass film preparation using AmimCl system, (d) TEMPO-oxidised cellulose/PS blend packaging films, (e) Ozonolysis-derived NFC packaging films, (f) AX composite films developed from thermo-processed AXase material, and (g) EDA-complexation-derived lignocellulose composite hydrogels. Source: Fig. 6a reproduced from Hou et al. [59], with permission from the Royal Society of Chemistry. Fig. 6c, d and f reproduced from Li et al. [60], Fujisawa [61], and Espino-Pérez et al. [62], respectively; with permissions. Fig. 6e and g from Akkus et al. [63] and J. Xia et al. [64], respectively under Creative Commons Attribution-NonCommercial 3.0 Unported Licence. Fig. 6c, © Shahi et al. [65], published by MDPI, 2020; with permission.

obtained from various lignocellulosic sources using alkaline or AHP hydrolysis are relatively higher [95]. Often alkaline and AHP hydrolysis are used in tandem with repetitions to improve the quality and functional performance of the extracted cellulose [37,65]. However, both approaches exhibit certain drawbacks, including high energy consumption in the case of alkaline hydrolysis and potential health and safety concerns though the use of H_2O_2 is relatively safer in comparison.

3.1.3.3. Ionic liquid extraction (ILE). Ionic liquids (ILs) have gained considerable attention as effective solvents for the extraction of cellulose from LB, offering a promising avenue for sustainable packaging materials. Notably, the use of specific ILs, specifically methylimidazolium acetate derivatives such as 1-ethyl-3-methylimidazolium acetate (EMIMAc), has demonstrated high efficiency in cellulose dissolution at moderate temperatures [103]. The significance of reaction parameters, including the EMIMAc concentration (*e.g.*, 10–15% *v*/v) and temperature (*e.g.*, 120–140 °C), in facilitating the selective extraction of cellulose with high purity (>90%) [104,105]. The derived cellulose exhibited remarkable properties, such as improved crystallinity and thermal stability, as observed in various studies, positioning it as a promising candidate for sustainable packaging materials with enhanced mechanical strength and barrier properties [106,107]. However, challenges such as high costs, energy-intensive processes, and the need for extensive solvent recovery systems underline the necessity for further optimisation and cost-effective strategies to facilitate the widespread utilisation of ILs in cellulose extraction [108].

Notably, IL recovery *via* fractional distillation requires the use of volatile co-solvents (*e.g.* acetone, EtOH, and MeOH) to compensate for the low vapour pressure [109]. The co-solvents both extract ILs and regenerate the extracted cellulose. Additionally, entrapment of residual ILs can occur with the amorphous cellulose regions which can lead to a plasticising effect in these disordered regions [110,111]. Extraction yields for the regenerated cellulose can further vary from one lignocellulosic feedstock to the other, as demonstrated by Carmichael et al. [110]. Earle et al. [112] demonstrated that ILs could be distilled more efficiently under low pressures and high temperatures; which would imply the use of vacuum conditions and greater inputs – increasing the cost of production. Such challenges could prove relatively unsuited for marketable sustainable packaging applications if not adequately optimised.

A transesterification using vinyl laurate and hemicelluloses was reported in EMIMAc at 80 °C for 1 h. The hemicellulose laurate films were produced possessing high hydrophobicity, mechanical strength (34 MPa), high water vapour permeability (WVP) values of 3.21×10^{-2} to 4.51×10^{-2} g/(m^2·d) and high oxygen permeability (OP) coefficient value of *ca.* 0.011 cm^3·cm/(m^2·s·Pa) [113]. Li et al. [60] reported the use of 1-allyl-3-methylimidazolium chloride (AMIMCl) for preparing wood/straw lignocellulose films with high tensile strength (62 MPa), high UV resistance, and low degree of crystallinity (33%). Suzuki et al. [114] mentioned the preparation of FACEs from sugarcane bagasse lignocellulose and mixed acyl groups (1:4 decanoyl/acetyl) *via* a one-pot, two-step homogenous IL-assisted transesterification reaction. The IL systems used were EMIMAc/DMSO and the transesterification occurred under an inert atmosphere using vinyl decanoate at 80 °C for 30 min and, then, with isopropyl acetate at 80 °C for 30 min. The corresponding polysaccharide acetate/decanoate was injection-moulded at 205 °C despite the high molar mass value of $1.5 \cdot 10^6$ g/mol; indicating sufficiently high tensile and flexural strengths of approximately 50 and 80 MPa, respectively, and with low degree of crystallinity. The degree of crystallinity amounted to *ca.* 80% for cellulose oleates prepared at 50 or 100 °C for 4 h to 24 h. Lease et al. [115] reported an IL-assisted mechanochemical cellulose oleate preparation using *p*-TsCl and 1-butyl-3-metylimidazolium acetate (BMIMAc). The reaction system involved kneading in a magnetic mortar at 150 rpm for 1 h, followed by the addition of *p*-TsCl at 50–100 °C for 4–24 h. The DS obtained varied from 0.001 to 0.210, where increasing DS corresponded with the retention of Cellulose I despite a loss in crystallinity amounting to *ca.* 5.7% on average relative to MCC.

3.1.3.4. TEMPO oxidation. TEMPO (2,2,6,6-tetramethylpiperidine-1-oxyl)-mediated oxidative chemical valorisation involves the selective extraction of cellulose from LB, holding significant potential for sustainable packaging materials [116]. Notably, the use of TEMPO-mediated oxidation, in combination with sodium bromide (NaBr) and sodium hypochlorite (NaClO), has been shown to effectively facilitate the conversion of lignocellulose into cellulose nanofibrils. Research by Isogai et al. [117] emphasized the critical role of reaction parameters, including the TEMPO loading (*e.g.*, 0.5–1% *w*/w) and reaction time (*e.g.*, 2 h to 4 h), at pH = 4.8, with(out) NaClO, NaBr or other oxidants, in achieving high yields of cellulose nanofibrils with uniform dimensions and excellent mechanical properties [117,116]. Aspect ratios are also reportedly high with TEMPO-oxidised celluloses (60–100) (M. [118]). The resultant cellulose exhibited enhanced tensile strength and improved thermal stability, as evidenced by studies conducted to date [119], highlighting its potential for sustainable packaging applications requiring robust and thermally resistant materials. Fujisawa [61] reported the use of TEMPO-oxidised nanofibrilliated cellulose (NFCs) in *in-situ* polymerisation with PS. The process yields shelled nanoparticles with an average diameter of 3 μm, with a NFC coating of 8 nm thickness. The resulting sheets were initially opaque and later complete transparency due to a post-heat-treatment at 160 °C for 30 s. The tensile strength of the NFC/PS films was 50 MPa. Fibre diameters from this process were relatively narrower, *i.e.*, 5.6 ± 1.5 nm with a moderate crystallinity value of 55%. The loss in crystallinity degrees and shortening of fibre lengths in NFCs as opposed to CNCs owes to the increase in the amorphous regions of the NFCs (*i.e.* loss of Cellulose I structure) owing to the surface modification. Papers prepared from TEMPO-oxidised celluloses from lignocellulose wastes have a relatively higher tensile strength than their neat cellulose counterparts [120]. However, challenges such as the need for precise control of oxidation conditions and potential environmental impacts of chemical reagents underscore the importance of further optimization and eco-friendly alternatives in TEMPO-mediated oxidation for sustainable packaging materials. Though, much progress has been made in developing recyclable and greener TEMPO derivatives such as Tempol (4-hydroxy-TEMPO) and polymer-supported TEMPO-based oligomeric catalysts such as Oxynitrox S100, Merrifield's TEMPO-functionalised PS resin, and silica-supported TEMPO (Silicat TEMPO) [121].

3.1.3.5. Ozonolysis. Ozonolysis acts *via* strongly exothermic electron-rich components in lignocellulose such as lignin than the carbohydrates [122]. These have been defined by near-ambient operation conditions with reaction times of *ca.* 1–2 h, with temperatures *ca.* 0–40 °C using 4–6% and 26% w/w ozone, depending on the plant source of the LB [123,124,125]. Solvent-based ozonolysis has been used to depolymerise lignocelluloses for obtaining biopolymers suited for blending with petroleum-based polymers. For instance, Espino-Pérez et al. [62] applied ozonolysis to microcrystalline cellulose (MCC) and starch for tandem hydrolysis and *in situ* grafting with PS in a 1.56 styrene/glucose unit ratio for starch and 0.25 for crystalline nanocellulose (CNC). The properties of the novel blend cellulose-*g*-PS and starch-*g*-PS nanocomposite films have controllable lower WVP values of 1.85×10^{-1} g/(m^2·d·Pa). Higher contact angles further indicate greater hydrophobicity. Fibre lengths achieved with the ozonolysis-grafting polymerisation led to CNCs with 92 ± 61 nm length, while 53 ± 9 nm for starch nanocrystals. Thermal stability was higher than 100 °C (*i.e.,* T_g for PS) for both grafted cellulosic biopolymers. While ozonolysis is generally considered environmentally friendly, there are substantial requirements for safety and hazard reduction with its use on pilot-scales. Further, the use of ozonolysis, incurs a considerable cost (0.135 €/kg) and high energy demand, dedicated maintenance and reactor design features that reduce the viability of this valorisation/pre-treatment approach in contrast to other methods [122]. Few studies such as the above-mentioned exist regarding the use of ozonolysis for developing grafted biopolymers [62,122]. The use of ozonolysis has predominantly been associated with a pre-treatment method, setting the stage for subsequent enzymatic hydrolysis to yield glucose, organic acids and EtOH.

3.1.4. Biochemical/enzymatic approach

Martínez-Abad et al. [126] mentioned the use of various enzymes that are proving competitive and often much more lucrative than conventional oxidative, mechanical and chemical-based methods for lignocellulosic hydrolysis. The authors indicated that enzymatic treatments occur at milder conditions (pH 4.0–7.0; 50–60 °C), though a pre-treatment stage is usually required to increase the accessibility of the glycosidic bonds in lignocelluloses for the enzymes. Pre-treatments are typically alkaline, acidic or AHP hydrolysis; aim to fractionate the lignocellulose by removing lignin [39,40,52]. The use of carbohydrate-active enzymes (CAZymes) is a key aspect of ongoing research in biochemical lignocellulosic hydrolysis, featuring the use of diverse enzymes and their families for transesterification, synthesis and depolymerisation of the lignocellulose [127]. For instance, glycoside hydrolases (GH) such as endoglucanases, carbohydrate esterases (CEs), glycosyltransferases (GTs), lytic polysaccharide monooxygenases (LPMOs) and lignin-degrading enzymes [128] have generally considered to optimal in terms of sustainability and control of the morphology of the derived nanostructures, often better than chemical methods.

The use of enzymes such as xyloglucanases (XyG; a GH-type) allows for the fine-tuning of the degree of polymerisation, the molecular weight and likely the filmogenicity of cellulosic nanofiber films derived from lignocellulosic polysaccharides [126]. Such films possess higher oxygen barrier properties and mechanical strengths. The thermal properties of XyG-derived films increase as shown by the high T_g value of 245 °C for such materials which limits their use in thermal processing [129,130]. Often chemical crosslinkers have been used to increase packaging films of optimal mechanical strengths using glyoxal and zircomium (IV) carbonate complexes $[Zr(CO_3)_4]^{4-}$ [131]. Laccases can also act as crosslinkers by themselves and can link lignin moieties with each other, thereby improving polymer strength [132]. Notably, the recyclability of such materials reduces with increasing crosslinking, and barrier properties also increase with loss of free volume of the amorphous material with increasing cross-linking.

The filmogenicity of low molecular weight hemicellulose extracts from the enzymatic hydrolysis by arabinoxylanases (AX) and glucogalactomannanases (GGM) has not yielded optimal results as with XyG [126]. Such lignocellulosic extracts are blended with other cellulosic materials such as microfibres, nanofibers and bacterial cellulose [133]. The presence of salts and the water sensitivity of lignocellulosic polysaccharides affect the capacity and efficiency of enzymatic, as well as chemical hydrolysis [134]. As hemicelluloses possess high moisture susceptibility, the plasticisation is impacted leading to sub-optimal mechanical and barrier properties. AX films could be produced *via* thermo-processing at 90 °C, at an annealing of 1 h and ambient conditioning for a week [63]. The mechanical strength of thermo-processed AX bioplastics is relatively higher than most films produced by solvent casting [126]. Debranching has also been known to increase thermal stability while reducing the water sensitivity of such films [135]. As enzymes (such as laccases) are highly specific functionalities, their use could be leveraged in grafting-type syntheses onto the cellulosic surfaces, such as that reported by Wei et al. [136].

3.1.5. Advances in other approaches and processes (hybrids and tandem approaches)

3.1.5.1. Cellulose-based composites and blends with petroleum-derived commodity polymers. Cellulose research has much focused on the blending of the material with existing high-performing yet less sustainable materials and to imbue further optimisation of their functionalities. To this end, (ligno)cellulose nanofibers have found much use in blending applications with many renewable biomass-derived biopolymers such as poly(lactic acid) (PLA), cellophane (CP) or cellulose acetate (CA); petroleum-derived polymer recyclates such as rPET; and petroleum-derived biodegradable polymers such polycarbonate (PC), poly(glycolic acid) (PGA), poly(hydroxyalkanoate)s (PHAs) like poly(3-hydroxybutyrate) (PHB) and poly(3-hydroxybutyrate-*co*-3-hydroxyvalerate) (PHBV) [137,138,139,140]. The use of nanofibrilliated starch and nanofibrilliated cellulose (NFC) has been well-reported to improve the barrier, biodegradability and mechanical performance of PHBV, PHAs and PLA [86,141]. Though the blend compositions contain up to 3–5% of NFCs or particles by polymer weight percentage (Wu et al., 2019), the blend composites are more suited for short-term commerciality and market viability for sustainable packaging [138]. Blending has also involved the use of the fruit or soy-based biomasses directly with cellulosic materials such as starch to obtain packaging films, with high tensile strength (8.20 ± 0.02 MPa), excellent water resistance, and low moisture permeability (50 g/m^2/day) [142,143].

The blending of other thermoplastics with lignocellulose or cellulose is predominantly focused on fine-tuning more hydrophilicity or hydrophobicity of the base polymer material for the particular bioplastic application [144]. For instance, lignocellulose nanofibers were blended with polycaprolactone (PCL) *via* electrospinning to improve their functional performance in biomedical applications which could potentially prove viable for packaging owing to the improved strength, thermal stability, and biodegradability [145]. Additionally, blending with other biopolymers that are in commercial use, such as PLA; increases thermoplasticity and hydrogen bonding between lignin, holocellulose and xylans, *i.e.*, higher strength [146]. Despite the inclusion of a newer material into the materials design, the blending with lignocellulosic nanofibers reportedly lowers downstream processing costs for performance optimisation and enhancing the lifecycle of the thermoplastic [138]. The introduction of lignocellulose biopolymer with poly (butylene adipate-*co*-terephthalate) (PBAT) led to significant enhancement of the polymer film's UV-resistance and improved barrier properties [147,148].

3.1.5.2. Other esterification & surface functionalisation approaches. In addition to the various transesterification techniques that have been discussed prior in Sections 3.2.3., certain other surface functionalisation and transesterification procedures have also been discussed as follows. DMAc/LiCl, NMMO, Py/TsOH and DMSO-TBAF, as well as the various ILs mentioned prior, have been typically used for esterification-related surface modifications of cellulose with cellulose ester yields ranging from 77 to 86% with a tuneable degree of crystallinity, DS values of 1.0–2.5 and improved hydrophobicity [5,69]. Innovative approaches such as that of Onwukamike et al. [149] performed cellulose and fatty acid ester grafting (FACE synthesis) using a DMSO-CO_2/1,8-diazabicyclo[5.4.0]undec-7-ene (DBU) switchable solvent system with high oleic sunflower oil; in a purged esterification system at 115 °C for 24 h. DS achieved ranged from 0.34 to 1.59, with improved thermal stability up to 360 °C and high elastic moduli up to 478 MPa and a maximum stress value of 22 MPa.

Tedeschi et al. [6] reported a transesterification of cellulose acetate with oleic acid in a mixed anhydride system that is proving to be popular owing to its higher recyclability, reaction efficiency and formation of cellulose acetate with the FACE that imparts greater mechanical strength. Tedeschi et al. [6] used TFA/TFAA-$CHCl_3$ system at 80 °C for

30 min, leading to 76% decrease in WVTR from 670 g/(m^2·d) to 2800 g/(m^2·d) and 90% decrease in OTR values from 105,000 cm^3/(m^2·d) to 10,200 cm^3/(m^2·d) of the cellulose acetate/oleate films in comparison to acetate ones. Stress at break was lower for the former, *i.e.*, up to 6.6 MPa with greater elasticity as shown by the elongation at break by 14.4%. A higher degree of crystallinity led to a lower T_m of 63 °C for the former material in contrast to that for the latter, though similar to PCL (64 °C) and PEO (66 °C). Water uptake was lower for cellulose acetate/oleate films up to 16 mJ/m^2 *vs.* CA's 45 mJ/m^2. Heredia-Guerrero et al. [150] reported the use of the mixed anhydride system to prepare FACEs using aleuritic acid (*rel*-(9*R*,10*S*)-9,10,16-trihydroxyhexadecanoic acid), yielding relatively similar results with DS values of 0.51–2.60, stress at break of 3 MPa, and a T_g value of −17 °C.

Kulomaa et al. [151] reported a FACE synthesis using hydrochlorinated tail oil fatty acids (TOFA) in a modified Py/$CHCl_3$ esterification system. The thermal stability improved, ranging between 7 and 22 °C after certain modifications were made. The measured T_g values were relatively low, falling between 104 and 119 °C. The maximum strain, which could go up to 101%, and the elastic moduli, between 30 and 50 MPa, were found to be similar to those seen in commercial products. The FACE films exhibited high WVTR, with values from 21.65 to 22.35 g./(m^2·d) - comparable to low-density polyethylene (LD-PE), *i.e.*, 20 g/(m^2·d) - and OP of *ca.* 2.95 × 10^{-9} to 4.51 × 10^{-9} cm^3 cm/(m^2·s·Pa). Moreover, partially hydrogenated fatty acids led to higher WVTR values in the FACE films, *i.e.*, 43.4 g/(m^2·d).

3.1.5.3. Hydrolysis and nano-defibrillation. Research also reports the use of metal chloride pre-treatment such as $CuCl_2$, $AlCl_3$, and $FeCl_3$ before the AHP hydrolysis to further facilitate hydrolysis and cellulose nanofibrillation. The process occurred in tandem with a biochemical/enzymatic saccharification and cellulose nanofibrillation method. The reported process removed lignin on the fibre surface and produced lignocellulose nanofibers with thin diameters between 9 and 25 nm [152]. The degree of crystallinity was reportedly highest with $CuCl_2$ pre-treatment, *i.e.*, around 52%.

Rampazzo et al. [153] mentioned the use of persulfate-based hydrolysis of cotton linters and kraft pulp to extract nanofibrillated celluloses (NFCs) using $(NH_4)_2S_2O_8$, which is known for its oxidative power and water solubility. The resulting NFCs were blended with virgin PET to yield high O_2 and CO_2 barrier films with diffusion coefficients being 8–10 times lower than PVA and 50–60 times lower than PVDC. NFC lengths were 130–170 nm with high polydispersity indices, with thermal stability up to 369–388 °C. Guo et al. [154] reported the use of conventional soda/anthraquinone (soda/AQ), sodium salicylate hydrotropic and organosolv to extract lignin and cellulose for preparing composite films for packaging. Their research revealed higher antioxidant activities of the cellulose/lignin films derived from organosolv and soda/AQ; owing to the higher amount of phenolic hydroxyls retained in contrast to other methods such as hydrotrope, kraft and DES (lactic acid and betaine). Xia et al. [64] reported the preparation of thermo-sensitive lignocellulose composite hydrogels using a semi-interpenetrating network (sIPN) reagent *N*-isopropylacrylamide (NIPAM). The lignocellulose was prepared from ethylene diamine (EDA) complexation in the LiCl/DMSO solvent system. The prepared hydrogel/film possessed a rapid conversion capacity from hydrophobic behaviour at 20 °C to hydrophobic behaviour at 45 °C.

Kwon et al. [155] reported the preparation of lignocellulosic nanofibrils from pine-based LWs *via* a two-step microwave-assisted reaction. The said reaction was characterised by its use of a DES (ChCl/LA) pre-treatment and high-pressure homogenisation (1361 atm). Reaction parameters for the DES pre-treatment were as high as 110–130 °C, followed by a 110 s microwave-assisted nanofibrillation with excellent lignin removal (70%) and hemicellulose extraction (90%). Lignocellulosic nanofibrils pre-treated at 110 °C demonstrated 2 times more optimal tensile strengths (137–155 MPa) than the microwave-assisted nanofibrils, as well as high thermal stabilities (310 °C). The films produced were hydrophobic and had UV-shading capacities (highest for lignocellulosic nanofibrils pre-treated at 110 °C). Microwave-assisted reactions yield inefficient nanofibrillation without DES pre-treatment with diameters of 60–90 nm with degree of crystallinity values near 64–70%. This contrasted with 6–60 nm diameter and a degree of crystallinity of 65–69% for those that were pre-treated at 110 °C. Ballesteros et al. [156] mentioned the use of an electric pulse field-induced hydrolysis process for lignocellulose hydrolysis. Reaction conditions for this novel electrochemical method involved 5–20 kV/cm, and short pulse times (100 μs) at room temperature. The electrochemical processing technique ruptures cell walls, exposing cellulosic microfibrils for subsequent hydrolytic reactions.

3.2. Developments in process design for the development of lignocellulosic biopolymers for sustainable packaging

3.2.1. Lignocellulosic material processing designs

Process intensification, cost reduction and effective optimisation are key considerations for the mass manufacture and industrialisation of any material. Particularly, for cellulosic materials, the associated with the polymer shaping, solution chemistry and material synthesis considerations, *e.g.*, inclusion of additives and performance enhances, lead to costs greater than contemporary fossil fuel-derived plastics [157,158]. Extensive need for chemical modification to control moisture retention, barrier properties, and thermal and mechanical behaviour of the prepared cellulose packaging films has most often led to poorer trade-off between cost, performance and environmental footprint [159,160]. However, complexity in both materials design and packaging preparation has significantly progressed since the 2010s, though much progress still remains to improve the lignocellulosic or lignocellulosic-derived packaging material's end-user performance across its lifecycle, as well its cost-effectiveness and sustainability.

3.2.1.1. Developments in in situ polymerisation reactors – Types and systems. *In situ* polymerisation has been attempted *via* various valorisation and post-valorisation modification routes such as those described earlier. The rationale of such systems is to yield versatile lignocellulosic or lignocellulose-derived materials that provide for improved mechanical, thermal, functional and barrier properties than their predecessors. Current proof-of-concepts for such systems aim for convenient, one-pot preparation of packaging materials [2,114]. For instance, *in situ* polymerisation is typically associated with blending preparations for packaging materials; involving simultaneous hydrolysis of the lignocellulose, and the subsequent cross-linking or grafting with aromatic or electron-rich polymers.

As discussed previously, Espino-Pérez et al. [62] utilised an *in situ* ozonolytic and graft polymerisation process according to their proposed two-stage synthesis method for cellulose-g-PS and starch-g-PS composite films. Their process featured the use of an electric discharge ozone generation in a 2% *w*/w sodium acetate (NaOAc) bath at pH 3.5. The ozonolysis temperature was kept at 10 °C using 0.85 wt% of ozone (O_3) at 50 L/h. The use of O_3 further allowed for conducting a subsequent persulfate-assisted free radical polymerisation under an inert atmosphere in a conventional stirred glass reactor at 57–77 °C for 36 h. A continuous stirring reactor system was also employed by Sain et al. [161] where jute-derived cellulose-g-PMMA composite films were prepared in a PVOH-assisted suspension polymerisation (6% w/w to MMA) with 10% w/w CNPs at 85–90 °C for 5 h. The composite prepared from the *in situ* method yields more thermo-resistive composites (T_m = 125 °C).

Wang et al. [147,148] mentioned an aqueous one-pot synthesis featuring a laccase-assisted (Metzyme) oxidation and *in situ* polymerisation reaction between MCC and lignin extracted using a sequential $C_{1–3}$ alcoholic (*i*-PrOH, EtOH and MeOH) fractionation. The processing featured the use of a mechanically-refined (milled) bleached Kraft birch pulp, then high-pressure homogenisation at 100 atm per pass that was followed by incubation with the laccase for 39 °C with ambient air circulation under gentle agitation (400 rpm). The thermal properties featured T_g values of *ca.* 89–162 °C for the birch- and 78–161 °C for the spruce-lignin/MCC composite films, respectively. Birch-derived lignin/MCC composite films had relatively higher mechanical strengths, *i.e.*, up to 92 MPa. The authors found that the *in situ* polymerisation was more prominent in the birch lignocellulosic material, where a homogenous coating of lignin nanoparticles was observed within <40 nm of the MCC network.

Oliaei et al. [162] reported a process using bleached fibres and the MCC derived from spruce pulp in an *in situ* polycaprolactone (PCL) oligomer synthesis. The authors reported the use of a glycerol-assisted ring opening polymerisation with end-capping with succinic acid. The resulting ε-PCL succinate was dissolved and allowed to impregnate the MCC (size <100 nm) after which the *in situ* polymerisation was initiated in the presence of $Sn(Oct)_2$ at 140 °C for 14 h. Thermoplastic homopolymer sheets were prepared *via* hot-pressing at 1 MPa pressure and 60 °C for 3 min. The sheets had high mechanical strengths of up to 82 GPa for 77% w/w hot-pressed spruce fibre/PCL composite for a 50.7% degree of crystallinity and 62 GPa for a 20% degree of crystallinity for a 50% MCC/PCL composite. Interestingly, Oliaei et al. [162] showed that lignin-containing wood fibres/PCL composites (as much as 16% lignin) can have improved performances than MCC/PCL composites. ε-PCL in the lumen region of the wood fibres or bonding with residual lignin could have led to increased mechanical strengths for such films [163].

3.2.1.2. Developments in torrefaction and percolation reaction systems. Berthet et al. [164] reported the use of a solvent-free torrefaction pretreatment for the functionalisation of cellulose and subsequent melt-extrusion with PHBV to produce filler composites. The torrefaction process used a horizontal tubular oven and later with an oven-heated medium-sized reactor both with an N_2 sweeping setup (to purge O_2). This allows for rapid defibrillation and lignin depolymerisation at optimal levels before charring and holocellulose breakdown [165]. The sample treatment involved gradual incremental changes to the temperature by a cold-hot-cold regime for 45 min at 230 °C. The torrified MCC fibres were subject to melt-extrusion with PHBV pellets using a twin-screw compounder at 160–180 °C at 300 rpm using a rod die. The composite pellets were thermo-compressed at 170 °C and 150 atm for 5 min to obtain composite films. Torrified fibres had greater aspect ratios (28 × 2.2 μm at 230 °C) and higher hydrophobicity (contact angle values of 115–117° as opposed to 28–38°). The colour of the wheat fibres darkened due to hemicellulose breakdown, and the thermal properties remained relatively unchanged at *ca.* 115–119 °C with a degree of crystallinity of 60–64%. The torrefaction process yielded an increased WVTR of 7.3–15.7 $g/(m^2{\cdot}d)$ for a 3:10 w/w wheat MCC/PHBV composite. Higher permeation was attributable to the percolating effects of the N_2-swept thermal treatment, and better fibre/matrix adhesion despite little impact on mechanical strength.

3.2.1.3. Developments in continuous reaction systems. Continuous stirred tank reactors (CSTRs), particularly batch or semi-batch configurations, are a common configuration employed concerning the lignocellulosic valorisation and modification techniques employed for lignocellulosic functional materials [166]. Their use, as Ballesteros et al. [156] mentioned, is typically confined to the lab- to mid-scale pulping, and acid/alkali or enzymatic hydrolyses. Said reactors are often pressurised, and operate typically between 40 and 170 °C and from short to moderate reactor residence times depending on the type of technique employed. Current innovation has often featured the use of higher pretreatment temperatures to reduce the energy input downstream, *i.e.*, in the subsequent hydrolysis step [167]. This typically boosts wet oxidation and improves lignocellulosic breakdown to yield higher lignin quantities and holocellulose.

Birch [168] mentioned the use of liquid foam reactors (LFRs) for handling value-added foams and transporting solid particulates. Birch's research concerned the synthesis of 2,5-furandicarboxylic acid (FDCA)-based blend polymer precursors from lignocellulose breakdown products such as hydroxymethylfurfural (HMF). LFRs feature the use of flow polymerisation for a reportedly higher temperature and mixing control. Continuous flow reactors such as the LFR also possess a higher economic viability potential. The LFR featured the use of an *in situ* peroxyacetic-induced enzymatic hydrolysis and polymerisation reaction using CAL-B (*Candida antarctica* lipase); with high selectivity at 95%. Birch [168] reported various reactor configurations for the continuous flow polymerisation process involving: (i) CSTR (Fig. 7d)., (ii) coiled tube setting, (iii) tubular setting, (iv) tube-in-tube sparging setup, and (v) cross-piece *cum* tubular setting. Of these five LFR configurations, the CSTR configuration outperformed the other configurations as it demonstrated efficient capability for particulate transport, temperature control and lower mass balance losses. Solid build-up and finer foam were produced by the CSTR/active mixing with residence times up to 1–10 min, and enzymatic activity was also better retained. (See Fig. 8.)

Bondancia et al. [180] reported the use of a parametrically-modified CSTR for the enzymatic production of NFCs, where optimised hydrolysis has been achieved at an impeller speed rotation of 470 rpm (turbulent flow regime). The turbulent flow was created using the elephant ear impellers (Fig. 7e). The prepared NFCs have an excellent fibre diameter of 18–31 nm, a degree of crystallinity of 72–81%, and thermal stability up to 310 °C. The dual impellers led to improved mixing and mass transfer (higher turbulence; Re: 5.72–7.36 × 10^4 for 24–48 h of enzymatic hydrolysis), while also resulting in decreased shear forces and lowered energy usage. Optimised power consumption for the CSTR reported above, amounted to 161–2017 W·h at a 10 mg/g enzyme loading with 10% *w/v* solids. As with Birch [168], active mixing was found to incur a significant impact on the hydrolysis of lignocellulose and subsequent polymerisation or defibrillation, respectively.

The use of dual impellers such as anchor stirrers is also reported by Amoroso et al. [172] for preparing NFCs from bleached carrot pomace *via* an alkaline chlorite bleaching pre-treatment. This was followed by high-shear mixing in the dual-blade anchor-stirred batch glass reactor, with subsequent a two-chamber microfluidisation process. The process featured 10 passes at 40–50 L/h at 8 atm. While microfluidisation improved fibre quality and homogenisation, it led to unwanted clogging and the need for manual interventions to clear said issues. Their use can ensure effective mixing to promote an adequate bleaching of lignocellulosic fibres. Yang et al. [170,171] reported a plug-flow-based reactor system for the surface modification of NFC cake. The modification with maleic acid, a cross-linking dicarboxylic acid, allowed for a higher degree of substitution of 0.17 at ambient temperature within 25 min. The NFCs were later subsequently *blend*-modified with poly(acrylamide-*co*-acrylic acid) (PAA) to form nanocomposite hydrogels with an extensive semi-interpenetrating network (sIPN), known to possess higher mechanical strength and functional properties [181]. Yang et al. [170,171] procedure relied on the existence of nanochannels in NFC cake which have a thickness greater than the diameters of nanochannels, thereby preventing back-mixing. The facile solvent exchange and impregnation with maleic acid monoester led to little loss of the NFCs. The plug-flow relied on the gravimetric pull, as a dead-end vacuum filtration set-up was used. The prepared maleic acid monoester-modified NFCs had a relatively high degree of crystallinity (68%), with 15–40 nm diameter and micron lengths. Thermal stability lowered from 258 to 230 °C, owing to the conjugated carboxylate groups.

3.2.1.4. Developments in sonochemical reactors. Kuna et al. [182] reported the use of sonochemical approaches that have been integrated into concurrent reaction systems, that induce physical and chemical changes using short-pulse, high-temperature (5000 °C at a rate of

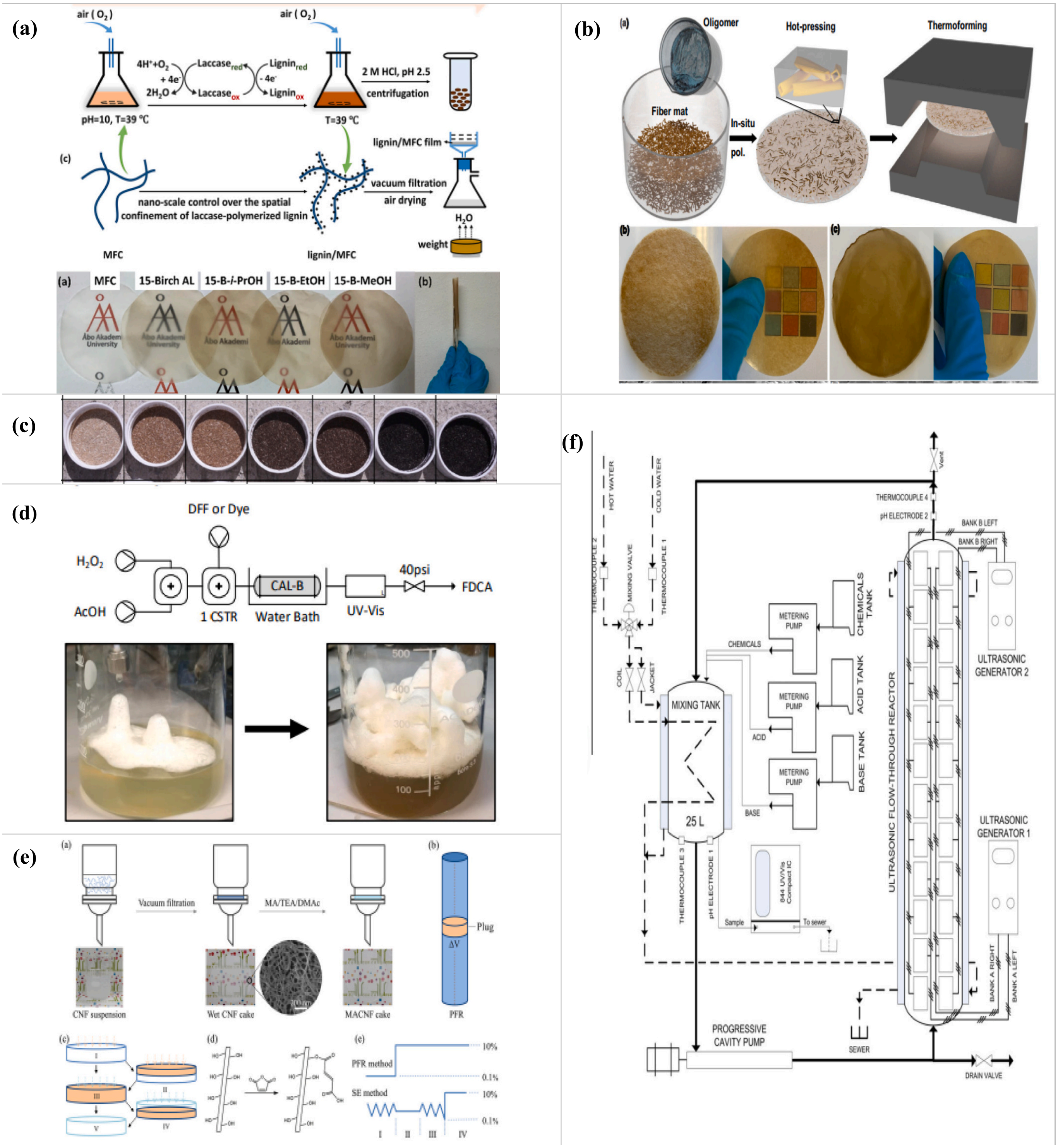

Fig. 7. Lignocellulosic Material Processing Designs. (a) Aqueous one-pot synthesis featuring a laccase-assisted (Metzyme) oxidation, (b) *in situ* polycaprolactone (PCL) oligomer synthesis and PCL thermoforming process, (c) torrefaction-extrusion process, (d) Continuous Liquid Foam Reactor (LFR), (e) NFC cake plug-flow reactor, and (f) sonochemical reactor (Scaled Weissler Method). Source: Fig. 7a reprinted (adapted) with permission from Wang et al. [147,148], Copyright 2021 American Chemical Society 2021, under CC-BY-NY. Fig. 7b reproduced from Oliaei et al. [162], published by Springer Nature, with permission under CC-BY-NY. Fig. 7c and f reproduced with permission from Berthet et al. [164] and [169], respectively, Copyright 2013, 2016 Elsevier; Fig. 7d reproduced with permission from Birch [168], Copyright 2021 University of Leeds, under Creative Commons Attribution NonCommercial ShareAlike 4.0 International Licence. Fig. 7e, reprinted (adapted) with permission from Yang et al. [170,171], Copyright 2019 American Chemical Society.

10^{10} °C/s) and high-pressure hydrodynamic cavitations (*ca.* 1000 atm). Ultrasonication parameters impacting the hydrolysis and shear of lignocellulose depend on parameters such as s frequency, acoustic power, temperature, pressure, solvent, and geometrical design of reactors; which impact the bubble cavitation formation [65]. Cavitational activity is impacted by horn tip diameters as well as their proximity [183]. Paquin et al. [169] reported the use of a continuous flow-through system ("Scaled Weissler's Method") instead of the batch/

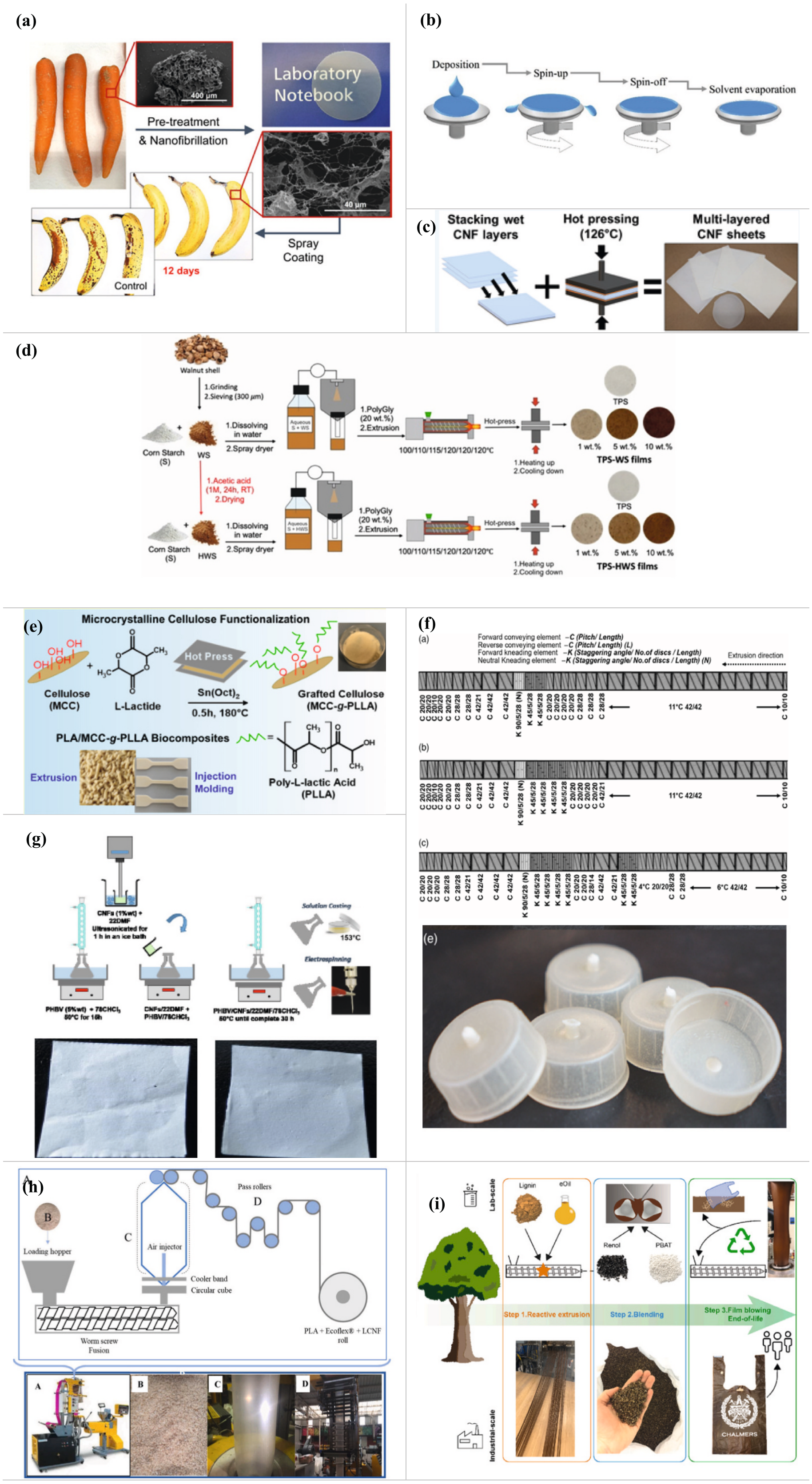

(caption on next page)

Fig. 8. Developments in Packaging Processes Technologies: (a) NFC spray coating process, (b) spin-coating, (c) wet-stacking lamination of multilayer microfibrillated NFC sheets by hot-pressing, (d) melt-extrusion and compression moulding of walnut lignocellulose and starch thermoplastic composites, (e) poly(L-Lactide) cross-linked MCC-*g*-PLLA composites prepared by thermo-compression and extrusion-*cum*-injection moulding process, (f) bottle screw caps prepared from PCL-CNC *via* extrusion-*cum*-injection moulding, (g) electrospun sisal lignocellulose and rPET, (h) lignocellulose-reinforced blow-casted PLA:Ecoflex® packaging films, and (i) reactive melt-processing of lignin with methyl 9,10-epoxystearate to produce Renol packaging films. Source: Fig. 7a and c reprinted (adapted) with permission from Amoroso et al. [172], and El Awad Azrak et al. [173]. Copyright 2019, 2020 American Chemical Society. Fig. 7b, h and g reprinted (adapted) with permission from Shojaeiarani et al. [174], Bascón-Villegas et al. [175] and Santos et al. [176]. Copyright 2015, 2019, 2020 Elsevier. Fig. 7d and e reprinted (adapted) with permission from Quilez-Molina et al. [85], and Genovese et al. [177]. Copyright 2022, American Chemical Society; under CC-BY. Fig. 7f reprinted (adapted) with permission from Venkatesh et al. [178]. Copyright 2022, John Wiley and Sons; under CC-BY. Fig. 7i reprinted (adapted) with permission from Avella et al. [179]. Copyright 2023 Elsevier; under CC-BY.

semi-batch glass reactor configuration whereby the tandem ultrasonicator increased reaction rate by 36% and reduced overall energy consumption by 87%. Carboxylate formation was the highest at 250 W or 16.4 W/L (*i.e.*, 651.2 mmol/kg), which was achieved at a constant flow-rate of lignocellulose/TEMPO-reactant mixture at 40.8 L/min and an ultrasound of 11.2 s/cycle.

Qin et al. [184] reported the use of a TEMPO-assisted oxidative hydrolysis of cotton linter pulp lignocellulose for NFC at 40 kHz. The generation of active oxidation species is optimised at 40 kHz and typically increases from 20 to 500 kHz. The resulting NFCs had high aspect ratios (5–10 nm, 100–400 nm, L/D: 20–40) and degree of crystallinity values of *ca.* 84%, well-suited to packaging applications and bioplastic blending. Carboxylation was relatively lower than the scaled Weissler's method reported by Paquin et al. [169]. Hou et al. [185] further mentioned sonochemically-assisted cellulose derivatisation using oleic acid, with a ranging DS of 0.37–1.71, where cellulose oleates with DS equal to 1.23 had higher thermoplasticity (*i.e.,* greater elongation at break of 75.6%) and T_g values of *ca.* 160–173 °C. Ultrasonication at 300 W/m^2 had improved the degree of substitution, using DMSO and DMAc, although pyridine was said to have led to higher yields and degree of substitution up to 1.7 owing to dispersibility and optimised anhydroglucose unit OH to polar solvent interactions. The thermoplastic films were produced in a blend formation with poly(L-lactide) (PLLA) that exhibited a high mechanical strength value of 40 MPa compared to blend films using regenerated MCC or PLLA.

3.2.2. Developments in cellulose shaping technologies

Wendler et al. [186] mentioned various modification attempts to contemporary cellulose packaging films and bioplastic sheets produced using the Lyocell Process. The authors in their work identified the use of various fibre geometry modification approaches across cellulose fibre-spinning techniques; each with their distinctive cellulose shaping features and impacts on the mechanical and functional performance of the fibres. The solvent properties of the fibre-spinning solution prepared in *N*-methylmorpholine N-Oxide (NMMO) have undergone extensive reformulation with different additives such as 2D carbon nanomaterials and superabsorbent polymers, *i.e.*, carbamates to fine-tune fibre diameters for additive particle sizes ≤10 μm [187]. ILs have found extensive use in this regard, as cellulose shaping additives. Shaping spinneret tool geometries can allow for versatile cellulose shaping where round bulk fibres could be shaped into flat, trilobal and hollow cross-sections for a range of applications based on variations in the functional properties of the material [186]. Advances in altering shearing fields have also improved the sphere-forming and fibrillation properties of the shaped cellulose. Moriam et al. [188] performed an IL-based cellulose shaping using DBNHAc which led to an increase in the aspect ratio (L/D) by 1–2, with a reported toughness of 93 MPa and tensile strength of 60 cN/tex of round bulk fibres.

3.2.3. Developments in packaging process technologies

3.2.3.1. Solvent/blade casting/roll-to-roll coating. Wendler et al. [186] mentioned a parametrically modified and upscaled, continuous roll-to-roll iterations of the CELSOL/BIOCELSOL Process for preparing cellulosic 60 × 80 cm, 500 μm thick sheets of film for adequate size on a spinning line at 10 °C. The cellulose solution used was first deaerated, filtered and cast into film rolls at 10 °C, and then in subsequent sulfite/sulphuric acid coagulation baths (often with ZnO as an additive) for 10 min. Subsequent film storage was performed at 30 °C and dried by plate drying. Yoon et al. [189] reported a roll-to-roll process for the preparation of cellulose paper films, featuring an upscaled iteration of the classical doctor blade coating system over a PET belt and a tandem drying-winding process. The casting solution was prepared in LiCl/DMAc and later replaced by deionised water in the curing step. The authors' work provided key insights as to how hole defects can form owing to the rheological characteristics of the cellulose solutions, *via* poor yield stresses and increased viscosity under the blade. Further, film thickness is much more sensitive to the gap size rather than the casting speed. Zamani et al. [190] reported a twin-roll forming process for micro- and nanofibrillated cellulosic films derived from birch hardwood kraft pulp, using twin-rollers at 6 MPa for 1 min in 13 cycles, to give high-consistency cellulose films with comparable strength values of *ca.* 45–60 MPa and optical properties to those of conventionally casted films.

Droguet et al. [191] reported a roll-to-roll coating-based photonic film fabrication by solvent evaporation-driven self-assembly. Their method features the use of a corona discharge activation of PET substrates that leads to enhanced wetting of the low-viscosity aqueous NCC suspension; improving flow control and thus thickness consistency. Casting was performed using a slot-die with the dispense of the suspension at 6 mL/min. The drying was performed either statically in the air or by passing through a heated chamber at 30–40 °C. Free-standing films were obtained by peeling them off using a blade from the activated PET web. Qiao et al. [192] reported the use of an IL-assisted roll coating process using BMIMCl and LiCl as plasticizers and yielding high cellulose ratio films cast at 65 °C, with high tensility values of 74 MPa, and high transparency (81%). The use of a roll-to-roll dual-layer slot die method has been known to yield low OP bilayer thin films in contrast to spray-coated thin films, *i.e.*, up to 0.37–1.39 $cm^3{\cdot}cm/(m^2{\cdot}s{\cdot}Pa)$ [193]. Thicknesses in roll-to-roll coatings are apparently higher (by as much as 25%). Cazón et al. [194] reported the use of an alkaline-urea cellulose dissolution at ambient conditions, with freeze-thawing and solution casting in a PVA bath, and 2.5–5% *w/w* glycerol as a plasticiser. PVA bath led to improved toughness and burst strength in the cellulose films prepared as well as the WVP by 222%.

3.2.3.2. Spray coating. Spray coating is also a common industrial technique used to coat foodstuffs to prolong their shelf-life and sustain quality. The rheological behaviour of spraying suspension should by design feature shear-thinning behaviour to ensure adequate coating thickness during spraying/atomisation. Amoroso et al. [172] mentioned the preparation of bleached NFC films and spray coatings from carrot pomace; first preparing NFCs *via* the NaOH/$NaClO_3$ bleaching method in an acetate buffer. 0.5% w/w carrot NFC aqueous suspensions were sprayed twice using an atomizer onto banana fruits. The carrot NFC spray demonstrated low shear rates, *i.e.*, 0.001 Hz resting viscosity. Further, bleached carrot NFCs had higher viscosities than unbleached carrot NFCs (82–219 Pa·s against 109–176 Pa·s for 1% w/w suspension). The bananas had a prolonged shelf-life of 12 days. OP barrier performance for bleached carrot NFCs was higher and ranged up to 0.05–1.12

$cm^3 \cdot cm/(m^2 \cdot s \cdot Pa)$ from fresh carrots and 0.10–1.43 $cm^3 \cdot cm/(m^2 \cdot s \cdot Pa)$ from stale ones.

Spray-coating has been particularly applied for improving the mechanical and barrier properties of packaging bags and paper packaging using NFCs and other performance enhancers such as nano-clay fillers (hydrophilic bentonite: $H_2Al_2O_6Si$; ≤ 25 μm). de Oliveira et al. [195] reported such an NFC/nanoclay spray-coating over sack kraft paper with as much as 10–20 g/m^2; leading to a 44–66% increase in the tensile properties of the Kraft paper. The authors further developed multilayered spray-coated NFC/NC Kraft papers. The WVTR amounted to 263–274 $g/(m^2 \cdot d)$ for NFC/NC Kraft papers. Mirmehdi et al. [196] further reported a similar use of nanoclays with bleached eucalyptus-derived NFCs (46–54 nm in diameter) on printing and writing papers, leading to improved WVTR, which were the highest at 28.5 $g/(m^2 \cdot d)$ for a 29 μm thick coating, owing to the hydrophilic nature of the nanoclay. Similar effects were not as prominent for the OTR. Prior to the spray coating, Mirmehdi et al. [196] applied a continuous electric discharge of 10 kV to increase surface wettability pre-coating of the printing and writing papers. The spray formulation featured a 1.4% *w*/w NFC/nanoclay aqueous suspension (5% w/w nanoclay); sprayed under 5 atm from 15 cm distance with vacuum dewatering to consistently remove water and improve drying. Coated sheets were then thermo-compressed at 103 °C for 1 h at 1 atm.

3.2.3.3. Spin coating. Spin coating has also grown in popularity in preparing cellulosic coating films, characterised by parametric optimisations of coating thickness, roughness, and uniformity of the spin-coated films, *via* rotational speed, spinning cycles and suspension concentration/formulation variations [197]. For instance, Shojaeiarani et al. [174] reported spin-coated PLA-*g*-CNC composites having higher mechanical storage modulus values than their film counterparts, *i.e.*, 2000 MPa for PLA *vs.* 2056–2849 MPa for the blends. Shear-thinning led to higher dispersity of the blend components where non-Newtonian fluidic nature becomes dominant at lower shear rates [198]. Molecular weight retention of the NCC is more prominent in spin-coated preparations for the PLA-*g*-CNC composites. T_g values were also the highest for spin-casted blend films. In another study, Shojaeiarani et al. [199] reported that spin coating leads to the formation of macroaggregates by 1–5% w/w NCCs and that high drying rates reduced NCC self-assembly. This reportedly leads to a higher degree of crystallinity values that are *ca.* 19–57% higher than solvent-casted films for spin-coated films based on PLA grafted CNC (PLA-*g*-CNC). WVP and WVTR were also lower for spin-coated films with values up to 1.82×10^{-6}–1.9×10^{-6} $g/(m^2 \cdot d \cdot Pa)$ and 11.8–12.5 $g/(m^2 \cdot d)$, respectively.

3.2.3.4. Vac filter/hot-pressing in tandem film-forming processes. As described earlier, the use of thermo-compressing or hot-pressing is typically considered for lignocellulosic materials or derived cellulosic with poor degree of crystallinity values - owing to higher lignin contents or micro-aggregation [162]. The loss of crystallinity is typical with cellulose blending with different sustainable polymers such as PCL, PLA and others, which necessitate the use of thermo-compression, Additionally, given the high moisture intake and water permeation capacities of NCCs or NFCs, filter cakes (derivatised or bleached) are typically fabricated into papers or films using vacuum dewatering and hot-pressing methods [172,164,196]. El Awad Azrak et al. [173] reported the use of a hot-pressing approach to prepare multi-layered microfibrillated NFC sheets that yield 500 μm high tensile strength films up to 205–209 MPa. Azrak and co-workers' method featured an aqueous NFC suspension casting with subsequent vacuum dewatering (capillary suction and filtration by gravity) and sponge soaking. The resulting 7% w/w NFC web was sandwiched between two metal meshes and slip-rolled to obtain individual 10% w/w stacks that were stacked and hot-pressed at 126 °C for 2 h. The processing step leads to significantly higher mechanical strengths that are as much as 6 times more than PS. Though, hot-pressing likely reduces the OTR for hot-pressed TEMPO-derived NFC films by 68%–80%; < 500 cm^3/min, in exchange for higher film flexibility. Tear strength is reduced after NFC addition in papers but returns to original strengths by hot-pressing [200]. The extent of fibrillation has little impact on the synergistic effects between NFC and hot-pressing on the film strength. Huang et al. [201] reported the use of hot-pressing of regenerated wood cellulose films, which led to remarkable drying effects, and highly improved mechanical strengths with a value of *ca.* 85 MPa and with a WVP value of 5.32×10^{-4}–5.76×10^{-4} $g/(m^2 \cdot d \cdot Pa)$. Preservation effects lasted 16 days at most for the hot-pressed regenerated wood cellulose films.

Genovese et al. [177] prepared surface-functionalised MCC-*g*-PLLA composite films *via* a solvent-free grafting process in a compression moulding setup. Superhydrophobization achieved resulted in a higher water vapour barrier, degree of crystallinity, and stiffness compared to both pure PLA and formulations, and non-functionalised MCCs. The MCC-*g*-PLLA composites were first prepared using L-Lactide in a Sn $(Oct)_2$-catalysed surface functionalisation reaction where the composites were then compression moulding using a hot press at 180 °C for 5–120 min between two metal plates covered with PTFE.

3.2.3.5. Melt-processing and melt-intercalation. Aside from high energy intensively, melt-intercalation for the preparation of cellulose composites has been known to lead to poor fibre quality and deformation owing to poor thermal control and mixing of the blend composites [162]. Despite challenges, melt intercalation or melt processing is extensively used for most plant-derived biocomposites [202]. To improve upon NFC quality throughout the melt-processing and impart greater mechanical strength to cellulosic biocomposites, an *in situ* PS-cellulose grafting process has been successfully demonstrated utilising dispersion polymerisation coupled with melt intercalation/pressing [61]. Fujisawa's NFC-*g*-PS, as discussed previously was able to attain porous transparent films with relatively high mechanical strengths and adequate crystallinity and thermal processability (T_g of 100 °C owing to PS). Avella et al. [179] reported a novel preparation of lignin-based Renol and PBAT blend packaging films using a reactive melt-extrusion process. Briefly, the process featured softwood-derived Kraft lignin and 12% *w*/w methyl 9,10-epoxystearate (eOil) being stirred till homogeneity, and then reactive extrusion using a twin-screw extruder at a temperature profile of 120/160/150/150 °C (feeder to die), at 60 rpm and a round hole die; with a 15 min residence time. 40% w/w of the resulting blend of Renol and PBAT were further processed in a subsequent melt-extrusion step.

3.2.3.6. Extrusion and thermocompression in tandem with injection moulding. Quilez-Molina et al. [85] further reported a novel melt-extrusion process for the preparation of corn starch and walnut lignocellulose thermoplastic composites. The thermoplastic starch composites featured a batch process involving the spray drying of a 5% w/w aqueous 1:1 walnut lignocellulose and starch formulation with 20% *w*/w polyglycerol as a plasticiser. Post-drying, the blend formulation was melt-extruded using a twin-screw extruder at 50 rpm in the following temperature profile: 100/110/115/120/120/120/120 °C with a filament die. The thermoplastic walnut lignocellulose-starch composite filaments were thermo-compressed at 30 °C for 10 min. The degree of crystallinity of the thermoplastic dramatically reduced to 5% owing to the addition of the polyglycerol. The T_g of the composites ranged from −36 to −31 °C owing to the higher lignin content in the blending component (walnut shell lignin). The thermal resistance was however improved considerably up to 300 °C owing to the hydrolysed walnut shell lignocellulose used as a filler for the starch thermoplastics. The hydrolysed lignocelluloses led to improved WVP values of 0.58×10^{-9}–2.31×10^{-9} $g/(m^2 \cdot d \cdot Pa)$, OP values of 1.84×10^{-11} $cm^3 \cdot cm/(m^2 \cdot s \cdot Pa)$, and opacity for the composite films produced. Higher lignin led to relatively lower tensile strengths for the films (<10 MPa).

Moran et al. [203] reported the preparation of PLA-cellulose nanowhisker composites using a twin-screw extrusion process with injection moulding at temperature, screw speed and residence time were set at 190 °C, 90 rpm and for 1 min. The dispersion of cellulose nanowhiskers is particularly challenging owing to the poor dispersibility in non-polar polymer matrices, which leads to extensive aggregation upon drying. The cellulose nanowhisker was melt-mixed with a plasticiser - 18% *w*/w; glycerin polyglycidyl ether (GPE) - to improve PLA processability. PLA-cellulose nanowhisker composites with a 12% formulation of the latter led to optimal mechanical strengths with tensile stress at a break of 27–31 MPa. Thermal stability was also observed up to 224 °C (at a low degree of crystallinity of 13.6%), which allows a possibility for injection moulding of the composites.

Venkatesh et al. [178] reported the production of carton screw caps using poly(ethylene-*co*-acrylic acid) (PEAA), PCL and prepared NCC fibres (3–9 nm diameter; 191–411 nm length) and thermomechanical pulp derived from acid hydrolysis of Norwegian spruce pulp. The NCC-PEAA composites were prepared by mixing in water and the thermomechanical pulp (TMP) composites by dry mixing. Following a dual-step twin-screw extrusion using a screw L/D: 1144/26 at a temperature profile of 120/140/200/200/170/170 °C first and then compounded into pellets at a profile of 0/90/130/130/120/120 °C for NCC-PCL composites. The compounded pellets were injection moulded into screw bottle caps at a backpressure of 1.5 MPa and screw speed of 20 m/min. Tensility amounted to 15–16 MPa for both NCC-PEAA and TMP-PEAA composites and 15–25 MPa for both NCC-PCL and TMP-PCL composites. Elasticity improved with NCC and/or TMP inclusion, though morphological properties indicated aggregation. NCC aggregations were observed and prominent in the composite formulations, attributed to the sub-optimal dispersibility, low shear homogenisation and Leidenfrost effects observed during the mixing of NCC-PCL or NCC-PEEA composites [204]. Nevertheless, the structural stiffness was relatively similar to HDPE for NCC-PCL and the TMP-PCL composites (32–36 N/mm and 40–42 N/mm, respectively, *vs* HDPE's 43–49 N/mm). The degree of crystallinity remained unaffected as well as the melting point relative to NCC or TMP addition. Changing injection mould temperature across 70–130 °C also leads to improved mechanical properties for the addition of NCC fibres in soy protein-derived bioplastics [205]. Beaugrand and Berzin [206] also reported their work on a PCL-lignocellulose (hemp) fibre reinforcement composite, where similar results were obtained, though it was found that the ratio of screw length-to-diameter (L/D) does not fully encapsulate the dimensions of the fibre or bundle.

PLA/MCC-PLLA composites have further been prepared by extrusion at 180 °C, with a screw rate of 150 rpm and a residence time of the material of *ca.* 1 min in a single screw extruder with a length-to-diameter ratio (L/D) of 20 [177]. Further processing involved micro-injection moulding of the extruded pellets *via* conducting systematic plasticisation (210 °C) and injection (205 °C) with an injection pressure of 100 atm. Specifically, the materials exhibited an increase in the degree of crystallinity ranging from 12% to 33%, which was associated with the content and functionalization of MCC. This acted as a catalyst for PLA, without significantly altering its thermal stability. Concurrently, the addition of MCC resulted in a significant decrease in permeability, ranging from 45% to 66%.

Fekete et al. [207] reported the preparation of thermoplastic starch/wood composites from thermo-compression and injection moulding, after blending with lignocellulosic wood fibres at 150 °C for 10 min at 50 rpm. The melt was compression moulded to obtain the thin film composites. Alternatively, injection moulding has also been used where fibre aspect ratios impacted the wood lignocellulose's reinforcement effect [208]. The amount of fibre present greatly influences modulus and tensile strength; however, they are not affected by the size of the particles or their aspect ratio. Fekete et al. [207] mentioned that injection moulding allows for better fibre orientation and potential improvement to the mechanical and thermal strengths of the composites. Montanes et al. [209] also prepared lignocellulosic filled wood plastic composites with bio-PET *via* injection moulding, where increasing lignocellulosic fibre content led to increasing viscosity and thus lower processability at low shear rates. Though the shear thinning effect of pseudoplastic fluids is observed at higher shear rates, melt viscosity and rheological behaviour further prevented lignocellulosic filler homogenisation.

3.2.3.7. Electrospinning. Santos et al. [176] prepared ultrathin nanofibre mats from electrospun sisal lignocellulose and rPET in TFA solutions. The electrospinning utilised an optimised 20 g/L concentration threshold that restricted gelation after dissolution. Additionally, fibres were electrospun at ambient conditions for 80 min at 20 kV and a flow rate of 5.5 μL/min. The addition of sisal led to stiffer mats and higher T_g values relative to a neat PET mat. Fibre diameters ranged from 185 to 284 nm from sisal lignocellulose-PET/TFA solutions, with random orientations. Hydrophilicity was further enhanced with the addition of the sisal lignocellulose fibres. In another paper, Passos de Oliveira et al. [210] reported the mechanical strength of the sisal lignocellulose-PET fibre mats was the highest possible tensile strength, 2.5 MPa, was achieved at 40% *w*/w sisal lignocellulose.

Nanocellulose has also been electrospun with PHAs, which formed multilayered functional fibres having adequate hydrophilicity, mechanical properties, and higher barrier performance against water vapour in comparison to the neat nanopapers [211]. Water barrier performance (WVP) reduced significantly for electrospun lignocellulose nanofibre blends with PHB and PHBV, by as much as 115 times and 133 times, respectively. OTR was also reduced for PHA-lignocellulose nanofibre electrospun films against neat lignocellulose nanofibers by 35%. The PHB and PHBV polymer blends with NCC were prepared *via* high-shear defibrillation-assisted microfluidisation. The nanopapers were prepared by solution casting after a plasma arc activation of the substrate to allow for film property control. The PHB or PHBV was then electrospun over the nanopapers at 25 °C, for 2 h under a steady flow-rate of 6 mL/h, 16 kV, and a distance to the collector of 15 cm. The electrospun fibre mats had a thickness of 30–140 μm based on the multilayering approach followed. Arguably, tensile strength reduced with the multilayered electrospun fibres in relation to their neat counterparts.

Benini et al. [212] reported a comparative assessment of PHBV/NFC mats prepared from electrospinning and solution casting. The former parameters involved a needle 20 × 10, drum collector rotation of 27 rpm, and a working distance of 10 cm. The addition of NFCs had led to little changes in film transparency for solution casting, though electrospun mats had better transparency. The degree of crystallinity was also relatively lower for electrospun PHBV/NFC mats (56% as opposed to 64% in solution casting). T_g was higher by a factor of 3 for electrospun PHBV/NFC mats. Crystallisation had occurred in full for both techniques. Yang et al. [91,92] mentioned a blending electrospinning process (15% *w*/w in formic acid) using PVA/ethyl cellulose/TEA polyphenol, yielding fibres of 213–432 nm diameter, and lower water stability and water barrier properties, as WVP reduced *ca.* 40%. The TEA polyphenol improved the antioxidant and antibacterial properties of the cellulose film. ILs have also been used to improve cellulose fibre dissolution in the electrospinning solution or melt, leading to improved fibre lengths relative to lower IL loadings with polar aprotic co-solvents such as DMAc, DMF and DMSO. Finally, optimal fibres were obtained in a 5% w/w wood lignocellulose to EMIMLac solution [213].

3.2.3.8. Solution blowing. Bascón-Villegas et al. [175] reported a pilot scale trial of an agri-food lignocellulose packaging polymer blend with PLA and poly(butylene adipate-*co*-terephthalate) (PBAT; Ecoflex®). The authors reported significant improvements in the blow cast 70:30 PLA: Ecoflex® with 0.5 and 1% lignocellulose nanofibre reinforcement. The lignocellulose nanofibres were produced by soda pulping of wheat straw using alkaline hydrolysis, followed by enzymatic pre-treatment using Quimizime B to assist subsequent defibrillation and high-pressure homogenisation. A dehydration step using PEG was conducted at 40 °C and the PEG-lignocellulose nanofibre melt was pelletised with PLA and Ecoflex®, and extruded a multilayer film extruder. The tensile strength of the films was optimised for the blow cast 70:30 PLA:Ecoflex® packaging films with 0.5 and 1% lignocellulose nanofibre reinforcement, at 43 MPa and 41 MPa, respectively. Decomposition temperatures for both films were 322 °C, with 99.65–99.88% UV-barrier properties yet lowered transparency scores ($< 36\%$). The OTR for the former was around 600 $cm^3/(m^2{\cdot}d)$ and WVP was equal to 4.5×10^{-7}–5.1×10^{-7} $g/(m^2{\cdot}d{\cdot}Pa)$. The packaging films allowed for a 21-day shelf life for fresh-cut lettuce before significant degradation of both the packaging film and the packaged material.

Avella et al. [179] further mentioned that a Renol-PBAT packaging bag with a T_g value of 112 °C was also prepared by film-blowing with a die temperature of 160 °C. The single-screw extruder was used for palletisation, set at a temperature profile of 120/160/150/120 °C (feeder to die) and extruded through a film-blowing die with a cooling ring. The blown films were collected and pulled by rotating rolls at the top of the die. The films exhibited high mechanical strength when the lignin content was relatively lower in proportion to the eOil (12% w/w.) and PBAT (60% *w*/w) The films were highly recyclable/compostable, water-insoluble over 72 h and had a maximum degradation time of 90 days.

Table 2 provides a comprehensive summary of various agro-industrial LB-derived cellulosic materials from various valorisation, utilisation and processing techniques for lignocellulose thermoplastics and packaging films. The table also indicates their use for packaging or having potential for said purpose, for which significant literature has been tabulated and summarised below. Processes or methods with FP as n.a. (not available), are typically those that do not confirm certain functional properties such as mechanical films as no film preparation was reported.

3.3. Process structure property performance relations

A graphical illustration of the correlation of property variations, on the micro- and macro-structure and subsequently the functional properties of the lignocellulosic material is presented in Fig. 9. The property variations are in terms of the presence of lignin (as LC) and NFC or LCNF (characterised by extent of defibrillation, DE). Further, the correlations herein refer to the various findings reported in the literature as above. The table is a summarisation of the impacts across a two-colour intensity scale, ranging from lowest correlation (white) to moderate correlation (lime green) to highest correlation (green).

A literature review has revealed the relatively complex Process-Structure-Property-Performance relations governing the transformation of lignocellulosic materials into functional lignocellulose packaging and coatings. Various valorisation and utilisation processes indicate distinct impacts on cellulose properties, particularly crystallinity, and the functional attributes of lignocellulosic materials (Fig. 10). The interplay between cellulose fibres and lignin significantly influences the functional properties of lignocellulosic materials. In terms of barrier properties, cellulose's crystalline structure enhances the material's barrier properties. Simultaneously, lignin, with its hydrophobic nature, contributes to water resistance and can augment the overall barrier performance. However, the impact of lignin on barrier properties becomes nuanced, as excessive lignin content might introduce porosity, potentially compromising the barrier characteristics [96]. Optical properties are influenced by cellulose's transparency and light-scattering features, with highly crystalline cellulose regions enhancing transparency. Conversely, lignin's inherent colouration imparts a brown hue, reducing overall transparency [76]. Nonetheless, lignin's UV-absorbing capacity can be advantageous in protecting cellulose fibres from UV radiation.

Lignin acts as a matrix or dispersant media, while hemicelluloses are the binding agents that disperse cellulose fibres in the plant cell wall acting as coupling agents [3,216]. Additionally, pectins further facilitate this cellulose-lignin dispersion and permit spatial arrangement of cellulose in the lignin matrix, especially in the middle lamella region [217]. These binding interactions are illustrated in Fig. 11. Alternatively, individual cellulose chains can undergo crosslinking and simultaneous defibrillation by dicarboxylic acids that contribute to an increased binding effect [89], which can lead to increased hydrophobisation (as AGU hydroxyls partake in crosslinking) and increased mechanical strength [218]. Additionally, delignification reduces amorphousness rather than increases crystallinity. Further, lignin removal facilitates functional properties (barrier, elasticity, porosity, etc) of lignocellulosic materials and their products. Delignification, in general, can reduce amorphousness in lignocellulose, leading to a more ordered and crystalline structure.

Alkaline hydrolysis and steam-explosion enhance aspect ratios and crystallinity in sugarcane bagasse-derived lignocellulose, while acid hydrolysis and oxalate pre-treatment lead to high crystallinity and improved transparency in cotton nanocellulose ([82]; J. [219]). Reactive processes, including the production of FACEs and CNC-*g*-PS shelled nanoparticles, exhibit enhanced mechanical and thermal strengths [179,62]. Sonochemical treatments, exemplified by the production of sugarcane bagasse NFCs, result in improved thermal resistance and mechanical strength [65]. Furthermore, the choice of fatty acid and its esterification impacts the hydrophobicity, crystallinity, and thermal stability of the cellulose esters [220,59,71,151]. Additionally, bio-based and torrefaction approaches demonstrate unique influences. Biochemical/enzymatic processes, such as soda pulping and enzymatic hydrolysis, lead to enhanced mechanical strength and extended shelf life in wheat straw LCNF/PLA and LCNF/PBAT composites [154,215,221]. Torrefaction of wheat straw MCC/PHBV composites affects holocellulose fibre breakdown and mechanical strength, while microwave-assisted nanofibrillation enhances tensile strengths and UV-shading capacities in pine-based lignocellulose [164].

Filler-matrix interaction is reportedly a challenge for achieving appreciable mechanical and thermal strength for NCC-polymer composites though the poor dispersibility characteristics of the former prove difficult to optimise [222]. Wang et al. [214] studied various melt-processing trials for the preparation of NFC/thermoplastic composites with appropriate dispersibility, mechanical strength and thermal properties. The authors attempted to address the challenges associated with the moisture absorption properties of lignocellulosic precursors that reduced wet melt-processing capacities. Films with better thermal, mechanical and functional properties than their solvent-cast counterparts. Negro et al. [200] found that thermomechanical film-forming processes, *e.g.*, thermo-compression and hot-pressing methods, yield NFC and LCNF.

In terms of thermal behaviour, cellulose fibres contribute to the material's thermal stability due to their ordered structure and high decomposition temperature. An excessive amount of lignin may introduce complexity and potentially lead to lower thermal stability [223]. The mechanical strength of lignocellulosic materials is predominantly attributed to cellulose, with its crystalline regions and strong intermolecular bonding. Excess lignin may further compromise mechanical strength due to its more amorphous nature compared to cellulose [149].

3.4. Techno-economical feasibility of lignocellulosic waste valorisation for packaging

Notably, the use of LBs has been further encouraged by the competitiveness of lignocellulosic materials against conventional plastics, in terms of functional properties (*i.e.*, printability, transparency, gloss), thermo-mechanical properties (*i.e.*, flexibility, stability, durability), barrier efficiency and processability aspects [10]. Arguably, cost-effectiveness and carbon emission (CO_2e) reduction could be inducted across the value chain [224]. These features are unique selling points for LWs as sustainable packaging materials. The recyclability and integrability of lignocellulosic biopolymers have inspired many ongoing

Table 2
Process design characteristics for sustainable lignocellulosic packaging bioplastic and biopolymers.

	Lignocellulosic material(s)	Process Chemistry & Design Summary			Micro- and Macro- Structure Property	Functional Property (Performance)	Refs
		RP[a]	S/P[b]	FF[c]			
Mechanochemical	Regenerated Nanocellulose Fibres	Alkaline Hydrolysis	Alkaline planetary Ball-milling for 90 min with 8% w/w NaOH. Thermocompressing at 120 °C.	tc/ hp.	☐ High crystallinity ☐ Cellulose I morphology retained ☐ Fibre diameter of 25–50 nm	☐ High Young's Modulus (9.3 GPa) ☐ Tensile strength of 100 MPa. ☐ Translucent films. ☐ Cellulose I yields higher mechanical strength.	Abe [44]
Mechanochemical	Sugar Palm NFCs – Starch composites	Alkaline Hydrolysis	Ball-milling, High-pressure Homogenisation under normal conditions	sc	☐ High crystallinity (81.2%) ☐ Fibre diameter of 5.5 ± 0.99 nm and micro meter lengths ☐ Structure deformations, pores and cracks in starch matrices	☐ High Young's Modulus (59–121 MPa) ☐ Translucent films ☐ H-bonding interactions between sugar palm NFCs and starch matrices	Ilyas et al. [68]
Mechanochemical	Fatty acid cellulose esters (cellulose octanoate, palmitate, laurates)	Acid Hydrolysis	Mechanochemical synthesis in an Ac$_2$O/TFA anhydride system, a 1:3 AGU-to-fatty acid ratio under normal conditions	sc	☐ High agglomeration of FACEs ☐ Large particles with rough morphologies ☐ High amorphousness ☐ Higher cellulose defibrillation. ☐ DS achieved: 2.04–2.4 (C$_8$), 1.8–2.7 (C$_{12}$), and 2.1–2.3 (C$_{16}$).	☐ Translucency and elasticity. Higher adhesion of cellulose esters than fatty acid substituents.	Hu et al. [71]
Mechanochemical	Fatty acid cellulose esters (cellulose oleate), Regenerated cellulose acid cake	Acid Hydrolysis; Reactive	Solventless mechanochemical synthesis using carbodiimide, DMAP and a low dose AGU-to-fatty acid ratio (6 mmol/AGU) at 300–500 rpm, for 2–6 h at ambient temperature. Subsequent hot-pressing at 160 °C to prepare films.	tc/ hp	☐ Powderisation was lower at rotations ≥400 rpm, forming crystalline monoliths. ☐ FACE aggregation is prominent with pore-forming and network formation between cellulose fibres and the fatty acid. ☐ Fatty acids prevent cellulose I nanocrystal regularisation. ☐ FACE particle roughness and irregularity.	☐ DS achieved: 1.3–2.55 with increasing ball milling time ☐ Transparent films that are melt-processable at 160 °C. ☐ High tensile strength of FACEs prepared at 400 rpm, 4 h (8.3 MPa) ☐ The highest glass transition temperature at 54 °C–173 °C.	Hou et al. [59]
Mechanochemical	Fatty acid cellulose (cellulose oleate)	Ionic Liquid Extraction	Mechanochemical cellulose oleate preparation with p-TsCl and BMIMAc at 50–100 °C for 4–24 h.		☐ DS: 0.001–0.210, ☐ Cellulose I morphology was retained with higher DS despite decrystallisation. ☐ High crystallinity <82%, a reduction from MCC's 86% ☐ Low amorphousness ☐ The crystallite size was ≤4.89 nm. ☐ Rod-like bundles with porous fibre structures	☐ Glass transition increases with increasing DS, up to 116.5 °C. ☐ Thermal stability was reduced with FACE formation. ☐ Decrystallisation is linked with lower thermal strength.	Lease et al. [115]
	Lignocellulosic material(s)	Process Chemistry & Design Summary			Micro- and Macro-Structure Property	Functional Property (Performance)	Refs
		RP[a]	S/P[b]	FF[c]			
Thermomechanical/ Thermochemical (Fluidised)	Sugarcane bagasse-derived lignocellulose micro-nanofibrils, nanocrystals and nanospheres	Alkaline Hydrolysis	Steam-explosion at 195 °C for 7.5 and 15 min, followed by alkaline/ hypochlorite pulping and endoglucanase hydrolysis with high-pressure homogenisation for 60 or 180 min.	n.a.	☐ High aspect ratios (78.5) for steam-exploded LCNF at 15 min of steam-explosion treatment and 180 min alkaline/ hypochlorite pulping. ☐ Fibre widths were lower by <20 nm in the above process ☐ Crystallinity was also higher (77%).	☐ Pretreatment severity and the extent of alkaline delignification or hypochlorite bleaching impact defibrillation and NFC formation	Fontes et al. [81]
Chemical	Cotton nanocellulose oxalate	Acid Hydrolysis	Oxalic acid pre-treatment under high-pressure homogenisation under	sc	☐ High crystallinity (75–83%)	☐ Higher carboxylic (809 μmol/g) content	Zhao et al. [73]

(continued on next page)

Table 2 (*continued*)

	Lignocellulosic material(s)	Process Chemistry & Design Summary			Micro- and Macro-Structure Property	Functional Property (Performance)	Refs
		RP[a]	S/P[b]	FF[c]			
			1300 atm (5 cycles), at 45 min of reaction		☐ Cross-linking and defibrillation by oxalic acid hydrolysis. ☐ Retention of Cellulose I morphology ☐ Shorter NFC lengths and diameters with oxalate hydrolysis at a 10:2 oxalate/cotton fibre ratio	led to higher transparency ☐ Transparent films ☐ High transparency, 81% at 600 nm transmittance ☐ High thermal resistance (< 333 °C) ☐ High tensile strength (161.9 MPa)	
Chemical	Corn starch and walnut lignocellulose thermoplastic composite	Acid Hydrolysis	Acetic acid hydrolysis at ambient conditions for 24 h. Spray drying of 5% *w*/w aqueous 1:1 walnut lignocellulose and starch formulation with PEG.	sp, tc, me	☐ High lignin content (60%) ☐ Particle size was reduced by 25% and pore-formation with holocellulose delignification ☐ Opaque films ☐ PEG reduced crystallinity to 5%. ☐ Film strengths are better conserved by thermo-compression.	☐ WVP: 0.83–0.33 g/(m^2.d.Pa) ☐ OP: 1586.8 cm^3.μm/(m^2 d atm) ☐ High thermal resistance due to starch, up to 300 °C ☐ Lower tensile strengths due to lignin (<10 MPa)	Quilez-Molina et al. [85]
Chemical	Softwood nanocellulose oxalate	Acid Hydrolysis	Solventless one-pot cellulose hydrolysis and esterification by molten oxalic acid dihydrate at 110 °C for 30–60 min.	sc	☐ Fibre aspect ratios (L/W) of 9.35 to 11. ☐ 68–71% crystallinity ☐ High lignin removal (81%) ☐ The high molecular weight of nanocellulose oxalates (40 kDa)	☐ Powder-shaped nanocrystals are capable of providing improved mechanical and thermal strengths. ☐ Lowering the ordering of fibril surfaces during esterification reduces crystallinity	Li et al. [89]
Chemical	Carrot pomace NFCs	Alkaline/chlorite Hydrolysis	NaOH/$NaClO_3$ bleaching method in an acetate buffer, in a high-shear mixing and subsequent two-chamber microfluidisation process (10 passes for 40–50 L/h and 8 atm).	sp	☐ Higher viscosities of bleached carrot NFCs (82–219 Pa·s)	☐ OP for bleached carrot NFCs was higher, up to 46–966 cm^3μm/(m^2 day bar). ☐ Opaque/Translucent films ☐ Prolonged shelf-life of 12 days.	Amoroso et al. [172]
Chemical	Fatty acid cellulose (hemicellulose laurate)	Ionic Liquid Extraction	EMIMAc-assisted homogenous transesterification with a reaction time of 1 h at 80 °C.	sc	☐ Porous networks and fibrous structures ☐ Higher DS lead to higher honeycombing in the hemicellulose laurate.	☐ High water barrier properties, WVP: 3.21×10^{-2} to 4.51×10^{-2} g/(m^2·d) ☐ High oxygen barrier properties, OP 1.2–4.2 cm^3 μm/(m^2 d kPa) ☐ Transparency at 52% to 74% at 900 nm ☐ High hydrophobicity. ☐ Shelf-life extension by 15 days (chillies)	Zhang et al. [113]
Chemical	Fatty acid cellulose ester (polysaccharide acetate decanoate)	Acid Hydrolysis; Ionic Liquid Extraction	EMIMAc/DMSO and mixed acyl (1:4 decanoyl/acetyl) transesterification in an inert atmosphere at 80 °C for 30 min. Injection moulded at 205 °C	im	☐ High M_w of $1.5{\cdot}10^6$ g/mol ☐ High non-crystallinity	☐ High tensile and flexural strengths of approximately 50 and 80 MPa.	Suzuki et al. [114]
Chemical	PS-*g*-NFC shelled nanoparticles	TEMPO-oxidation	TEMPO-oxidised NFCs *in situ* polymerisation with PS at ambient condition	mi	☐ Shelled nanoparticles with an average diameter of 3 μm ☐ NFC coating of 8 nm thickness. ☐ Spherical NFCs with diametres about 5.6 ± 1.5 nm. ☐ Moderate crystallinity: 55%.	☐ The tensile strength of the NFC/PS films was 50 MPa. ☐ Thermal stability *ca.* 100 °C owing to PS ☐ Porous transparent films.	Fujisawa [61]

(*continued on next page*)

Table 2 (*continued*)

	Lignocellulosic material(s)	Process Chemistry & Design Summary			Micro- and Macro-Structure Property	Functional Property (Performance)	Refs
		RP[a]	S/P[b]	FF[c]			
Chemical	CNC-*g*-PSl Starch-*g*-PS	Ozonolysis; Reactive	Ozone-assisted hydrolysis and *in situ* grafting with PS (1.56 and 0.25 Sty/AGU ratio with starch and CNC),	sc	☐ CNCs with 91.7 ± 60.8 nm length, ☐ 53.2 ± 9.4 nm length for starch nanocrystals ☐ High hydrophobicity	☐ Thermal stability >100 °C. ☐ Both starch and CNC grafted PS films had lower WVP of 1.85×10^{-1} g/(m^2·d·Pa)	Espino-Pérez et al. [62]
Chemical	Fatty acid cellulose ester (cellulose oleate)	Reactive	Modified acetic anhydride system using TFA/TFAA-$CHCl_3$ system at 80 °C for 30 min; with oleic acid	sc	☐ Higher crystallinity ☐ High hydrophobicity ☐ Densely packed, porous fibre matrix. ☐ Ellipsoidal cells	☐ 76% decrease in WVTR (2800 g/(m^2·d) CO to 670 g/(m^2·d) CA) ☐ 90% decrease in OTR (105,000 cm^3/(m^2·d) CO to 10,200 cm^3/(m^2·d) CA) ☐ Low water uptake ☐ Higher elasticity (14.4%) and lower tensility (6.6 MPa) ☐ Low melting point (63 °C)._	Tedeschi et al. [6]
Chemical	Fatty acid cellulose ester (cellulose aleuritate)	Reactive	Same system as Tedeschi et al. [6], except with aleuritic acid, a polyhydroxy acid.	sc	☐ DS 0.51–2.60 ☐ High amorphousness	☐ Stress at break of 3 MPa ☐ Glass transition of −17 °C, low thermal stability.	Heredia-Guerrero et al. [150]
Chemical	Fatty acid cellulose ester (cellulose isostearate)	Reactive	FACE synthesis using hydrochlorinated tail oil fatty acids (TOFA) in a modified Py/$CHCl_3$ esterification system.	sc	☐ Loss of fibrillar morphology. ☐ Densely packed, porous network and bundled cellulose ester fibres.	☐ Thermal stability improved by 7–22 °C against natural cellulose. ☐ Elastic moduli improved between 30 and 50 MPa ☐ Higher permeability from 2.55 to 3.90 g mm/(m^2 d kPa). ☐ Transparent films	Kulomaa et al. [151]
Chemical	MCC-*g*-PCL	Reactive	*In-situ* polycaprolactone (PCL) oligomer synthesis with succinic acid capping and glycerol medium in the presence of $Sn(Oct)_2$ at 140 °C for 14 h. Hot-pressing at 1 MPa pressure and 60 °C for 3 min	tc/hp	☐ 51% crystallinity for 77% w/w hot-pressed spruce fibre/PCL composite. ☐ 20% crystallinity for a 50% MCC/PCL composite. ☐ Lignin <20% ☐ ε-PCL in the lumen region of the wood fibres. ☐ Fibrous, porous matrices with a dense packing morphology ☐ Micro-aggregation due to lignin.	☐ High mechanical strength of up to 82.1 GPa for 77% w/w hot-pressed spruce fibre/PCL composite ☐ High mechanical strength of 62 GPa for a 50% MCC/PCL composite ☐ Bonding with residual lignin could have led to increased mechanical strengths	Oliaei et al. [162]
Chemical	CNC-*g*-PAA	Reactive	Plug-flow, solvent exchange-based design surface modification of NCC cake with maleic acid at ambient temperature within 25 min, and blend modification with PAA.	ors	☐ Low DS: 0.17 ☐ Nanochannelling in NCC cake. ☐ High crystallinity (68%), ☐ Fibres of 15–40 nm diameter and micron lengths ☐ Formation of sIPN with use of acrylamides	☐ Thermal stability lowered from 258 °C to 230 °C	Yang et al. [170,171]
Chemical	Softwood Kraft Ligning derived Renol-PBAT	Reactive	Reactive extrusion using Kraft Lignin and an epoxy stearate with a twin-screw extruder at a temperature profile of 120/160/150/150 °C (feeder to die), 60 rpm and a round hole die; with a 15 min residence time	me, bf	☐ Monophasic structure (good miscibility between Renol and PBAT) ☐ Low crystallinity: 11–13% ☐ Densely packed layers.	☐ Mechanical strength when the lignin content was relatively lower in proportion to the epoxy stearate. ☐ Glass transition temperature of 112 °C ☐ Highly recyclable/compostable.	Avella et al. [179]

(*continued on next page*)

Table 2 (*continued*)

	Lignocellulosic material(s)	Process Chemistry & Design Summary			Micro- and Macro-Structure Property	Functional Property (Performance)	Refs
		RP^a	S/P^b	FF^c			
						☐ Water-insoluble over 72 h ☐ Degradation *ca.* 90 days. ☐ Opaque films	
Chemical	MCC-*g*-PLLA	Reactive	Solvent-free grafting process in a compression moulding setup, involving an L-Lactide in a Sn(Oct)$_2$-catalysed surface functionalisation reaction and then compression moulding using a hot press at 180 °C for 5–120 min. Further preparation by micro-injection moulding and extrusion	tc/hp., me, im	☐ Crystallinity ranges from 12% to 33%, with higher MCC grafting with PLLA.	☐ Little changes in thermal stability. ☐ Significant decrease in water permeability from 66% to 45% ☐ Plastication occurs at 210 °C.	Genovese et al. [177]
Chemical	CNC-PEAA, TMP-PEAA, CNC-PCL	Reactive	Wet-mixing for CNC-PEAA and dry-mixing for TMP-PEAA, using an extrusion process at <170 °C for the former and 120 °C for the latter	me, im	☐ CNC aggregations ☐ Low shear homogenisation ☐ L/D of screw extruder poses impacted CNC fibre aspects, bundling and size, relative to the blend polymer matrix.	☐ Elasticity improved with NCC and/or TMP inclusion. ☐ Tensility: 15–16 MPa for NCC- PEAA and TMP-PEAA for 15–25 MPa ☐ Structural stiffness: 32–36 MPa NCC/PCL and 40–42 MPa NCC-PEAA	Venkatesh et al. [178]
Torrefaction	Wheat Straw MCC/PHBV	Reactive	Percolated/Thermal treatment in an inert sweeping environment for rapid defibrillation and lignin depolymerisation by a cold-hot-cold regime for 45 min at 230 °C. Melt-extrusion with PHBV at 160–180 °C, 300 rpm using a rod die; and thermo-compressed at 170 °C, 150 atm for 5 min	tc/hp., me	☐ Holocellulose fibre breakdown ☐ Crystallinity of 60–64% ☐ Higher fibre/matrix adhesion.	☐ Thermal properties remained relatively unchanged *ca.* 115–119 °C ☐ Increased WVP of 7.3–15.7 g/(m^2 d) for a 3:10 w/w wheat MCC/PHBV composite. ☐ Lower mechanical strength ☐ Darkening increases with increasing torrefaction time (holocellulose breakdown)	Berthet et al. [164]
Microwave-assisted	Pine-based lignocellulose	Reactive; DES pretreatment	110–130 °C DES (ChCl/LA) pretreatment and high-pressure homogenisation (1360.9 atm). Followed by a microwave-assisted nano-fibrillation at 5–20 kV/cm, short pulse times (100 μs) at RTP.	sc	☐ Fibres without DES pretreatment had diameters of 60–90 nm and crystallinity near 64–70%. ☐ Fibres without DES pretreatment had diameters of 6–60 nm and crystallinity near 65–69%,	☐ DES pretreatment improved tensile strength (137–155 MPa). ☐ High thermal stabilities (310 °C). ☐ Hydrophobic ☐ UV-shading capacities	Kwon et al. [155]
Sonochemical	Sugarcane Bagasse NFC	Alkaline Hydrolysis	AHP hydrolysis for 4 h at ambient conditions followed by ultrasonically-assisted defibrillation in 1% H_2O_2 $_{(aq)}$ for 1–3 h.	sc, tc/hp	☐ Moderate to low crystallinity (61%). ☐ Bundled, entangled holocellulosic structures with fibres having diameters of 6–100 nm. ☐ Higher ultrasonication and AHP at 2 h led to improved defibrillation.	☐ High thermal resistance (300 to 350 °C). ☐ Hot-pressed NFC films had higher mechanical strength than solvent-cast ones (8×; 25 MPa *vs* 3.5 MPa)	Shahi et al. [65]
Sonochemical	Fatty acid cellulose ester (cellulose oleate), CO/PLLA	Reactive	Sonochemically-assisted cellulose derivatisation using oleic acid. Ultrasonication at 300 W/m^2 in DMSO, DMAc and pyridine		☐ DS: 0.37–1.71 ☐ Higher crystallinities are attained due to defibrillation. ☐ Rod-like fibre bundles ☐ High aspect ratios.	☐ DS of 1.23 led to higher thermoplasticity and glass transition temperatures *ca.* 160–173 °C	Hou et al. [185]

(*continued on next page*)

Table 2 (*continued*)

	Lignocellulosic material(s)	Process Chemistry & Design Summary			Micro- and Macro-Structure Property	Functional Property (Performance)	Refs
		RP[a]	S/P[b]	FF[c]			
						☐ CO/PLLA blends had a high tensile strength of 40.3 MPa.	
Biochemical/ Enzymatic	Corn cob-derived xylan/starch	Alkaline hydrolysis followed by enzymatic hydrolysis (xylanase)	Potash hydrolysis (24% w/w) in ambient conditions, followed by xylanase-driven hydrolysis at similar conditions	me	☐ Lignin content <13% ☐ The monophasic layering of starch and xylans (high miscibility)	☐ High tensile strength (120 MPa). ☐ Elastic modulus (1.2 GPa) ☐ Equilibrium moisture content decreased with increasing heat-treatment temperature (60–150 °C). ☐ Reduced hydrophilicity due to cellulose decrystallisation	Akkus et al. [63]
Biochemical/ Enzymatic	Wheat straw LCNF/ PLA and LCNF/ PBAT	Alkaline hydrolysis (Soda pulping), with enzymatic hydrolysis (Quimizime B)	Conventional soda pulping process, with enzymatic pretreatment for defibrillation and high-pressure homogenisation. The dehydration step using PEG was conducted at 40 °C prior to extrusion	bf, me	☐ Amourphousness ☐ A high degree of PLA branching	☐ Lignocellulose nanofibre reinforcement increased mechanical strength (<43 MPa) ☐ High thermal stability: 322 °C. ☐ < 99.9% UV-barrier property ☐ OTR: 600 $cm^3/(m^2{\cdot}d)$ ☐ WVP: 4.5×10^{-7}– 5.1×10^{-7} $g/(m^2{\cdot}d{\cdot}Pa)$. ☐ Low transparency (<36%) ☐ Shelf life increased by 21 days.	Bascón-Villegas et al. [175]
Biochemical/ Enzymatic	Birch Kraft pulp MCC and Lignin	Alcoholic fractionation with enzymatic hydrolysis (MetZyme)	Laccase-assisted (Metzyme) oxidation and *in-situ* polymerisation. Further involving, high-pressure homogenisation at 100 atm/pass.	sc	☐ A homogenous coating of lignin nanoparticles was observed within <40 nm of the MCC network.	☐ Thermal properties featured T_g *ca.* 89–162 °C for the birch and 78–161 °C spruce lignin/MCC composite films	Wang et al. [147,148]

[a] Reactive preparation type for the film precursors, *e.g.*, pretreatment, bleaching or hydrolysis step involved, [b] S/P - Synthetic/ Preparative, [c] FF – Film-forming; bf – blow-forming, im – injection moulding, me – melt extrusion, mi – melt-intercalation, ors – other, sc – solution casting, *sp.* – spray drying, tc/hp. – Thermocompressing/ Hot-pressing.

research, development and commercialisation projects such as the R3Pack, and the Sulachange Project to develop versatile consumer packaging materials from natural fibres and resources such as those derived from agro-industrial LBs [225,226].

TEV scores were assigned based on a similar approach taken by Qasem et al. [227]. The scores have been assigned based on the above discussion and the reported studies in the literature. TEV scores provide a semi-qualitative assessment of the supposed implications for each packaging front-end and back-end technology for potential packaging purposes. Further, the sustainability assessments performed by various LCA researchers on NFCs and LCNFs have been summarised and presented as follows in Table 3. The colorimetric scoreboard assigns ‘1’ (red box) for the lowest rating, ‘2’ (orange) for low, ‘3’ (yellow) for neutral, ‘4’ (lime green) for high, and ‘5’ (dark green) for highest rating against each sustainability parameter (see footnote, Table 3).

The data for the table has considered certain cases of Lignocellulose V/U approaches or packaging/film-forming processes that share similar operating requirements. The system boundaries, definitions and key assumptions can be found in the respective works cited herein.

For the various case processes set in Table 3. the mechanochemical valorisation and lignocellulose utilisation techniques have low TEV scores and low CC and CED scores, though these processes are more likely to integrate 12 Principles of Green Chemistry, proposed by DeVierno Kreuder et al. [241]. The use of materials and energy inputs, especially chemicals and reagents such as TEMPO (5.95 €/kg), APS (3.45 €/kg), with high-pressure homogenisation or other energy-intensive defibrillation techniques in addition to conventional mixing and reactive setups (0.98–2.21 €/kg) [242]. Such costing of material inputs, as well as energy inputs, significantly impacts the cost-effectiveness and marketability of the material’s life-cycle. In this regard, ILs offer a relatively cheaper option (<2.6–5.3 €/kg) [243].

Biochemical and chemical V/U processes are relatively more sustainable though the former is more prominent as a sustainable process than the former. Despite their innovativeness, microwave-assisted and sonochemical methods possess the lowest scores overall, predominantly owing to the energy demand-driven CC and CED that increase operating costs and other TEVs. While extrusion, injection moulding and thermo-compression processes are more technically mature, their CC, CED and CY scores are relatively borderline optimal and vary by material design requirements. Solvent coating and roll-coating are apparently much sustainable though technological maturity and other TEVs require certain improvements.

3.5. *Opportunities and persistent challenges*

Lignocelluloses have high moisture absorption characteristics that can often lead to poor barrier efficiency needed for packaging. Additionally, polymer-to-monomer conversion *via* valorisation techniques has been challenged by attaining consistent functional performance, subject to the effects of structural, crystallinity and lignin incrustation - lignin-carbohydrate complexation [170,171]. While these problems have been a major challenge for the use of lignocelluloses as biofuel

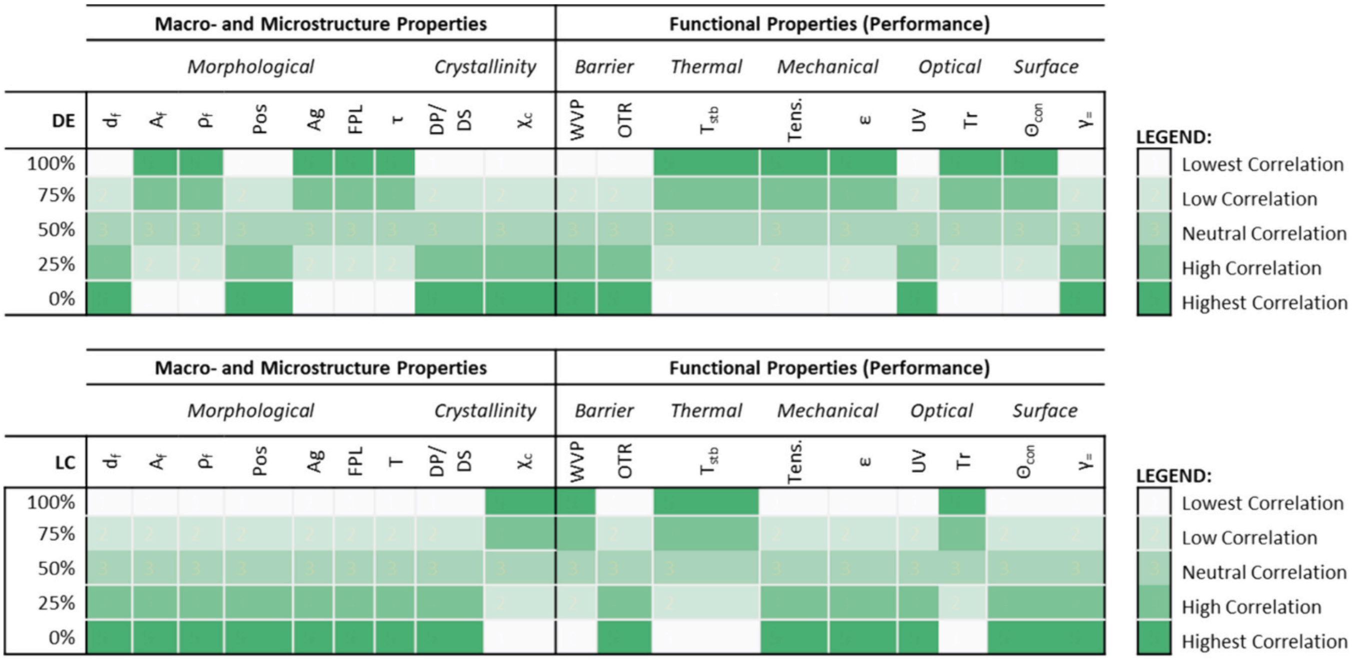

	Macro- and Microstructure Properties									Functional Properties (Performance)								
	Morphological								Crystallinity	Barrier		Thermal	Mechanical		Optical		Surface	
DE	d_f	A_f	ρ_f	Pos	Ag	FPL	τ	DP/ DS	χ_c	WVP	OTR	T_{stb}	Tens.	ε	UV	Tr	Θ_{con}	$\gamma_=$
100%	1	5	5	1	5	5	5	1	1	1	1	5	5	5	1	5	5	1
75%	2	4	4	2	4	4	4	2	2	2	2	4	4	4	2	4	4	2
50%	3	3	3	3	3	3	3	3	3	3	3	3	3	3	3	3	3	3
25%	4	2	2	4	2	2	2	4	4	4	4	2	2	2	4	2	2	4
0%	5	1	1	5	1	1	1	5	5	5	5	1	1	1	5	1	1	5

LEGEND:
Lowest Correlation
Low Correlation
Neutral Correlation
High Correlation
Highest Correlation

	Macro- and Microstructure Properties									Functional Properties (Performance)								
	Morphological								Crystallinity	Barrier		Thermal	Mechanical		Optical		Surface	
LC	d_f	A_f	ρ_f	Pos	Ag	FPL	T	DP/ DS	χ_c	WVP	OTR	T_{stb}	Tens.	ε	UV	Tr	Θ_{con}	$\gamma_=$
100%	1	1	1	1	1	1	1	1	5	5	1	5	1	1	1	5	1	1
75%	2	2	2	2	2	2	2	2	4	4	2	4	2	2	2	4	2	2
50%	3	3	3	3	3	3	3	3	3	3	3	3	3	3	3	3	3	3
25%	4	4	4	4	4	4	4	4	2	2	4	2	4	4	4	2	4	4
0%	5	5	5	5	5	5	5	5	1	1	5	1	5	5	5	1	5	5

LEGEND:
Lowest Correlation
Low Correlation
Neutral Correlation
High Correlation
Highest Correlation

Fig. 9. Simplified property-performance correlation table between cellulose nanofibril (NFC) content and lignin (L) content impact on macro- and microstructure properties and functional properties (performance). *Note*: DE – Defibrillation Extent, LC – Lignin Content, d_f – Fibre Diametre, A_f – area of fibre, DP/DS is the degree of polymerisation or substitution, χ – degree of crystallinity, Ag – aggregation, FPL – Fibril packing and layering, τ – the thickness (of the film), ρ_f – fibre density, Pos – Porosity, WVP – water vapour permeation, T_{stb} – Thermal stability, Tens. – tensility, ε – elasticity, UV – UV barrier, Tr – transparency, OTR – oxygen permeation rate, θ_{con} – contact angle, γ - Surface charge/tension (of fibre). Data from the literature above including Jiang et al. [48], Negro et al. [200], and Wang et al. [214].

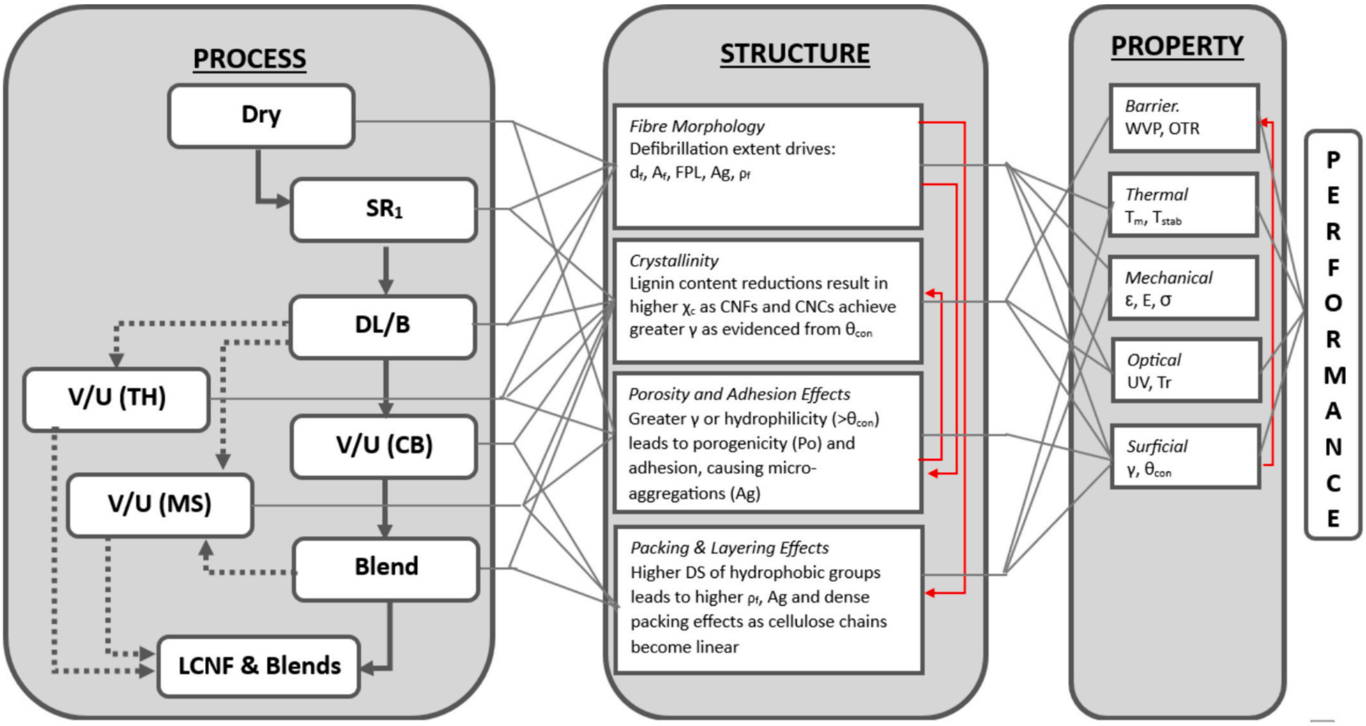

Fibre Morphology
Defibrillation extent drives: d_f, A_f, FPL, Ag, ρ_f

Crystallinity
Lignin content reductions result in higher χ_c as CNFs and CNCs achieve greater γ as evidenced from θ_{con}

Porosity and Adhesion Effects
Greater γ or hydrophilicity ($>\theta_{con}$) leads to porogenicity (Po) and adhesion, causing micro-aggregations (Ag)

Packing & Layering Effects
Higher DS of hydrophobic groups leads to higher ρ_f, Ag and dense packing effects as cellulose chains become linear

Fig. 10. A summative overview of the LCNF and blended LCNF Material Processing, Property, Structure, and Performance Relationship, *i.e.*, LCNF filler-matrix interaction and resulting outcomes. Data from the literature above including Jiang et al. [48], Negro et al. [200], Wang et al. [214], Koppolu et al. [215] and others in this work. *Note:* Dry – Drying process, pre-treatment handling, *e.g.*, sun-drying or oven-drying; SR_2 – Size reduction by mechanical means (microfibrillation and/or powderisation) for subsequent hydrolysis pre-treatment; DL/B – Partial Delignification, Bleaching (pre-treatment or hydrolysis reaction); V/U (TH) – Valorisation and utilisation by thermal means, V/U (MS) – Valorisation and utilisation by mechanical or sonicated means, V/U (CB) – Valorisation and utilisation by chemical or biochemical means.

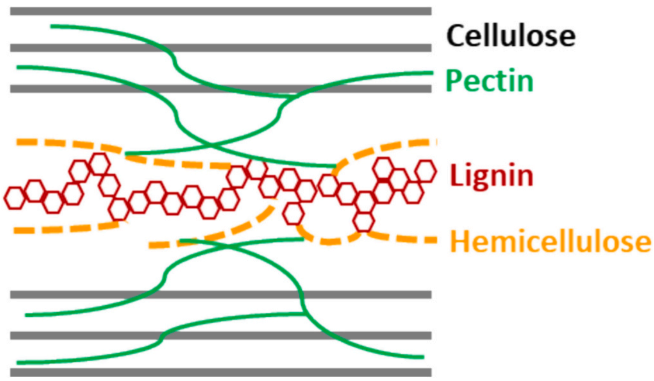

Fig. 11. A simplified schematic representing Cellulose-Hemicellulose-Lignin interactions within the cell walls.

precursors [86], these are anticipated to not be as impeding and discouraging as their potential for packaging plastics. In other words, the presence of lignin incrustation in agro-industrial lignocellulosic biomass and the bioplastics derived from them can add to desired biodegradability, mechanical strength, functionality and consumer features - transparency and haze - to an appreciable extent [244]. Alternative applications could see the conversion of lignocellulosic biomas to non-cellulosic yet sustainable green polymers such as L-polylactic acid (PLA) from plum biomass *via* a $SnCl_2$-based microwave-assisted polymerisation process, which offers cost-effective and alternative methods to conventional CO_2e-prone production processes [245]. The cost associated with a closed-loop circular production of green biopolymers is expected to have as little auxiliary/additive/reagent input as possible [246]. This has often been the converse case for contemporary lignocellulosic bioplastics preparations and formulations reported to date. Additives are typically considered to improve plasticity and other functional properties. Their addition is a common process/step for improving consumer-end performance (*i.e.*, the lifecycle of use, function, and mechanical properties) for other bioplastic materials [51].

Table 3
Sustainability assessment and TEV scoreboard for the process(es) for lignocellulose thermoplastic/bioplastic/packaging. Data acquired from corresponding literature [190,228–240]

	TEV Scores[1]							
	TR[2]	CE[3]	GC/GE[4]	CY[5]	CC[6]	CED[7]	**Process Description and Reported CO2e/GHGe & Electricity Consumption; per kg material produced**	**Ref**
Pre-treatment/Hydrolysis								
Mechanochemical Valorisation	2	2	4	2	3	1	TEMPO oxidation + mechanical refinement; 0.75-1.0 per kg CO_2e; s 100 kWh	Li *et al.*, (2013); Nascimento *et al.* (2016)
Thermomechanical Valorisation	3	2	2	3	2	4	NFC-epoxy composite preparation using mechanical defibrillation with thermo-compression, injection moulding and reactive processes (VARI); 1.9 per kg CO_2e; 5.25 kWh	Hervy *et al.*, (2015); Josset *et al.* (2014)
Chemical Valorisation	4		4	4	2	3	TEMPO oxidation, Acid hydrolysis; 1.0-1.8 per kg CO_2e; 190-1160 per kg NCC; 1.095-11.289 kWh	Li *et al.*, (2013); de Figueirêdo *et al.* (2012); Foroughi *et al.* (2021)
Biochemical /Enzymatic Valorisation	3	4	5	3	2	4	Enzymatic + HPH; MFC liberated (Enzymatic + homogenisation) + Wet spinning by adding Sodium Alginate; 1.2-3.1 kg CO_2e; 1.5-1.6 per 10 g of MCC; 0.198 kWh	Piccinno *et al.* (2015)
Sonochemical Valorisation	1	1	3	1	5	2	Extraction of CNC with high-powered ultrasound; 0.207 kg CO_2e; 5.93-15.36 kWh	Li *et al.*, (2013)
Microwave-assisted Valorisation	1	1	3	1	1	3	Microwave-assisted mercerisation with and without AHP and NaOH; 7 per kg CO_2e; 6.79 kWh	Camani *et al.* (2020)
Plasticisation/Packaging Process(es)								
Solvent/Blade Casting/Roll-to-Roll Coating	4	4	3	5	4	4	TEMPO NFC involving solvent casting, 7.53 per kg CO_2e; 24 kWh	Arfelis *et al.*(2023); Vohra *et al.* (2022); Moon *et al.* (2017)
Spray coating	4	3	4	4	3	3	n.a.; though qualitative data for said process using different materials provides a tentative baseline	Vohra *et al.* (2022);
Spin coating	2	2	2	2	3	2		Tu *et al.* (2020)
Melt-processing and Melt-intercalation	5	4	4	5	2	1		Banerjee and Ray, (2022)
Extrusion and Thermo-compression, Injection Moulding	5	3	3	5	2	1		Banerjee and Ray, (2022)
Electrospinning	4	3	4	5	4	2		Tu *et al.* (2020)
Solution Blowing	5	4	4	5	2	1		Arfelis *et al.*(2023)

[1]TEV - Techno-economic Viability, [2]TM – Technological Readiness, [3]CE – Cost-effectiveness, [4]GC/GE – Green Chemistry/Green Engineering Integration, [5]CY – commerciality, [6]CC – Climate Change Impact, as per CO_2e/GHGe – Carbon dioxide or greenhouse gas emission balance, [7]CED – Cumulative Energy Demand in kWh/kg.

These auxiliary materials add to production complexities and additional costs that could lead to poorer competitiveness of lignocellulosic biopolymers against other emerging or established candidates like poly (lactic acid) (PLA), poly(hydroxyalkanoates) (PHAs), poly(butylene succinate) (PBS) and poly(butylene adipate-*co*-terephthalate) (PBAT). Arguably, these so-called 'biopolymers' are still derived from fossil fuels and lack the desired biodegradability characteristics to mitigate microplastic pollution (European [56]).

4. Conclusion

Achieving an optimal balance between cellulose and lignin content is crucial for tailoring these materials to meet specific functional requirements in diverse applications. The type of process and treatment applied to lignocellulosic materials, along with the cellulose properties and lignin content, have a direct impact on the resulting functional properties, including crystallinity, mechanical strength, thermal stability, transparency, and barrier properties. The relations are complex and depend on the specific conditions and treatments applied during the processes.

Recent processing innovations have allowed us to achieve near-similar efficiency for lignocellulose bioplastics as their petroleum-based counterparts, such as *via* film extrusion, spinning, injection moulding, thermoforming and sheet-forming. The cost-effectiveness and optimal efficiency of these processes is an ongoing area of extensive research and development towards continuous improvement. While lignocellulose bioplastics offer consumer-end environmental safety and sustainability; the product value chain can involve extraction and processing steps that could undermine the zero-waste generation and carbon neutral or zero goals that are considered the 'sweet-point' for the circular plastic economy. These challenges present significant hurdles to the widespread adoption of lignocellulosic materials in packaging. However, ongoing research and development efforts continue to explore ways to overcome these challenges and make the use of these materials more feasible and sustainable.

4.1. Future perspectives

Most of the current cellulose-based materials rely on solvent-based processing methods that involve harmful solvents. However, natural cellulose products are difficult to produce using eco-friendly thermoplastic processing methods. There is a need to improve the processability of cellulose bioplastics, which have, to date, been attempted using relatively expensive materials that are often scarcely available despite their efficiency, offering an impractical option for the less developed and the developing world. Agro-industrial LB has been used to develop nanocellulose, simple cellulose esters (modified/composite cellulose acetate, oxalate and other carboxylate derivatives), or $C_{12–16}$ fatty acid cellulose esters (FACEs: cellulose oleate, stearate, laurate). The trade-off considerations between the performance/functionality and cost of the material limit the applicability and viability of these materials. This must be considered so that the adequate material is selected for optimum performance at an appreciable cost. This strategy may solve to a considerable extent, the issues mentioned prior. The intention to upcycle said wastes for thin-film technology applications presents a broad spectrum of reliable, high-efficiency, and ease in operational capabilities.

Funding

The authors have received no funding or research grants (and their source) received in the course of the study, research or assembly of the manuscript.

CRediT authorship contribution statement

M.J. Ahmed: Writing – review & editing, Writing – original draft, Visualization, Validation, Methodology, Investigation, Formal analysis, Data curation. **J. Ashfaq:** Writing – original draft, Methodology, Investigation, Formal analysis. **Z. Sohail:** Writing – original draft, Formal analysis, Data curation. **I.A. Channa:** Writing – review & editing, Supervision, Methodology, Conceptualization. **A. Sanchez-Ferrer:** Writing – review & editing, Validation, Conceptualization. **S.N. Ali:** Writing – review & editing, Supervision. **A.D. Chandio:** Writing – review & editing, Supervision.

Declaration of competing interest

The authors declare that they have no known competing financial interests or personal relationships that could have appeared to influence the work reported in this paper.

Data availability

All data used in the review paper are accessible within this paper and have been disclosed herein in its entirety.

Acknowledgement

Ahmed MJ would like to acknowledge the support of his supervisor, Dr.-Ing. Channa IA and co-supervisor Dr. Ali SN, who have provided unprecedented encouragement and support throughout his research in lignocellulosic materials for sustainable packaging. The first author would further express unyielding gratitude towards the Thin-Film Lab within the Advanced Materials and Surface Engineering (AMSE) Group, NED University of Engineering and Technology for the technical support and counsel offered to the researcher throughout his work and academic endeavour.

References

[1] H. Seddiqi, E. Oliaei, H. Honarkar, J. Jin, L.C. Geonzon, R.G. Bacabac, J. Klein-Nulend, Cellulose and its derivatives: towards biomedical applications, Cellulose 28 (4) (2021) 1893–1931, https://doi.org/10.1007/S10570-020-03674-W.

[2] H.S. Al-Battashi, N. Annamalai, N. Sivakumar, S. Al-Bahry, B.N. Tripathi, Q. D. Nguyen, V.K. Gupta, Lignocellulosic biomass (LCB): a potential alternative biorefinery feedstock for polyhydroxyalkanoates production, Rev. Environ. Sci. Bio/Technol. 18 (1) (2019) 183–205, https://doi.org/10.1007/S11157-018-09488-4.

[3] M. Brodin, M. Vallejos, M.T. Opedal, M.C. Area, G. Chinga-Carrasco, Lignocellulosics as sustainable resources for production of bioplastics – A review, J. Clean. Prod. 162 (2017) 646–664, https://doi.org/10.1016/J.JCLEPRO.2017.05.209.

[4] D. Kong, A.V. Dolzhenko, Cyrene: a bio-based sustainable solvent for organic synthesis, Sustain. Chem. Pharm. 25 (2022) 100591, https://doi.org/10.1016/j.scp.2021.100591.

[5] P. Willberg-Keyriläinen, J. Ropponen, Evaluation of esterification routes for long chain cellulose esters, Heliyon 5 (11) (2019), https://doi.org/10.1016/j.heliyon.2019.e02898.

[6] G. Tedeschi, S. Guzman-Puyol, U.C. Paul, M.J. Barthel, L. Goldoni, G. Caputo, L. Ceseracciu, A. Athanassiou, J.A. Heredia-Guerrero, Thermoplastic cellulose acetate oleate films with high barrier properties and ductile behaviour, Chem. Eng. J. 348 (2018) 840–849, https://doi.org/10.1016/J.CEJ.2018.05.031.

[7] European Commission, A European Strategy for Plastics. European Comission, July, 24, 2018, https://doi.org/10.1021/acs.est.7b02368.

[8] European Commission, Communication from the Commission to the European Parliament, the Council, the European Economic and Social Committee and the Committee of the Regions a New Circular Economy Action Plan For a Cleaner and More Competitive Europe. https://eur-lex.europa.eu/legal-content/EN/TXT/?qid=1583933814386&uri=COM:2020:98:FIN, 2020.

[9] European Commission, Improved Circular Economy Monitoring Framework Now Live, News Article., 2023. https://ec.europa.eu/eurostat/web/products-eurostat-news/w/wdn-20230515-1.

[10] A. Gil, Current insights into lignocellulose related waste valorization, Chem. Eng. J. Adv. 8 (2021) 100186, https://doi.org/10.1016/j.ceja.2021.100186.

[11] S. Asaadi, M. Hummel, S. Hellsten, T. Härkäsalmi, Y. Ma, A. Michud, H. Sixta, Renewable high-performance fibers from the chemical recycling of cotton waste utilizing an ionic liquid, ChemSusChem 9 (22) (2016) 3250–3258, https://doi.org/10.1002/cssc.201600680.

[12] F.H. Isikgor, C.R. Becer, Lignocellulosic biomass: a sustainable platform for the production of bio-based chemicals and polymers, Polym. Chem. 6 (25) (2015) 4497–4559, https://doi.org/10.1039/C5PY00263J.

[13] M.A. Mahmud, F.R. Anannya, Sugarcane bagasse - a source of cellulosic fiber for diverse applications, Heliyon 7 (8) (2021) e07771, https://doi.org/10.1016/J.HELIYON.2021.E07771.

[14] R. Khandanlou, G.C. Ngoh, W.T. Chong, Feasibility study and structural analysis of cellulose isolated from rice husk: microwave irradiation, optimization, and treatment process scheme, BioResources 11 (3) (2016), https://doi.org/10.15376/biores.11.3.5751-5766.

[15] N. Johar, I. Ahmad, A. Dufresne, Extraction, preparation and characterization of cellulose fibres and nanocrystals from rice husk, Ind. Crop. Prod. 37 (1) (2012) 93–99, https://doi.org/10.1016/j.indcrop.2011.12.016.

[16] N.D. Kambli, K.K. Samanta, S. Basak, S.K. Chattopadhyay, P.G. Patil, R. R. Deshmukh, Characterization of the corn husk fibre and improvement in its thermal stability by banana pseudostem sap, Cellulose 25 (9) (2018) 5241–5257, https://doi.org/10.1007/s10570-018-1931-z.

[17] L. Valentín, B. Kluczek-Turpeinen, S. Willför, J. Hemming, A. Hatakka, K. Steffen, M. Tuomela, Scots pine (*Pinus sylvestris*) bark composition and degradation by fungi: potential substrate for bioremediation, Bioresour. Technol. 101 (7) (2010) 2203–2209, https://doi.org/10.1016/j.biortech.2009.11.052.

[18] S. Pan, Y. Pu, M. Foston, A.J. Ragauskas, Compositional characterization and pyrolysis of loblolly pine and douglas-fir bark, Bioenergy Res. 6 (1) (2013) 24–34, https://doi.org/10.1007/s12155-012-9223-1.

[19] X. Duret, F. Emmanuel, P. Gérardin, E. Masson, Spruce bark hydrolysis to optimize phenolic content, Cellul. Chem. Technol. 46 (9–10) (2012) 541–550. https://www.researchgate.net/publication/263922483_Spruce_bark_hydrolysis_to_optimize_phenolic_content.

[20] F. Rusch, A.D. Wastowski, T.S. de Lira, K.C.C.S.R. Moreira, D. de Moraes Lúcio, Description of the component properties of species of bamboo: a review, Biomass Convers. Biorefinery 13 (3) (2023) 2487–2495, https://doi.org/10.1007/s13399-021-01359-3.

[21] Kalinowska Buzała, Boruszewski Małachowska, Krajewski, Przybysz, The effect of lignin content in Birch and beech Kraft cellulosic pulps on simple sugar yields from the enzymatic hydrolysis of cellulose, Energies 12 (15) (2019) 2952, https://doi.org/10.3390/en12152952.

[22] B.N. Kuznetsov, I.G. Sudakova, N.V. Garyntseva, A.M. Skripnikov, A.V. Pestunov, E.V. Gnidan, Birch wood biorefinery into microcrystalline, microfibrillated, and nanocrystalline celluloses, xylose, and adsorbents, Wood Sci. Technol. 57 (1) (2023) 173–196, https://doi.org/10.1007/s00226-022-01443-5.

[23] H.M. Boundzanga, B. Cagnon, M. Roulet, S. de Persis, C. Vautrin-Ul, S. Bonnamy, Contributions of hemicellulose, cellulose, and lignin to the mass and the porous characteristics of activated carbons produced from biomass residues by phosphoric acid activation, Biomass Convers. Biorefinery 12 (8) (2022) 3081–3096, https://doi.org/10.1007/s13399-020-00816-9.

[24] F. Rego, A.P. Soares Dias, M. Casquilho, F.C. Rosa, A. Rodrigues, Fast determination of lignocellulosic composition of poplar biomass by thermogravimetry, Biomass Bioenergy 122 (2019) 375–380, https://doi.org/10.1016/j.biombioe.2019.01.037.

[25] D. Díez, A. Urueña, R. Piñero, A. Barrio, T. Tamminen, Determination of hemicellulose, cellulose, and lignin content in different types of biomasses by thermogravimetric analysis and Pseudocomponent kinetic model (TGA-PKM method), Processes 8 (9) (2020) 1048, https://doi.org/10.3390/pr8091048.

[26] P. Pączkowski, A. Puszka, B. Gawdzik, Effect of eco-friendly Peanut Shell powder on the chemical resistance, physical, thermal, and thermomechanical properties of unsaturated polyester resin composites, Polymers 13 (21) (2021) 3690, https://doi.org/10.3390/polym13213690.

[27] C. Felgueiras, N.G. Azoia, C. Gonçalves, M. Gama, F. Dourado, Trends on the cellulose-based textiles: raw materials and technologies, Front. Bioeng. Biotechnol. 9 (2021), https://doi.org/10.3389/fbioe.2021.608826.

[28] G. Li, Y. Wang, D. Yu, P. Zhu, G. Zhao, C. Liu, H. Zhao, Ligninolytic characteristics of Pleurotus ostreatus cultivated in cotton stalk media, Front. Microbiol. 13 (2022), https://doi.org/10.3389/fmicb.2022.1035040.

[29] N. Stevulova, J. Cigasova, A. Estokova, E. Terpakova, A. Geffert, F. Kacik, E. Singovszka, M. Holub, Properties characterization of chemically modified hemp Hurds, Materials 7 (12) (2014) 8131–8150, https://doi.org/10.3390/ma7128131.

[30] S. Pirah, X. Wang, M. Javed, K. Simair, B. Wang, X. Sui, C. Lu, Lignocellulose extraction from sisal fiber and its use in green emulsions: a novel method, Polymers 14 (11) (2022) 2299, https://doi.org/10.3390/polym14112299.

[31] G. Zommere, A. Vilumsone, D. Kalnina, R. Solizenko, V. Stramkale, Comparative analysis of fiber structure and cellulose contents in flax and hemp fibres, Mater. Sci. Text. Cloth. Technol. 8 (2013) 96–104, https://doi.org/10.7250/mstct.2013.016.

[32] A. Álvarez, S. Cachero, C. González-Sánchez, J. Montejo-Bernardo, C. Pizarro, J. L. Bueno, Novel method for holocellulose analysis of non-woody biomass wastes, Carbohydr. Polym. 189 (2018) 250–256, https://doi.org/10.1016/j.carbpol.2018.02.043.

[33] TAPPI, Carbohydrate composition of extractive-free wood and wood pulp by gas-liquid chromatography, TAPPI Test Methods 5 (2004).

[34] G.W. Latimer (Ed.), Official Methods of Analysis of AOAC International, Oxford University PressNew York, 2023, https://doi.org/10.1093/9780197610145.001.0001.

[35] A. Sluiter, B. Hames, R. Ruiz, C. Scarlata, J. Sluiter, D. Templeton, D. Crocker, Determination of Structural Carbohydrates and Lignin in Biomass Laboratory Analytical Procedure (LAP) Issue Date: 7/17/2005. www.nrel.gov, 2008.

[36] R.G. Candido, A.R. Gonçalves, Synthesis of cellulose acetate and carboxymethylcellulose from sugarcane straw, Carbohydr. Polym. 152 (2016) 679–686, https://doi.org/10.1016/J.CARBPOL.2016.07.071.

[37] D.T.T. Nu, N.P. Hung, C. Van Hoang, B. Van der Bruggen, Preparation of an asymmetric membrane from sugarcane bagasse using DMSO as green solvent, Appl. Sci. 9 (16) (2019) 3347, https://doi.org/10.3390/APP9163347.

[38] J.G. Rosenboom, R. Langer, G. Traverso, Bioplastics for a circular economy, Nat. Rev. Mater. 7 (2) (2022) 117–137, https://doi.org/10.1038/s41578-021-00407-8.

[39] H.H. Cheng, L.M. Whang, Resource recovery from lignocellulosic wastes via biological technologies: advancements and prospects, Bioresour. Technol. 343 (2022) 126097, https://doi.org/10.1016/J.BIORTECH.2021.126097.

[40] H.-H. Cheng, L.-M. Whang, Resource recovery from lignocellulosic wastes via biological technologies: advancements and prospects, Bioresour. Technol. 343 (2022) 126097, https://doi.org/10.1016/j.biortech.2021.126097.

[41] A.R. Mankar, A. Pandey, A. Modak, K.K. Pant, Pretreatment of lignocellulosic biomass: a review on recent advances, Bioresour. Technol. 334 (2021) 125235, https://doi.org/10.1016/j.biortech.2021.125235.

[42] S. Periyasamy, V. Karthik, P. Senthil Kumar, J.B. Isabel, T. Temesgen, B. M. Hunegnaw, B.B. Melese, B.A. Mohamed, D.-V.N. Vo, Chemical, physical and biological methods to convert lignocellulosic waste into value-added products. A review, Environ. Chem. Lett. 20 (2) (2022) 1129–1152, https://doi.org/10.1007/s10311-021-01374-w.

[43] S. Islam, J.M. Cullen, Criteria for assessing sustainability of lignocellulosic wastes: applied to the cellulose nanofibril packaging production in the UK, Polymers 15 (6) (2023) 1336, https://doi.org/10.3390/polym15061336.

[44] K. Abe, Novel fabrication of high-modulus cellulose-based films by nanofibrillation under alkaline conditions, Carbohydr. Polym. 205 (2019) 488–491, https://doi.org/10.1016/j.carbpol.2018.10.069.

[45] M.M. Mahmud, A. Perveen, R.A. Jahan, M.A. Matin, S.Y. Wong, X. Li, M.T. Arafat, Preparation of different polymorphs of cellulose from different acid hydrolysis medium, Int. J. Biol. Macromol. 130 (2019) 969–976, https://doi.org/10.1016/j.ijbiomac.2019.03.027.

[46] H.V. Scheller, P. Ulvskov, Hemicelluloses, Annu. Rev. Plant Biol. 61 (1) (2010) 263–289, https://doi.org/10.1146/annurev-arplant-042809-112315.

[47] B. Saake, R. Lehnen, Lignin, in: Ullmann's Encyclopedia of Industrial Chemistry, Wiley, 2007, https://doi.org/10.1002/14356007.a15_305.pub3.

[48] Y. Jiang, X. Liu, Q. Yang, X. Song, C. Qin, S. Wang, K. Li, Effects of residual lignin on composition, structure and properties of mechanically defibrillated cellulose fibrils and films, Cellulose 26 (3) (2019) 1577–1593, https://doi.org/10.1007/s10570-018-02229-4.

[49] J. Pere, E. Pääkkönen, Y. Ji, E. Retulainen, Influence of the hemicellulose content on the fiber properties, strength, and formability of handsheets, BioResources 14 (1) (2019) 251–263, https://doi.org/10.15376/BIORES.14.1.251-263.

[50] G.P. Udayakumar, S. Muthusamy, B. Selvaganesh, N. Sivarajasekar, K. Rambabu, S. Sivamani, N. Sivakumar, J.P. Maran, A. Hosseini-Bandegharaei, Ecofriendly biopolymers and composites: preparation and their applications in water-treatment, Biotechnol. Adv. 52 (2021) 107815, https://doi.org/10.1016/J.BIOTECHADV.2021.107815.

[51] K. Ho, D. Tang, Lignocellulosic materials for green packaging: the prospects and challenges, Eng. Technol. J. 6 (7) (2021) 969–976, https://doi.org/10.47191/ETJ/V6I7.04.

[52] I. Haq, K. Qaisar, A. Nawaz, F. Akram, H. Mukhtar, X. Zohu, Y. Xu, M. Mumtaz, U. Rashid, W. Ghani, T. Choong, Advances in valorization of lignocellulosic biomass towards energy generation, Catalysts 11 (3) (2021) 309, https://doi.org/10.3390/catal11030309.

[53] V. Ashokkumar, R. Venkatkarthick, S. Jayashree, S. Chuetor, S. Dharmaraj, G. Kumar, W.-H. Chen, C. Ngamcharussrivichai, Recent advances in lignocellulosic biomass for biofuels and value-added bioproducts - A critical review, Bioresour. Technol. 344 (2022) 126195, https://doi.org/10.1016/j.biortech.2021.126195.

[54] European Bioplastics, Bioplastics Market Data. Report. https://www.european-bioplastics.org/market/, 2022.

[55] J. Poole, Bioplastics Boom: Global Production Will Triple in Five Years as Asia Dominates, Finds EUBP, 2021. Web Report. https://www.packaginginsights.com/news/bioplastics-boom-global-production-will-triple-in-five-years-as-asia-dominates-finds-eubp.html#:~:text=Bioplastics boom%3A Global production will triple in five,market data compiled in cooperation with the nova-Insti.

[56] European Bioplastics, Bioplastic Materials. https://www.european-bioplastics.org/bioplastics/materials/, 2022.

[57] Mordor Intelligence, Biodegradable Packaging Market Size & Share Analysis - Growth Trends & Forecasts (2023–2028), Business Report, 2023. https://www.mordorintelligence.com/industry-reports/gobal-biodegradable-packaging-solutions-market-industry.

[58] Y. Zhang, C. Zhang, Y. Wang, Recent progress in cellulose-based electrospun nanofibers as multifunctional materials, Nanoscale Adv. 3 (21) (2021) 6040–6047, https://doi.org/10.1039/D1NA00508A.

[59] D.F. Hou, M.L. Li, C. Yan, L. Zhou, Z.Y. Liu, W. Yang, M.B. Yang, Mechanochemical preparation of thermoplastic cellulose oleate by ball milling, Green Chem. 23 (5) (2021) 2069–2078, https://doi.org/10.1039/D0GC03853A.

[60] J. Li, X. Zhang, J. Zhang, Q. Mi, F. Jia, J. Wu, J. Yu, J. Zhang, Direct and complete utilization of agricultural straw to fabricate all-biomass films with high-strength, high-haze and UV-shielding properties, Carbohydr. Polym. 223 (2019) 115057, https://doi.org/10.1016/j.carbpol.2019.115057.

[61] S. Fujisawa, Material design of nanocellulose/polymer composites via Pickering emulsion templating, Polym. J. 53 (1) (2021) 103–109, https://doi.org/10.1038/s41428-020-00408-4.

[62] E. Espino-Pérez, R.G. Gilbert, S. Domenek, M.C. Brochier-Salon, M.N. Belgacem, J. Bras, Nanocomposites with functionalised polysaccharide nanocrystals through aqueous free radical polymerisation promoted by ozonolysis, Carbohydr. Polym. 135 (2016) 256–266, https://doi.org/10.1016/j.carbpol.2015.09.005.

[63] M. Akkus, E. Bahcegul, N. Ozkan, U. Bakir, Post-extrusion heat-treatment as a facile method to enhance the mechanical properties of extruded xylan-based polymeric materials, RSC Adv. 4 (107) (2014) 62295–62300, https://doi.org/10.1039/C4RA10478A.

[64] J. Xia, Z. Liu, Y. Chen, Z. Wang, Y. Cao, Fabrication of thermo-sensitive lignocellulose hydrogels with switchable hydrophilicity and hydrophobicity through an SIPN strategy, RSC Adv. 9 (51) (2019) 29600–29608, https://doi.org/10.1039/C9RA05575D.

[65] N. Shahi, B. Min, B. Sapkota, V.K. Rangari, Eco-friendly cellulose nanofiber extraction from sugarcane bagasse and film fabrication, Sustainability 12 (15) (2020) 6015, https://doi.org/10.3390/SU12156015.

[66] F. Jérôme, G. Chatel, K. De Oliveira Vigier, Depolymerization of cellulose to processable glucans by non-thermal technologies, Green Chem. 18 (14) (2016) 3903–3913, https://doi.org/10.1039/C6GC00814C.

[67] A. Shrotri, L.K. Lambert, A. Tanksale, J. Beltramini, Mechanical depolymerisation of acidulated cellulose: understanding the solubility of high molecular weight oligomers, Green Chem. 15 (10) (2013) 2761, https://doi.org/10.1039/c3gc40945g.

[68] R.A. Ilyas, S.M. Sapuan, R. Ibrahim, H. Abral, M.R. Ishak, E.S. Zainudin, M.S. N. Atikah, N. Mohd Nurazzi, A. Atiqah, M.N.M. Ansari, E. Syafri, M. Asrofi, N. H. Sari, R. Jumaidin, Effect of sugar palm nanofibrillated cellulose concentrations on morphological, mechanical and physical properties of biodegradable films based on agro-waste sugar palm (Arenga pinnata (Wurmb.) Merr) starch, J. Mater. Res. Technol. 8 (5) (2019) 4819–4830, https://doi.org/10.1016/j.jmrt.2019.08.028.

[69] P. Willberg-Keyriläinen, J. Vartiainen, A. Harlin, J. Ropponen, The effect of side-chain length of cellulose fatty acid esters on their thermal, barrier and mechanical properties, Cellulose 24 (2) (2017) 505–517, https://doi.org/10.1007/s10570-016-1165-x.

[70] Y. Zhang, L. Wei, H. Hu, Z. Zhao, Z. Huang, A. Huang, F. Shen, J. Liang, Y. Qin, Tribological properties of nano cellulose fatty acid esters as ecofriendly and effective lubricant additives, Cellulose 25 (5) (2018) 3091–3103, https://doi.org/10.1007/s10570-018-1780-9.

[71] H. Hu, H. Li, Y. Zhang, Y. Chen, Z. Huang, A. Huang, Y. Zhu, X. Qin, B. Lin, Green mechanical activation-assisted solid phase synthesis of cellulose esters using a co-reactant: effect of chain length of fatty acids on reaction efficiency and structure properties of products, RSC Adv. 5 (27) (2015) 20656–20662, https://doi.org/10.1039/C5RA02393A.

[72] C. Vaca-Garcia, M.E. Borredon, Solvent-free fatty acylation of cellulose and lignocellulosic wastes. Part 2: reactions with fatty acids, Bioresour. Technol. 70 (2) (1999) 135–142, https://doi.org/10.1016/S0960-8524(99)00034-6.

[73] Y. Zhao, J. Li, Q. Yu, K.D. Li, Q. Li, R. Zhou, R. Zhou, M. Ek, K.K. Ostrikov, Fabrication of multidimensional bio-nanomaterials from nanocellulose oxalate, Cellulose 30 (4) (2023) 2147–2163, https://doi.org/10.1007/s10570-022-05019-1.

[74] L. Szcześniak, A. Rachocki, J. Tritt-Goc, Glass transition temperature and thermal decomposition of cellulose powder, Cellulose 15 (3) (2008) 445–451, https://doi.org/10.1007/s10570-007-9192-2.

[75] X. Ouyang, Effect of simultaneous steam explosion and alkaline Depolymerization on corncob lignin and cellulose structure, Chem. Biochem. Eng. Q. 32 (2) (2018) 177–189, https://doi.org/10.15255/CABEQ.2017.1251.

[76] N. Ali, Q. Zhang, Z.-Y. Liu, F.-L. Li, M. Lu, X.-C. Fang, Emerging technologies for the pretreatment of lignocellulosic materials for bio-based products, Appl. Microbiol. Biotechnol. 104 (2) (2020) 455–473, https://doi.org/10.1007/s00253-019-10158-w.

[77] B. Deepa, E. Abraham, R.R. Koshy, L.A. Pothan, S. Thomas, Extraction and characterization of cellulose nanofibers from Banana plant, in: Handbook of Polymer Nanocomposites. Processing, Performance and Application, Springer, Berlin Heidelberg, 2015, pp. 65–80, https://doi.org/10.1007/978-3-642-45232-1_54.

[78] M.A. Hubbe, O.J. Rojas, L.A. Lucia, M. Sain, Cellulosic nanocomposites. A review, BioResources 3 (3) (2008) 929–980, https://doi.org/10.15376/biores.3.3.929-980.

[79] M. Michelin, D.G. Gomes, A. Romaní, M. de L.T.M. Polizeli, J.A. Teixeira, Nanocellulose production: exploring the enzymatic route and residues of pulp and paper industry, Molecules 25 (15) (2020) 3411, https://doi.org/10.3390/molecules25153411.

[80] H.P.S. Abdul Khalil, Y. Davoudpour, M.N. Islam, A. Mustapha, K. Sudesh, R. Dungani, M. Jawaid, Production and modification of nanofibrillated cellulose using various mechanical processes: A review, Carbohydr. Polym. 99 (2014) 649–665, https://doi.org/10.1016/j.carbpol.2013.08.069.

[81] A.M. Fontes, C.L. Pirich, G.R.O.A. Tanobe, Q. Tarrés, M. Delgado-Aguilar, L. P. Ramos, Micro/nanostructured lignonanocellulose obtained from steam-exploded sugarcane bagasse, Cellulose 28 (16) (2021) 10163–10182, https://doi.org/10.1007/s10570-021-04205-x.

[82] D. Chen, D. Lawton, M.R. Thompson, Q. Liu, Biocomposites reinforced with cellulose nanocrystals derived from potato peel waste, Carbohydr. Polym. 90 (1) (2012) 709–716, https://doi.org/10.1016/J.CARBPOL.2012.06.002.

[83] X. Yu, Y. Jiang, Q. Wu, Z. Wei, X. Lin, Y. Chen, Preparation and characterization of cellulose nanocrystal extraction from Pennisetum hydridum fertilized by municipal sewage sludge via sulfuric acid hydrolysis, Front. Energy Res. 9 (2021), https://doi.org/10.3389/fenrg.2021.774783.

[84] V.G. Firsty, J.Y. Jeong, Y.M. Gu, J.H. Lee, S.-J. Shin, High cellulose purity by acid hydrolysis pretreatment on Kenaf outer Bast, Appl. Sci. 13 (1) (2022) 334, https://doi.org/10.3390/app13010334.

[85] A.I. Quilez-Molina, U. Chandra Paul, D. Merino, A. Athanassiou, Composites of thermoplastic starch and lignin-rich agricultural waste for the packaging of fatty foods, ACS Sustain. Chem. Eng. 10 (47) (2022) 15402–15413, https://doi.org/10.1021/acssuschemeng.2c04326.

[86] R. Reshmy, D. Thomas, E. Philip, S.A. Paul, A. Madhavan, R. Sindhu, R. Sirohi, S. Varjani, A. Pugazhendhi, A. Pandey, P. Binod, Bioplastic production from renewable lignocellulosic feedstocks: a review, Rev. Environ. Sci. Biotechnol. 20 (1) (2021) 167–187, https://doi.org/10.1007/s11157-021-09565-1.

[87] A. Blasi, A. Verardi, C.G. Lopresto, S. Siciliano, P. Sangiorgio, Lignocellulosic agricultural waste valorization to obtain valuable products: an overview, Recycling 8 (4) (2023) 61, https://doi.org/10.3390/recycling8040061.

[88] Y. Liu, B. Chen, Y. Lv, X. Ye, C. Lin, M. Liu, Insight into the performance of lignin-containing cellulose nanofibers (LCNFs) via lignin content regulation by p-toluenesulfonic acid delignification, Cellulose 29 (4) (2022) 2273–2287, https://doi.org/10.1007/s10570-022-04432-w.

[89] D. Li, J. Henschen, M. Ek, Esterification and hydrolysis of cellulose using oxalic acid dihydrate in a solvent-free reaction suitable for preparation of surface-functionalised cellulose nanocrystals with high yield, Green Chem. 19 (23) (2017) 5564–5567, https://doi.org/10.1039/C7GC02489D.

[90] T. Huang, K.D. Li, M. Ek, Hydrophobization of cellulose oxalate using oleic acid in a catalyst-free esterification suitable for preparing reinforcement in polymeric composites, Carbohydr. Polym. 257 (2021) 117615, https://doi.org/10.1016/j.carbpol.2021.117615.

[91] X. Yang, S.R. Liew, R. Bai, Simultaneous alkaline hydrolysis and non-solvent induced phase separation method for polyacrylonitrile (PAN) membrane with highly hydrophilic and enhanced anti-fouling performance, J. Membr. Sci. 635 (2021) 119499, https://doi.org/10.1016/J.MEMSCI.2021.119499.

[92] Y. Yang, Y. Shi, X. Cao, Q. Liu, H. Wang, B. Kong, Preparation and functional properties of poly(vinyl alcohol)/ethyl cellulose/tea polyphenol electrospun nanofibrous films for active packaging material, Food Control 130 (2021) 108331, https://doi.org/10.1016/j.foodcont.2021.108331.

[93] J. Damaurai, T. Preechakun, M. Raita, V. Champreda, N. Laosiripojana, Investigation of alkaline hydrogen peroxide in aqueous organic solvent to enhance enzymatic hydrolysis of Rice straw, Bioenergy Res. 14 (1) (2021) 122–134, https://doi.org/10.1007/s12155-020-10152-5.

[94] M.C. Ho, V.Z. Ong, T.Y. Wu, Potential use of alkaline hydrogen peroxide in lignocellulosic biomass pretreatment and valorization – A review, Renew. Sust. Energ. Rev. 112 (2019) 75–86, https://doi.org/10.1016/j.rser.2019.04.082.

[95] E.D. Dutra, F.A. Santos, B.R.A. Alencar, A.L.S. Reis, R. de F.R. de Souza, K.A. da S. Aquino, M.A. Morais Jr., R.S.C. Menezes, Alkaline hydrogen peroxide pretreatment of lignocellulosic biomass: status and perspectives, Biomass Convers. Biorefinery 8 (1) (2018) 225–234, https://doi.org/10.1007/s13399-017-0277-3.

[96] G.T. Melesse, F.G. Hone, M.A. Mekonnen, Extraction of cellulose from sugarcane bagasse optimization and characterization, Adv. Mater. Sci. Eng. 2022 (2022) 1–10, https://doi.org/10.1155/2022/1712207.

[97] X. Cao, S. Sun, X. Peng, L. Zhong, R. Sun, D. Jiang, Rapid synthesis of cellulose esters by transesterification of cellulose with vinyl esters under the catalysis of NaOH or KOH in DMSO, J. Agric. Food Chem. 61 (10) (2013) 2489–2495, https://doi.org/10.1021/JF3055104.

[98] G. Zope, A. Goswami, S. Kulkarni, Isolation and characterization of cellulose nanocrystals produced by acid hydrolysis from Banana Pseudostem, BioNanoScience 12 (2) (2022) 463–471, https://doi.org/10.1007/s12668-022-00960-8.

[99] P. Abdeshahian, J.J. Ascencio, R.R. Philippini, F.A.F. Antunes, A.S. de Carvalho, M. Abdeshahian, J.C. dos Santos, S.S. da Silva, Valorization of lignocellulosic biomass and agri-food processing wastes for production of glucan polymer, Waste Biomass Valoriz. 12 (6) (2021) 2915–2931, https://doi.org/10.1007/s12649-020-01267-z.

[100] C.-L. Song, J.B. Othman, Synthesis and characterization of lignin-incorporated Carboxymethyl cellulose (CMC) films from oil palm lignocellulosic waste, Processes 10 (11) (2022) 2205, https://doi.org/10.3390/pr10112205.

[101] C. Aulin, G. Flodberg, G. Ström, T. Lindström, Enhanced mechanical and gas barrier performance of plasticized cellulose nanofibril films, Nordic Pulp & Paper Res. J. 37 (1) (2022) 138–148, https://doi.org/10.1515/npprj-2021-0061.

[102] H. Kargarzadeh, I. Ahmad, I. Abdullah, A. Dufresne, S.Y. Zainudin, R.M. Sheltami, Effects of hydrolysis conditions on the morphology, crystallinity, and thermal stability of cellulose nanocrystals extracted from kenaf bast fibers, Cellulose 19 (3) (2012) 855–866, https://doi.org/10.1007/s10570-012-9684-6.

[103] J. Zhang, J. Wu, J. Yu, X. Zhang, J. He, J. Zhang, Application of ionic liquids for dissolving cellulose and fabricating cellulose-based materials: state of the art and future trends, Mater. Chem. Front. 1 (7) (2017) 1273–1290, https://doi.org/10.1039/C6QM00348F.

[104] L. Szabó, R. Milotskyi, G. Sharma, K. Takahashi, Cellulose processing in ionic liquids from a materials science perspective: turning a versatile biopolymer into the cornerstone of our sustainable future, Green Chem. 25 (14) (2023) 5338–5389, https://doi.org/10.1039/D2GC04730F.

[105] S. Taokaew, W. Kriangkrai, Recent Progress in processing cellulose using ionic liquids as solvents, Polysaccharides 3 (4) (2022) 671–691, https://doi.org/10.3390/polysaccharides3040039.

[106] B. Azimi, H. Maleki, V. Gigante, R. Bagherzadeh, A. Mezzetta, M. Milazzo, L. Guazzelli, P. Cinelli, A. Lazzeri, S. Danti, Cellulose-based fiber spinning processes using ionic liquids, Cellulose 29 (6) (2022) 3079–3129, https://doi.org/10.1007/s10570-022-04473-1.

[107] Z. Xia, J. Li, J. Zhang, X. Zhang, X. Zheng, J. Zhang, Processing and valorization of cellulose, lignin and lignocellulose using ionic liquids, J. Bioresourc. Bioprod. 5 (2) (2020) 79–95, https://doi.org/10.1016/j.jobab.2020.04.001.

[108] N.A. Nguyen, K. Kim, C.C. Bowland, J.K. Keum, L.T. Kearney, N. André, N. Labbé, A.K. Naskar, A fundamental understanding of whole biomass dissolution in ionic liquid for regeneration of fiber by solution-spinning, Green Chem. 21 (16) (2019) 4354–4367, https://doi.org/10.1039/C9GC00774A.

[109] H. Wang, G. Gurau, R.D. Rogers, Ionic liquid processing of cellulose, Chem. Soc. Rev. 41 (4) (2012) 1519, https://doi.org/10.1039/c2cs15311d.

[110] E. Carmichael, E. Ghassemieh, G. Lyons, Biorefining of lignocellulosic feedstock and waste materials using ionic liquid, Mater. Sci. Eng. B 262 (2020) 114741, https://doi.org/10.1016/j.mseb.2020.114741.

[111] B. Kosan, C. Michels, F. Meister, Dissolution and forming of cellulose with ionic liquids, Cellulose 15 (1) (2008) 59–66, https://doi.org/10.1007/s10570-007-9160-x.

[112] M.J. Earle, J.M.S.S. Esperança, M.A. Gilea, J.N. Canongia Lopes, L.P.N. Rebelo, J. W. Magee, K.R. Seddon, J.A. Widegren, The distillation and volatility of ionic liquids, Nature 439 (7078) (2006) 831–834, https://doi.org/10.1038/nature04451.

[113] X. Zhang, N. Xiao, M. Chen, Y. Wei, C. Liu, Functional packaging films originating from hemicelluloses laurate by direct transesterification in ionic liquid, Carbohydr. Polym. 229 (2020) 115336, https://doi.org/10.1016/j.carbpol.2019.115336.

[114] S. Suzuki, H. Hikita, S.C. Hernandez, N. Wada, K. Takahashi, Direct conversion of sugarcane bagasse into an injection-moldable cellulose-based thermoplastic via homogeneous esterification with mixed acyl groups, ACS Sustain. Chem. Eng. 9 (17) (2021) 5933–5941, https://doi.org/10.1021/acssuschemeng.1c00306.

[115] J. Lease, T. Kawano, Y. Andou, Esterification of cellulose with long fatty acid chain through mechanochemical method, Polymers 13 (24) (2021) 4397, https://doi.org/10.3390/POLYM13244397/S1.

[116] J. Wu, X. Du, Z. Yin, S. Xu, S. Xu, Y. Zhang, Preparation and characterization of cellulose nanofibrils from coconut coir fibers and their reinforcements in biodegradable composite films, Carbohydr. Polym. 211 (2019) 49–56, https://doi.org/10.1016/J.CARBPOL.2019.01.093.

[117] A. Isogai, T. Saito, H. Fukuzumi, TEMPO-oxidized cellulose nanofibers, Nanoscale 3 (1) (2011) 71–85, https://doi.org/10.1039/C0NR00583E.

[118] M. Wang, C. Shao, S. Zhou, J. Yang, F. Xu, Preparation of carbon aerogels from TEMPO-oxidized cellulose nanofibers for organic solvents absorption, RSC Adv. 7 (61) (2017) 38220–38230, https://doi.org/10.1039/C7RA05506D.

[119] A. Naderi, T. Lindström, A comparative study of the rheological properties of three different nanofibrillated cellulose systems, Nordic Pulp & Paper Res. J. 31 (3) (2016) 354–363, https://doi.org/10.3183/npprj-2016-31-03-p354-363.

[120] L. Dai, J. Chen, B. Yang, Y. Su, L. Chen, Z. Long, Y. Ni, TEMPO-oxidized waste cellulose as reinforcement for recycled Fiber networks, Ind. Eng. Chem. Res. 56 (51) (2017) 15065–15071, https://doi.org/10.1021/acs.iecr.7b04135.

[121] R. Ciriminna, M. Pagliaro, Industrial oxidations with Organocatalyst TEMPO and its derivatives, Org. Process. Res. Dev. 14 (1) (2010) 245–251, https://doi.org/10.1021/op900059x.

[122] R. Travaini, J. Martín-Juárez, A. Lorenzo-Hernando, S. Bolado-Rodríguez, Ozonolysis: an advantageous pretreatment for lignocellulosic biomass revisited, Bioresour. Technol. 199 (2016) 2–12, https://doi.org/10.1016/j.biortech.2015.08.143.

[123] V. Gitifar, R. Eslamloueyan, M. Sarshar, Experimental study and neural network modeling of sugarcane bagasse pretreatment with H2SO4 and O3 for cellulosic material conversion to sugar, Bioresour. Technol. 148 (2013) 47–52, https://doi.org/10.1016/j.biortech.2013.08.060.

[124] N.A. Mamleeva, S.A. Autlov, N.G. Bazarnova, V.V. Lunin, Delignification of softwood by ozonation, Pure Appl. Chem. 81 (11) (2009) 2081–2091, https://doi.org/10.1351/PAC-CON-08-10-11.

[125] T. Sugimoto, K. Magara, S. Hosoya, S. Oosawa, T. Shimoda, K. Nishibori, Ozone pretreatment of lignocellulosic materials for ethanol production: improvement of enzymatic susceptibility of softwood, Holzforschung 63 (5) (2009) 537–543, https://doi.org/10.1515/HF.2009.091.

[126] A. Martínez-Abad, A.C. Ruthes, F. Vilaplana, Enzymatic-assisted extraction and modification of lignocellulosic plant polysaccharides for packaging applications, J. Appl. Polym. Sci. 133 (2) (2016), https://doi.org/10.1002/app.42523.

[127] B.L. Cantarel, P.M. Coutinho, C. Rancurel, T. Bernard, V. Lombard, B. Henrissat, The carbohydrate-active EnZymes database (CAZy): an expert resource for Glycogenomics, Nucleic Acids Res. 37 (Database) (2009) D233–D238, https://doi.org/10.1093/nar/gkn663.

[128] V. Lombard, H. Golaconda Ramulu, E. Drula, P.M. Coutinho, B. Henrissat, The carbohydrate-active enzymes database (CAZy) in 2013, Nucleic Acids Res. 42 (D1) (2014) D490–D495, https://doi.org/10.1093/nar/gkt1178.

[129] Z. Benkő, M. Siika-aho, L. Viikari, K. Réczey, Evaluation of the role of xyloglucanase in the enzymatic hydrolysis of lignocellulosic substrates, Enzym. Microb. Technol. 43 (2) (2008) 109–114, https://doi.org/10.1016/j.enzmictec.2008.03.005.

[130] N. Piqué, M. Gómez-Guillén, M. Montero, Xyloglucan, a plant polymer with barrier protective properties over the mucous membranes: an overview, Int. J. Mol. Sci. 19 (3) (2018) 673, https://doi.org/10.3390/ijms19030673.

[131] A.C. Alavarse, E.C.G. Frachini, R.L.C.G. da Silva, V.H. Lima, A. Shavandi, D.F. S. Petri, Crosslinkers for polysaccharides and proteins: synthesis conditions, mechanisms, and crosslinking efficiency, a review, Int. J. Biol. Macromol. 202 (2022) 558–596, https://doi.org/10.1016/j.ijbiomac.2022.01.029.

[132] M.B. Agustin, D.M. de Carvalho, M.H. Lahtinen, K. Hilden, T. Lundell, K. S. Mikkonen, Laccase as a tool in building advanced lignin-based materials, ChemSusChem 14 (21) (2021) 4615–4635, https://doi.org/10.1002/cssc.202101169.

[133] Y. Lu, Q. He, G. Fan, Q. Cheng, G. Song, Extraction and modification of hemicellulose from lignocellulosic biomass: a review, Green Proc. Synth. 10 (1) (2021) 779–804, https://doi.org/10.1515/gps-2021-0065.

[134] J.C. Martins-Vieira, P.C. Torres-Mayanga, D. Lachos-Perez, Hydrothermal processing of lignocellulosic biomass: an overview of subcritical and supercritical water hydrolysis, Bioenergy Res. 16 (3) (2023) 1296–1317, https://doi.org/10.1007/s12155-022-10553-8.

[135] W. Xia, K. Zhang, L. Su, J. Wu, Microbial starch debranching enzymes: developments and applications, Biotechnol. Adv. 50 (2021) 107786, https://doi.org/10.1016/j.biotechadv.2021.107786.

[136] Z. Wei, J.H. Yang, X.J. Du, F. Xu, M. Zrinyi, Y. Osada, F. Li, Y.M. Chen, Dextran-based self-healing hydrogels formed by reversible Diels–Alder reaction under physiological conditions, Macromol. Rapid Commun. 34 (18) (2013) 1464–1470, https://doi.org/10.1002/marc.201300494.

[137] S. Cichosz, A. Masek, Thermal behavior of green cellulose-filled thermoplastic elastomer polymer blends, Molecules 25 (6) (2020) 1279, https://doi.org/10.3390/molecules25061279.

[138] V. Kumar, R. Sehgal, R. Gupta, Blends and composites of polyhydroxyalkanoates (PHAs) and their applications, Eur. Polym. J. 161 (2021) 110824, https://doi.org/10.1016/j.eurpolymj.2021.110824.

[139] R. Santi, A. Cigada, B. Del Curto, S. Farè, Modulable properties of PVA/cellulose fiber composites, J. Appl. Biomater. Funct. Mater. 17 (1) (2019), https://doi.org/10.1177/2280800019831224, 228080001983122.

[140] Y. Xie, Y. Pan, P. Cai, Hydroxyl crosslinking reinforced bagasse cellulose/polyvinyl alcohol composite films as biodegradable packaging, Ind. Crop. Prod. 176 (2022) 114381, https://doi.org/10.1016/j.indcrop.2021.114381.

[141] D. Trache, A.F. Tarchoun, M. Derradji, T.S. Hamidon, N. Masruchin, N. Brosse, M. H. Hussin, Nanocellulose: from fundamentals to advanced applications, Front. Chem. 8 (2020), https://doi.org/10.3389/fchem.2020.00392.

[142] J. Ashfaq, I.A. Channa, A.A. Shaikh, A.D. Chandio, A.A. Shah, B. Bughio, A. Birmahani, S. Alshehri, M.M. Ghoneim, Gelatin- and papaya-based biodegradable and edible packaging films to counter plastic waste generation, Materials 15 (3) (2022) 1046, https://doi.org/10.3390/ma15031046.

[143] I.A. Channa, J. Ashfaq, M.A. Siddiqui, A.D. Chandio, M.A. Shar, A. Alhazaa, Multi-shaded edible films based on gelatin and starch for the packaging applications, Polymers 14 (22) (2022) 5020, https://doi.org/10.3390/polym14225020.

[144] M.M. Abe, J.R. Martins, P.B. Sanvezzo, J.V. Macedo, M.C. Branciforti, P. Halley, V.R. Botaro, M. Brienzo, Advantages and disadvantages of Bioplastics production from starch and lignocellulosic components, Polymers 13 (15) (2021) 2484, https://doi.org/10.3390/polym13152484.

[145] M. Sharahi, A. Hivechi, S.H. Bahrami, N. Hemmatinejad, P.B. Milan, Co-electrospinning of lignocellulosic nanoparticles synthesized from walnut shells with poly(caprolactone) and gelatin for tissue engineering applications, Cellulose 28 (8) (2021) 4943–4957, https://doi.org/10.1007/s10570-021-03709-w.

[146] A.A. Singh, M.E. Genovese, G. Mancini, L. Marini, A. Athanassiou, Green processing route for polylactic acid–cellulose fiber biocomposites, ACS Sustain. Chem. Eng. 8 (10) (2020) 4128–4136, https://doi.org/10.1021/acssuschemeng.9b06760.

[147] H.-M. Wang, T.-Q. Yuan, G.-Y. Song, R.-C. Sun, Advanced and versatile lignin-derived biodegradable composite film materials toward a sustainable world, Green Chem. 23 (11) (2021) 3790–3817, https://doi.org/10.1039/D1GC00790D.

[148] L. Wang, L. Tan, L. Hu, X. Wang, R. Koppolu, T. Tirri, B. van Bochove, P. Ihalainen, L.S. Seleenmary Sobhanadhas, J.V. Seppälä, S. Willför, M. Toivakka, C. Xu, On laccase-catalyzed polymerization of biorefinery lignin fractions and alignment of lignin nanoparticles on the nanocellulose surface via one-pot water-phase synthesis, ACS Sustain. Chem. Eng. 9 (26) (2021) 8770–8782, https://doi.org/10.1021/acssuschemeng.1c01576.

[149] K.N. Onwukamike, S. Grelier, E. Grau, H. Cramail, M.A.R. Meier, Sustainable transesterification of cellulose with high oleic sunflower oil in a DBU-CO2 switchable solvent, ACS Sustain. Chem. Eng. 6 (7) (2018) 8826–8835, https://doi.org/10.1021/ACSSUSCHEMENG.8B01186.

[150] J.A. Heredia-Guerrero, L. Goldoni, J.J. Benítez, A. Davis, L. Ceseracciu, R. Cingolani, I.S. Bayer, T. Heinze, A. Koschella, A. Heredia, A. Athanassiou, Cellulose-polyhydroxylated fatty acid ester-based bioplastics with tuning properties: acylation via a mixed anhydride system, Carbohydr. Polym. 173 (2017) 312–320, https://doi.org/10.1016/J.CARBPOL.2017.05.068.

[151] T. Kulomaa, J. Matikainen, P. Karhunen, M. Heikkilä, J. Fiskari, I. Kilpeläinen, Cellulose fatty acid esters as sustainable film materials – effect of side chain structure on barrier and mechanical properties, RSC Adv. 5 (98) (2015) 80702–80708, https://doi.org/10.1039/C5RA12671A.

[152] H. Bian, X. Wu, J. Luo, Y. Qiao, G. Fang, H. Dai, Valorization of alkaline peroxide mechanical pulp by metal chloride-assisted hydrotropic pretreatment for enzymatic Saccharification and cellulose Nanofibrillation, Polymers 11 (2) (2019) 331, https://doi.org/10.3390/polym11020331.

[153] R. Rampazzo, D. Alkan, S. Gazzotti, M.A. Ortenzi, G. Piva, L. Piergiovanni, Cellulose nanocrystals from lignocellulosic raw materials, for oxygen barrier coatings on food packaging films, Packag. Technol. Sci. 30 (10) (2017) 645–661, https://doi.org/10.1002/pts.2308.

[154] Tian Guo, Yang Shen, He Long, Zhang Song, Huang Zhu, Deng., Transparent cellulose/technical lignin composite films for advanced packaging, Polymers 11 (9) (2019) 1455, https://doi.org/10.3390/polym11091455.

[155] G.-J. Kwon, S.-W. Cho, R. Bandi, B.-S. Yang, R. Dadigala, S.-Y. Han, S.-Y. Ma, J.-K. Kim, N.-H. Kim, S.-H. Lee, Production of lignocellulose nanofibrils by conventional and microwave-assisted deep-eutectic-solvent pretreatments: mechanical, antioxidant, and UV-blocking properties, Cellulose 30 (7) (2023) 4277–4292, https://doi.org/10.1007/s10570-023-05164-1.

[156] L.F. Ballesteros, M. Michelin, A.A. Vicente, J.A. Teixeira, M.Â. Cerqueira, Lignocellulosic Materials: Sources and Processing Technologies, 2018, pp. 13–33, https://doi.org/10.1007/978-3-319-92940-8_2.

[157] K. Molenveld, T.M. Slaghek, Recent developments in biodegradable cellulose-based plastics, in: Biodegradable Polymers in the Circular Plastics Economy, Wiley, 2022, pp. 273–298, https://doi.org/10.1002/9783527827589.ch8.

[158] N.M. Stark, L.M. Matuana, Trends in sustainable biobased packaging materials: a mini review, Mater. Today Sustain. 15 (2021) 100084, https://doi.org/10.1016/j.mtsust.2021.100084.

[159] C. Amara, A. El Mahdi, R. Medimagh, K. Khwaldia, Nanocellulose-based composites for packaging applications, Curr. Opin. Green Sustain. Chem. 31 (2021) 100512, https://doi.org/10.1016/j.cogsc.2021.100512.

[160] S. Saedi, C.V. Garcia, J.T. Kim, G.H. Shin, Physical and chemical modifications of cellulose fibers for food packaging applications, Cellulose 28 (14) (2021) 8877–8897, https://doi.org/10.1007/s10570-021-04086-0.

[161] S. Sain, M. Bose, D. Ray, A. Mukhopadhyay, S. Sengupta, T. Kar, C.J. Ennis, P. K. Rahman, M. Misra, A comparative study of polymethylmethacrylate/cellulose nanocomposites prepared by in situ polymerization and ex situ dispersion techniques, J. Reinf. Plast. Compos. 32 (3) (2013) 147–159, https://doi.org/10.1177/0731684412449699.

[162] E. Oliaei, P. Olsén, T. Lindström, L.A. Berglund, Highly reinforced and degradable lignocellulose biocomposites by polymerization of new polyester oligomers, Nat. Commun. 13 (1) (2022) 5666, https://doi.org/10.1038/s41467-022-33283-z.

[163] C. Montanari, P. Olsén, L.A. Berglund, Sustainable wood nanotechnologies for wood composites processed by in-situ polymerization, Front. Chem. 9 (2021), https://doi.org/10.3389/fchem.2021.682883.

[164] M.-A. Berthet, J.-M. Commandré, X. Rouau, N. Gontard, H. Angellier-Coussy, Torrefaction treatment of lignocellulosic fibres for improving fibre/matrix adhesion in a biocomposite, Mater. Des. 92 (2016) 223–232, https://doi.org/10.1016/j.matdes.2015.12.034.

[165] Y. Zhu, Y.Y. Lee, R.T. Elander, Optimization of dilute-acid pretreatment of corn Stover using a high-solids percolation reactor, Appl. Biochem. Biotechnol. 124 (1–3) (2005) 1045–1054, https://doi.org/10.1385/ABAB:124:1-3:1045.

[166] E. Acciardo, S. Tabasso, G. Cravotto, S. Bensaid, Process intensification strategies for lignin valorization, Chem. Eng. Process. Process Intensif. 171 (2022) 108732, https://doi.org/10.1016/j.cep.2021.108732.

[167] L.F. Ballesteros, M. Michelin, A.A. Vicente, J.A. Teixeira, M.Â. Cerqueira, Processing, Production Methods and Characterization of Bio-Based Packaging Materials, 2018, pp. 49–63, https://doi.org/10.1007/978-3-319-92940-8_4.

[168] C.J. Birch, Evaluation of Cellulosic Materials for the Enzymatic Production of Bioplastics [The University of Leeds]. https://etheses.whiterose.ac.uk/29515/1/Calum/Birch-Thesis-Chemical-Engineering%282021%29.pdf, 2021.

[169] M. Paquin, É. Loranger, V. Hannaux, B. Chabot, C. Daneault, The use of weissler method for scale-up a kraft pulp oxidation by TEMPO-mediated system from a batch mode to a continuous flow-through sonoreactor, Ultrason. Sonochem. 20 (1) (2013) 103–108, https://doi.org/10.1016/j.ultsonch.2012.08.007.

[170] J. Yang, Y. Ching, C. Chuah, Applications of lignocellulosic fibers and lignin in Bioplastics: A review, Polymers 11 (5) (2019) 751, https://doi.org/10.3390/polym11050751.

[171] X. Yang, S.K. Biswas, H. Yano, K. Abe, Stiffened nanocomposite hydrogels by using modified cellulose nanofibers via plug flow reactor method, ACS Sustain. Chem. Eng. 7 (10) (2019) 9092–9096, https://doi.org/10.1021/acssuschemeng.9b01322.

[172] L. Amoroso, K.J. De France, C.I. Milz, G. Siqueira, T. Zimmermann, G. Nyström, Sustainable cellulose nanofiber films from carrot pomace as Sprayable coatings for food packaging applications, ACS Sustain. Chem. Eng. 10 (1) (2022) 342–352, https://doi.org/10.1021/acssuschemeng.1c06345.

[173] S.M. El Awad Azrak, C.M. Clarkson, R.J. Moon, G.T. Schueneman, J. P. Youngblood, Wet-stacking lamination of multilayer mechanically fibrillated cellulose Nanofibril (CNF) sheets with increased mechanical performance for use in high-strength and lightweight structural and packaging applications, ACS Appl. Poly. Mater. 1 (9) (2019) 2525–2534, https://doi.org/10.1021/acsapm.9b00635.

[174] J. Shojaeiarani, D.S. Bajwa, N.M. Stark, S.G. Bajwa, Rheological properties of cellulose nanocrystals engineered polylactic acid nanocomposites, Compos. Part B Eng. 161 (2019) 483–489, https://doi.org/10.1016/j.compositesb.2018.12.128.

[175] I. Bascón-Villegas, M. Pereira, E. Espinosa, M. Sánchez-Gutiérrez, A. Rodríguez, F. Pérez-Rodríguez, A new eco-friendly packaging system incorporating lignocellulose nanofibres from Agri-food residues applied to fresh-cut lettuce, J. Clean. Prod. 372 (2022) 133597, https://doi.org/10.1016/j.jclepro.2022.133597.

[176] R.P.O. Santos, B.V.M. Rodrigues, E.C. Ramires, A.C. Ruvolo-Filho, E. Frollini, Bio-based materials from the electrospinning of lignocellulosic sisal fibers and recycled PET, Ind. Crop. Prod. 72 (2015) 69–76, https://doi.org/10.1016/j.indcrop.2015.01.024.

[177] M.E. Genovese, L. Puccinelli, G. Mancini, R. Carzino, L. Goldoni, V. Castelvetro, A. Athanassiou, Rapid solvent-free microcrystalline cellulose melt functionalization with <scp>l</scp> -Lactide for the fabrication of green poly (lactic acid) biocomposites, ACS Sustain. Chem. Eng. 10 (29) (2022) 9401–9410, https://doi.org/10.1021/acssuschemeng.2c01707.

[178] A. Venkatesh, L. Forsgren, A. Avella, K. Banke, J. Wahlberg, F. Vilaseca, G. Lo Re, A. Boldizar, Water-assisted melt processing of cellulose biocomposites with poly (ε-caprolactone) or poly(ethylene-acrylic acid) for the production of carton screw caps, J. Appl. Polym. Sci. 139 (6) (2022), https://doi.org/10.1002/app.51615.

[179] A. Avella, M. Ruda, C. Gioia, V. Sessini, T. Roulin, C. Carrick, J. Verendel, G. Lo Re, Lignin valorization in thermoplastic biomaterials: from reactive melt processing to recyclable and biodegradable packaging, Chem. Eng. J. 463 (2023) 142245, https://doi.org/10.1016/j.cej.2023.142245.

[180] T.J. Bondancia, L.J. Corrêa, A.J.G. Cruz, A.C. Badino, L.H.C. Mattoso, J. M. Marconcini, C.S. Farinas, Enzymatic production of cellulose nanofibers and sugars in a stirred-tank reactor: determination of impeller speed, power consumption, and rheological behavior, Cellulose 25 (8) (2018) 4499–4511, https://doi.org/10.1007/s10570-018-1876-2.

[181] S. Perveen, S.G. Hussain, M.J. Ahmed, R. Khawar, T. Bin Siraj, M. Saleem, A viable and sustainable flat- membrane plate-and-frame module for spent acid regeneration and metal ion recovery, Heliyon 9 (8) (2023) e18344, https://doi.org/10.1016/j.heliyon.2023.e18344.

[182] E. Kuna, R. Behling, S. Valange, G. Chatel, Juan Carlos Colmenares, Sonocatalysis: a potential sustainable pathway for the valorization of lignocellulosic biomass and derivatives, 2017, pp. 1–20, https://doi.org/10.1007/978-3-319-90653-9_1.

[183] G. Chatel, K. De Oliveira Vigier, F. Jérôme, Sonochemistry: what potential for conversion of lignocellulosic biomass into platform chemicals? ChemSusChem 7 (10) (2014) 2774–2787, https://doi.org/10.1002/cssc.201402289.

[184] Z.-Y. Qin, G.-L. Tong, Y.C. Frank Chin, J.-C. Zhou, Preparation of ultrasonic-assisted high carboxylate content cellulose nanocrystals by TEMPO oxidation, BioResources 9 (2) (2011) 1136–1146. https://bioresources.cnr.ncsu.edu/resources/preparation-of-ultrasonic-assisted-high-carboxylate-content-cellulose-nanocrystals-by-tempo-oxidation/.

[185] D.-F. Hou, P.-P. Yuan, Z.-W. Feng, M. An, P.-Y. Li, C. Liu, M.-B. Yang, Sustainable conversion regenerated cellulose into cellulose oleate by sonochemistry, Front. Chem. Sci. Eng. 17 (8) (2023) 1096–1108, https://doi.org/10.1007/s11705-023-2317-9.

[186] F. Wendler, T. Schulze, D. Ciechanska, E. Wesolowska, D. Wawro, F. Meister, T. Budtova, F. Liebner, Cellulose products from solutions: film, fibres and aerogels, in: The European Polysaccharide Network of Excellence (EPNOE), Springer Vienna, 2012, pp. 153–185, https://doi.org/10.1007/978-3-7091-0421-7_6.

[187] V. Harish, M.M. Ansari, D. Tewari, A.B. Yadav, N. Sharma, S. Bawarig, M.-L. García-Betancourt, A. Karatutlu, M. Bechelany, A. Barhoum, Cutting-edge advances in tailoring size, shape, and functionality of nanoparticles and nanostructures: a review, J. Taiwan Inst. Chem. Eng. 149 (2023) 105010, https://doi.org/10.1016/j.jtice.2023.105010.

[188] K. Moriam, D. Sawada, K. Nieminen, Y. Ma, M. Rissanen, N. Nygren, C. Guizani, M. Hummel, H. Sixta, Spinneret geometry modulates the mechanical properties of man-made cellulose fibers, Cellulose 28 (17) (2021) 11165–11181, https://doi.org/10.1007/s10570-021-04220-y.

[189] S.J. Yoon, L. Zhai, H.C. Kim, J.W. Kim, R.M. Muthoka, D. Kim, J. Kim, Rheology design and experimental test of roll-to-roll process for electroactive cellulose film, Int. J. Precis. Eng. Manuf. 19 (9) (2018) 1377–1384, https://doi.org/10.1007/s12541-018-0162-4.

[190] E. Sharifi Zamani, H. Ahadian, T. Maloney, Twin-roll forming, a novel method for producing high-consistency microfibrillated cellulosic films, Cellulose 29 (18) (2022) 9627–9636, https://doi.org/10.1007/s10570-022-04884-0.

[191] B.E. Droguet, H.-L. Liang, B. Frka-Petesic, R.M. Parker, M.F.L. De Volder, J. J. Baumberg, S. Vignolini, Large-scale fabrication of structurally coloured cellulose nanocrystal films and effect pigments, Nat. Mater. 21 (3) (2022) 352–358, https://doi.org/10.1038/s41563-021-01135-8.

[192] H. Qiao, L. Li, X. Zhou, X. Gao, X. Li, Y. Wang, Y. Zhang, Y. Liao, X. Zhou, H. Zhou, D. Li, Efficient preparation of all cellulose composite films using a plasticizing-rolling method, Compos. A: Appl. Sci. Manuf. 158 (106968) (2022), https://doi.org/10.1016/j.compositesa.2022.106968.

[193] K. Jung, Y. Ji, T.-J. Jeong, P.N. Ciesielski, J.C. Meredith, T.A.L. Harris, Roll-to-roll, dual-layer slot die coating of chitin and cellulose oxygen barrier films for renewable packaging, ACS Appl. Mater. Interfaces 14 (39) (2022) 44922–44932, https://doi.org/10.1021/acsami.2c09925.

[194] P. Cazón, M. Vázquez, G. Velazquez, Cellulose-glycerol-polyvinyl alcohol composite films for food packaging: evaluation of water adsorption, mechanical properties, light-barrier properties and transparency, Carbohydr. Polym. 195 (2018) 432–443, https://doi.org/10.1016/j.carbpol.2018.04.120.

[195] M.L.C. de Oliveira, S. Mirmehdi, M.V. Scatolino, M.G. Júnior, A.R. Sanadi, R.A. P. Damasio, G.H.D. Tonoli, Effect of overlapping cellulose nanofibrils and nanoclay layers on mechanical and barrier properties of spray-coated papers, Cellulose 29 (2) (2022) 1097–1113, https://doi.org/10.1007/s10570-021-04350-3.

[196] S. Mirmehdi, P.R.G. Hein, C.I.G. de Luca Sarantópoulos, M.V. Dias, G.H.D. Tonoli, Cellulose nanofibrils/nanoclay hybrid composite as a paper coating: effects of spray time, nanoclay content and corona discharge on barrier and mechanical properties of the coated papers, Food Packag. Shelf Life 15 (2018) 87–94, https://doi.org/10.1016/j.fpsl.2017.11.007.

[197] H. Nadeem, M. Athar, M. Dehghani, G. Garnier, W. Batchelor, Recent advancements, trends, fundamental challenges and opportunities in spray

deposited cellulose nanofibril films for packaging applications, Sci. Total Environ. 836 (2022) 155654, https://doi.org/10.1016/j.scitotenv.2022.155654.

[198] M.A. Herrera, J.A. Sirviö, A.P. Mathew, K. Oksman, Environmental friendly and sustainable gas barrier on porous materials: nanocellulose coatings prepared using spin- and dip-coating, Mater. Des. 93 (2016) 19–25, https://doi.org/10.1016/j.matdes.2015.12.127.

[199] J. Shojaeiarani, D.S. Bajwa, N.M. Stark, T.M. Bergholz, A.L. Kraft, Spin coating method improved the performance characteristics of films obtained from poly (lactic acid) and cellulose nanocrystals, Sustain. Mater. Technol. 26 (2020) e00212, https://doi.org/10.1016/j.susmat.2020.e00212.

[200] C. Negro, G. Pettersson, A. Mattsson, S. Nyström, J.L. Sanchez-Salvador, A. Blanco, P. Engstrand, Synergies between fibrillated nanocellulose and hot-pressing of papers obtained from high-yield pulp, Nanomaterials 13 (13) (2023) 1931, https://doi.org/10.3390/nano13131931.

[201] K. Huang, A. Maltais, J. Liu, Y. Wang, Wood cellulose films regenerated from NaOH/urea aqueous solution and treated by hot pressing for food packaging application, Food Biosci. 50 (2022) 102177, https://doi.org/10.1016/j.fbio.2022.102177.

[202] E. Fortunati, W. Yang, F. Luzi, J. Kenny, L. Torre, D. Puglia, Lignocellulosic nanostructures as reinforcement in extruded and solvent casted polymeric nanocomposites: an overview, Eur. Polym. J. 80 (2016) 295–316, https://doi.org/10.1016/j.eurpolymj.2016.04.013.

[203] J.I. Moran, L.N. Ludueña, V.T. Phuong, P. Cinelli, A. Lazzeri, V.A. Alvarez, Processing routes for the preparation of poly(lactic acid)/cellulose-nanowhisker nanocomposites for packaging applications, Polym. Polym. Compos. 24 (5) (2016) 341–346, https://doi.org/10.1177/096739111602400505.

[204] M. Hietala, K. Oksman, Pelletized cellulose fibres used in twin-screw extrusion for biocomposite manufacturing: fibre breakage and dispersion, Compos. A: Appl. Sci. Manuf. 109 (2018) 538–545, https://doi.org/10.1016/j.compositesa.2018.04.006.

[205] S. Gamero, M. Jiménez-Rosado, A. Romero, C. Bengoechea, A. Guerrero, Reinforcement of soy protein-based Bioplastics through addition of lignocellulose and injection molding processing conditions, J. Polym. Environ. 27 (6) (2019) 1285–1293, https://doi.org/10.1007/s10924-019-01430-1.

[206] J. Beaugrand, F. Berzin, Lignocellulosic fiber reinforced composites: influence of compounding conditions on defibrization and mechanical properties, J. Appl. Polym. Sci. 128 (2) (2013) 1227–1238, https://doi.org/10.1002/app.38468.

[207] E. Fekete, D. Kun, J. Móczó, Thermoplastic starch/wood composites: effect of processing technology, interfacial interactions and particle characteristics, Period. Polytech. Chem. Eng. 62 (2) (2017) 129, https://doi.org/10.3311/PPch.11228.

[208] P. Müller, K. Renner, J. Móczó, E. Fekete, B. Pukánszky, Thermoplastic starch/wood composites: interfacial interactions and functional properties, Carbohydr. Polym. 102 (2014) 821–829, https://doi.org/10.1016/j.carbpol.2013.10.083.

[209] N. Montanes, L. Quiles-Carrillo, S. Ferrandiz, O. Fenollar, T. Boronat, Effects of lignocellulosic fillers from waste thyme on melt flow behavior and Processability of wood plastic composites (WPC) with biobased poly(ethylene) by injection molding, J. Polym. Environ. 27 (4) (2019) 747–756, https://doi.org/10.1007/s10924-019-01388-0.

[210] Passos de Oliveira, R. Santos, P. Fernanda Rossi, L. Ramos, E. Frollini, Renewable resources and a recycled polymer as raw materials: Mats from electrospinning of lignocellulosic biomass and PET solutions, Polymers 10 (5) (2018) 538, https://doi.org/10.3390/polym10050538.

[211] A. Cherpinski, S. Torres-Giner, J. Vartiainen, M.S. Peresin, P. Lahtinen, J. M. Lagaron, Improving the water resistance of nanocellulose-based films with polyhydroxyalkanoates processed by the electrospinning coating technique, Cellulose 25 (2) (2018) 1291–1307, https://doi.org/10.1007/s10570-018-1648-z.

[212] K.C.C. de C. Benini, M.O.H. Cioffi, H.J.C. Voorwald, PHBV/cellulose nanofibrils composites obtained by solution casting and electrospinning process, Matéria (Rio de Janeiro) 22 (2) (2017), https://doi.org/10.1590/s1517-707620170002.0170.

[213] M. Polaskova, R. Cermak, V. Verney, P. Ponizil, S. Commereuc, M.F.C. Gomes, A. A.H. Padua, P. Mokrejs, M. Machovsky, Preparation of microfibers from wood/ionic liquid solutions, Carbohydr. Polym. 92 (1) (2013) 214–217, https://doi.org/10.1016/j.carbpol.2012.08.089.

[214] L. Wang, D.J. Gardner, J. Wang, Y. Yang, H.L. Tekinalp, M. Tajvidi, K. Li, X. Zhao, D.J. Neivandt, Y. Han, S. Ozcan, J. Anderson, Towards industrial-scale production of cellulose nanocomposites using melt processing: a critical review on structure-processing-property relationships, Compos. Part B Eng. 201 (2020) 108297, https://doi.org/10.1016/j.compositesb.2020.108297.

[215] R. Koppolu, J. Lahti, T. Abitbol, C. Aulin, J. Kuusipalo, M. Toivakka, Tailoring the performance of nanocellulose-based multilayer-barrier paperboard using biodegradable-thermoplastics, pigments, and plasticizers, Cellulose 30 (11) (2023) 6945–6958, https://doi.org/10.1007/s10570-023-05281-x.

[216] X.-F. Sun, Fowler P. Sun, M.S. Baird, Extraction and characterization of original lignin and hemicelluloses from wheat straw, J. Agric. Food Chem. 53 (4) (2005) 860–870, https://doi.org/10.1021/jf040456q.

[217] D. Lin, P. Lopez-Sanchez, M.J. Gidley, Interactions of pectins with cellulose during its synthesis in the absence of calcium, Food Hydrocoll. 52 (2016) 57–68, https://doi.org/10.1016/j.foodhyd.2015.06.004.

[218] S. Rodríguez-Fabià, J. Torstensen, L. Johansson, K. Syverud, Hydrophobization of lignocellulosic materials part II: chemical modification, Cellulose 29 (17) (2022) 8957–8995, https://doi.org/10.1007/s10570-022-04824-y.

[219] J. Jiang, Y. Zhu, S. Zargar, J. Wu, H. Oguzlu, A. Baldelli, Z. Yu, J. Saddler, R. Sun, Q. Tu, F. Jiang, Rapid, high-yield production of lignin-containing cellulose nanocrystals using recyclable oxalic acid dihydrate, Ind. Crop. Prod. 173 (2021) 114148, https://doi.org/10.1016/j.indcrop.2021.114148.

[220] D.F. Hou, Z.Y. Liu, L. Zhou, H. Tan, W. Yang, M.B. Yang, A facile strategy towards heterogeneous preparation of thermoplastic cellulose grafted polyurethane from amorphous regenerated cellulose paste, Int. J. Biol. Macromol. 161 (2020) 177–186, https://doi.org/10.1016/J.IJBIOMAC.2020.05.203.

[221] P. Müller, B. Pukánszky, Structure-Property Correlations in Thermoplastic Starch Blends and Composites, Budapest University of Technology and Economics, 2015. https://repozitorium.omikk.bme.hu/server/api/core/bitstreams/9b119669-e967-4b18-bee8-53a03383dbaa/content.

[222] A.K. Bharimalla, S.P. Deshmukh, N. Vigneshwaran, P.G. Patil, V. Prasad, Nanocellulose-polymer composites for applications in food packaging: current status, future prospects and challenges, Polym.-Plast. Technol. Eng. 56 (8) (2017) 805–823, https://doi.org/10.1080/03602559.2016.1233281.

[223] C.M. Ewulonu, H. Wang, X. Liu, M. Wu, Y. Huang, Sustainable fabrication of hydrophobic lignocellulose micro and nanofibrils mulch films and spray coatings, Cellulose 29 (4) (2022) 2305–2322, https://doi.org/10.1007/s10570-022-04440-w.

[224] D. Feber, A. Granskog, D. Nordigården, S. Ponkshe, P. Berg, The Drive Toward Sustainability in Packaging - Beyond the Quick Wins, McKinsey & Company, 2020. February, https://www.mckinsey.com/industries/paper-forest-products-and-packaging/our-insights/the-drive-toward-sustainability-in-packaging-beyond-the-quick-wins.

[225] European Commission, A Sustainable Alternative to Plastic Packaging. 1–2, 2018.

[226] European Commission, Reduce, Reuse, Rethink PACKaging: Towards Novel Fiber-based Packaging and Reuse Schemes Uptake, 2023, https://doi.org/10.3030/101060806.

[227] N.A.A. Qasem, R.H. Mohammed, D.U. Lawal, Author correction: removal of heavy metal ions from wastewater: a comprehensive and critical review, Npj Clean Water 4 (1) (2021) 52, https://doi.org/10.1038/s41545-021-00144-z.

[228] S. Arfelis, R.J. Aguado, D. Civancik, P. Fullana-i-Palmer, M.À. Pèlach, Q. Tarrés, M. Delgado-Aguilar, Sustainability of cellulose micro−/nanofibers: A comparative life cycle assessment of pathway technologies, Sci. Total Environ. 874 (2023) 162482, https://doi.org/10.1016/j.scitotenv.2023.162482.

[229] R. Banerjee, S.S. Ray, Sustainability and life cycle assessment of thermoplastic polymers for packaging: A review on fundamental principles and applications, Macromol. Mater. Eng. 307 (6) (2022), https://doi.org/10.1002/mame.202100794.

[230] P.H. Camani, B.F. Anholon, R.R. Toder, D.S. Rosa, Microwave-assisted pretreatment of eucalyptus waste to obtain cellulose fibers, Cellulose 27 (7) (2020) 3591–3609, https://doi.org/10.1007/s10570-020-03019-7.

[231] M.C.B. de Figueirêdo, M.D.F. Rosa, C.M.L. Ugaya, M. de S.M. de Souza Filho, A.C. C. da Silva Braid, L.F.L. de Melo, Life cycle assessment of cellulose nanowhiskers, J. Clean. Prod. 35 (2012) 130–139, https://doi.org/10.1016/j.jclepro.2012.05.033.

[232] F. Foroughi, E. Rezvani Ghomi, F. Morshedi Dehaghi, R. Borayek, S. Ramakrishna, A review on the life cycle assessment of cellulose: from properties to the potential of making it a low carbon material, Materials 14 (4) (2021) 714, https://doi.org/10.3390/ma14040714.

[233] M. Hervy, S. Evangelisti, P. Lettieri, K.-Y. Lee, Life cycle assessment of nanocellulose-reinforced advanced fibre composites, Compos. Sci. Technol. 118 (2015) 154–162, https://doi.org/10.1016/j.compscitech.2015.08.024.

[234] S. Josset, P. Orsolini, G. Siqueira, A. Tejado, P. Tingaut, T. Zimmermann, Energy consumption of the nanofibrillation of bleached pulp, wheat straw and recycled newspaper through a grinding process, Nord. Pulp Pap. Res. J. 29 (1) (2014) 167–175, https://doi.org/10.3183/npprj-2014-29-01-p167-175.

[235] Q. Li, S. McGinnis, C. Sydnor, A. Wong, S. Renneckar, Nanocellulose life cycle assessment, ACS Sustain. Chem. Eng. 1 (8) (2013) 919–928, https://doi.org/10.1021/sc4000225.

[236] D. Moon, M. Sagisaka, K. Tahara, K. Tsukahara, Progress towards sustainable production: environmental, economic, and social assessments of the cellulose nanofiber production process, Sustainability 9 (12) (2017) 2368, https://doi.org/10.3390/su9122368.

[237] D.M. do Nascimento, A.F. Dias, C.P. de Araújo Junior, M. de F. Rosa, J.P. S. Morais, M.C.B. de Figueirêdo, A comprehensive approach for obtaining cellulose nanocrystal from coconut fiber. Part II: environmental assessment of technological pathways, Ind. Crop. Prod. 93 (2016) 58–65, https://doi.org/10.1016/j.indcrop.2016.02.063.

[238] F. Piccinno, R. Hischier, S. Seeger, C. Som, Life cycle assessment of a new technology to extract, functionalize and orient cellulose nanofibers from food waste, ACS Sustain. Chem. Eng. 3 (6) (2015) 1047–1055, https://doi.org/10.1021/acssuschemeng.5b00209.

[239] H. Tu, K. Xie, D. Ying, L. Luo, X. Liu, F. Chen, B. Duan, Q. Fu, L. Zhang, Green and economical strategy for spinning robust cellulose filaments, ACS Sustain. Chem. Eng. 8 (39) (2020) 14927–14937, https://doi.org/10.1021/acssuschemeng.0c04890.

[240] V. Vohra, N.T. Razali, R. Wahi, L. Ganzer, T. Virgili, A comparative study of low-cost coating processes for green & sustainable organic solar cell active layer manufacturing, Optic. Mater.: X 13 (2022) 100127, https://doi.org/10.1016/j.omx.2021.100127.

[241] A. DeVierno Kreuder, T. House-Knight, J. Whitford, E. Ponnusamy, P. Miller, N. Jesse, R. Rodenborn, S. Sayag, M. Gebel, I. Aped, I. Sharfstein, E. Manaster, I. Ergaz, A. Harris, L. Nelowet Grice, A method for assessing greener alternatives between chemical products following the 12 principles of green chemistry, ACS Sustain. Chem. Eng. 5 (4) (2017) 2927–2935, https://doi.org/10.1021/

ACSSUSCHEMENG.6B02399/ASSET/IMAGES/LARGE/SC-2016-02399F_0002.JPEG.

[242] I. Filipova, F. Serra, Q. Tarrés, P. Mutjé, M. Delgado-Aguilar, Oxidative treatments for cellulose nanofibers production: a comparative study between TEMPO-mediated and ammonium persulfate oxidation, Cellulose 27 (18) (2020) 10671–10688, https://doi.org/10.1007/s10570-020-03089-7.

[243] H. Mahmood, M. Moniruzzaman, S. Yusup, T. Welton, Ionic liquids assisted processing of renewable resources for the fabrication of biodegradable composite materials, Green Chem. 19 (9) (2017) 2051–2075, https://doi.org/10.1039/C7GC00318H.

[244] G. Albornoz-Palma, D. Ching, O. Valerio, R.T. Mendonça, M. Pereira, Effect of lignin and hemicellulose on the properties of lignocellulose nanofibril suspensions, Cellulose 27 (18) (2020) 10631–10647, https://doi.org/10.1007/s10570-020-03304-5.

[245] L. Senila, O. Cadar, E. Kovacs, E. Gal, M. Dan, Z. Stupar, D. Simedru, M. Senila, C. Roman, L-poly(lactic acid) production by microwave irradiation of lactic acid obtained from lignocellulosic wastes, Int. J. Mol. Sci. 24 (12) (2023) 9817, https://doi.org/10.3390/ijms24129817.

[246] C. Achillas, D. Bochtis, Toward a green, closed-loop, circular bioeconomy: boosting the performance efficiency of circular business models, Sustainability 12 (23) (2020) 10142, https://doi.org/10.3390/su122310142.